DISSERTATION | DOCTORAL THESIS

Titel | Title

Exploring the mode of action of ichthyotoxins from *Prymnesium parvum* (Prymnesiophyceae) and *Karlodinium armiger* (Dinophyceae)

verfasst von | submitted by

Hélène-Christine Prause BSc MSc

angestrebter akademischer Grad | in partial fulfilment of the requirements for the degree of

Doktorin der Naturwissenschaften (Dr.rer.nat.)

Wien | Vienna, 2025

Studienkennzahl lt. Studienblatt | Degree programme code as it appears on the student record sheet:	UA 796 605 419
Dissertationsgebiet lt. Studienblatt | Field of study as it appears on the student record sheet:	Chemie
Betreut von | Supervisor:	Univ.-Prof. Dr. Doris Marko
Mitbetreut von | Co-Supervisor:	DI Dr. Elisabeth Varga

Abstract

Blooms of ichthyotoxic microalgae are responsible for many fish kills worldwide. The haptophyte *Prymnesium parvum* and the dinoflagellate *Karlodinium armiger* are examples of toxic species producing allelochemical compounds, prymnesins and karmitoxin respectively. Prymnesins comprise a large group of analogs categorized into A-, B-, and C-types. The mode of action (MoA) for prymnesins and karmitoxin is widely unknown. Current hypotheses propose pore-formation causing an increase in membrane permeability and subsequent cell disruption. A high affinity to sterols may aid them in their toxic mechanism. This project focused on the exploration of their MoA, by expanding the knowledge on their toxic profile and investigating the involvement of sterols.

A quick onset of adverse effects caused by prymnesins and karmitoxin was observed, with comparable potencies for cytotoxicity and hemolysis. Prymnesins generally followed the pattern of most to least potent as A>C>B. Individual analogs were found to direct prymnesin potency. Interestingly, the prymnesin types appear to differ in their MoAs, likely due to differing affinities as well as binding to selected sterols. This variance might explain the significant variation in potency between A- and B-type prymnesins. Irrespective thereof, altering cholesterol content in the target cells did not affect cytotoxicity. The involvement of Cl^- and Ca^{2+} in prymnesin toxicity was further highlighted in live-cell fluorescent imaging. For karmitoxin, a high sterol-affinity was measured, yet also for this ichthyotoxin a modulation of cellular cholesterol had no impact on potency.

Prymnesin and karmitoxin toxicity seems to be more complex than previously hypothesized. While sterol-affinity remains a key factor of pore-formation, these results suggest that the MoA includes other crucial steps. Moreover, it should be considered that the three types of prymnesins do not follow the same MoA. Future studies may focus on exploring cellular responses on a more molecular level.

Zusammenfassung

Blüten von ichthyotoxischen Mikroalgen sind weltweit für viele Fischsterben verantwortlich. Der Haptophyt *Prymnesium parvum* und der Dinoflagellat *Karlodinium armiger* sind Beispiele für toxische Spezies, die allelochemische Verbindungen, Prymnesine bzw. Karmitoxin, produzieren. Prymnesine umfassen eine große Gruppe von Analoga, die in A-, B- und C-Typen eingeteilt werden. Die Wirkungsweise von Prymnesinen und Karmitoxin ist weitgehend unbekannt. Aktuelle Hypothesen gehen von einer Porenbildung aus, die zur Erhöhung der Membranpermeabilität und Zelltod führt. Eine hohe Affinität zu Sterolen könnte dabei eine wichtige Rolle spielen. In diesem Projekt wurde der Fokus auf die Erforschung der Wirkmechanismen gelegt, indem das toxische Profil erweitert und die Mitwirkung von Sterolen untersucht wurde.

Bei Prymnesinen und Karmitoxin wurde eine rasche Beeinträchtigung der Zellviabilität beobachtet, mit vergleichbarer Wirksamkeit für Zytotoxizität und Hämolyse. Die Potenz der Prymnesine konnte nach dem Muster A>C>B, von stärkster zu schwächster Wirkung, eingeteilt werden. Es wurde festgestellt, dass einzelne Analoga die Prymnesin-Potenz direkt beeinflussen. Interessanterweise scheinen sich die Prymnesin-Typen in ihren Mechanismen zu unterscheiden, was wahrscheinlich auf unterschiedliche Sterolaffinitäten und Komplexbildung zurückzuführen ist. Dies könnte die signifikanten Unterschiede in der Wirksamkeit zwischen A- und B-Typen erklären. Unabhängig davon hatte die Veränderung des Cholesterolgehalts in den Zielzellen keinen Einfluss auf die Zytotoxizität. Die Beteiligung von Cl^- und Ca^{2+} an der Prymnesin-Toxizität wurde durch Fluoreszenzaufnahmen weiter verdeutlicht. Auch für Karmitoxin wurde eine hohe Sterol-Affinität gemessen, doch auch hier hatte eine Modulation des zellulären Cholesterols keinen Einfluss auf die Toxizität.

Der Wirkmechanismus von Prymnesinen und Karmitoxin scheint komplexer zu sein als bisher angenommen. Die Sterolaffinität ist zwar nach wie vor ein Schlüsselfaktor für die Porenbildung, doch deuten diese Ergebnisse darauf hin, dass weitere Schritte entscheidend für die Toxizität sind. Außerdem ist zu bedenken, dass die drei Prymnesin-Typen nicht demselben Mechanismus folgen. Zukünftige Studien könnten sich auf Reaktionen in der molekularen Ebene konzentrieren.

Acknowledgements

The last four years I dedicated to this PhD project were nothing short of a rollercoaster ride, and I am glad for every single second and for all the lessons – scientific and personal – that I learned along the way. It would be untruthful to say I enjoyed each moment, and yet I would not change a thing if I could. As I am writing this, it means that my journey as a *PhD student* is almost officially over, and this was in no way an accomplishment I achieved by myself. So, I want to take the time (and space) to express my gratitude and appreciation for everyone involved in this project and for all those who accompanied me on this journey and made it worthwhile.

First and foremost, I want to thank my supervisor, Elisabeth Varga. I am grateful for the opportunity to work on this project and to have been immersed in the fascinating world of microalgae. I truly appreciate all the time and effort you put into my project, for listening to me, and most of all for encouraging me in my pursuits. If it were not for your support, my PhD and thus my life would be very different right now.

Next, I would like to express my gratitude to Doris Marko for giving me the chance to be part of this amazing working group and to realize my research in this department. I appreciate your support and am glad for the invaluable growth and achievements I gained while working with you.

I am also very grateful to Giorgia Del Favero, whose guidance and knowledge was an immense aid to this project and myself. Thanks for all the input and advice you have given me over the years.

Of course, I cannot write this section and leave out Allen Place, who has been one of my biggest allies. I am deeply thankful for your guidance and insights, for all the times you lent me an ear, a hand, and a foot, and not to mention the opportunity to work with you and your lab group. Thank you for welcoming me to your lab family, your encouragement, and for being a friend.

It goes without saying that none of this would have been nearly as enjoyable if not for the wonderful people of the LMC group. We truly created a family in the last couple of years, and I am so touched by all the love you have shown me. Thank you so much for the fun times and for being there during the bad times. Without you I probably would not have lasted, and it will be the hardest thing to leave you.

I also want to acknowledge all my loved ones, who believed in me, cheered me on, and were there for me when I needed them. Thank you for the late-night talks, the countless trips we took, and the hours spent together either celebrating or getting my mind off work troubles. You gave me comfort and strength, and I am deeply grateful to each and every one of you.

And finally, Luke, thank you for understanding when I had to put work first, and for putting me first even when I could not. There are no words to describe how much it meant to me to have you as my rock. I definitely would not be here without you, my biggest cheerleader.

~ Thank you

Table of contents

1 Introduction

Microalgae are crucial for the food web, providing nutrients and representing a food source for bivalves and crustaceans[1,2]. They can also be considered a novel food source for humans, since they are rich in lipids, proteins, and vitamins. Some microalgal species, however, produce toxins, many of which are known to be harmful towards humans, while some toxins are relevant for their allelochemical properties[2,3]. Allelopathy is defined as the production of secondary metabolites providing the microalga in question a competitive advantage over other organisms and serve as a defense against grazers[2,4]. When allelopathic compounds affect fish, it is called ichthyotoxicity.

Toxin-producing microalgae can become particularly problematic during harmful algal blooms (HABs, Figure 1), during which microalgae proliferate very rapidly[1,5]. HABs occur worldwide and can have a detrimental impact on the ecosystem[6,7]. Most noticeable are discoloration of the water and massive kills or beaching of aquatic life forms. Human intervention in aquatic ecosystems as well as the exploitation thereof and climate change have led to an increase in the occurrence and intensity of HABs[1,5,6]. Among the most common HAB-forming microalgae are dinoflagellates and diatoms, although HAB events caused by other types of microalgae have been observed[3,5]. Allelochemical properties were demonstrated in several algal groups as well, including dinoflagellates, haptophytes, and cyanobacteria[2,8]. Toxins are often released when the bloom dies off, due to cell rupture, but can also be released by living cells. Importantly, toxin quantity is not directly related to the number of toxin-producing cells[6].

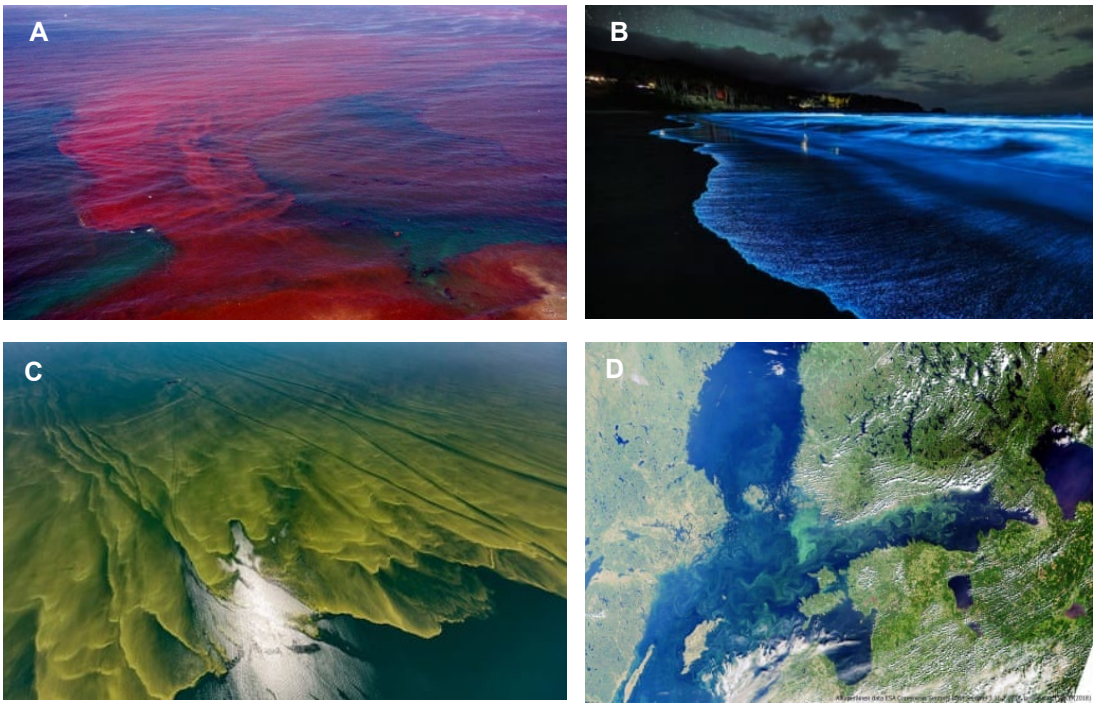

*Figure 1 – **A** Harmful algal bloom (HAB) caused by a so-called "red tide" in San Diego County, USA in 2018. Photograph: Kai Schumann. Retrieved 3rd February 2025 from www.noaa.gov. **B** Bioluminescence caused by "red tide" microalgae in Tasmania, Australia in 2024. Photograph: Toby Schrapel. **C** HAB in Lake Erie, Canada/USA in 2017. Photograph: Zachary Haslick. **D** Blue-green algal bloom in the Baltic Sea in 2018. Photograph: ESA/Finnish Environment Institute. Retrieved 3rd February 2025 from www.theguardian.com.*

Prymnesium parvum is an example of a haptophyte alga that has been associated with several fish kills following a HAB event, and their ichthyotoxins, the group of prymnesins, are believed to be the underlying reason for it. Prymnesins have been studied extensively in the last couple of years and gained even more attention due to a recent bloom in the Odra/Oder River[9]. Prymnesins are supersized (16 – 23 kDa) ladder-frame polyether compounds, with a primary amine group on their lipophilic arm (Figure 2)[10,11]. Unlike most identified ichthyotoxins, they are largely cell-bound[1,12,13].

Aside from this haptophyte species, dinoflagellate algae are generally well known for their involvement in HABs. Among the dinoflagellates, the genus of *Karlodinium* has caught the attention of researchers for their production of bioactive extracellular compounds and HAB-formation. Among these, the best described ichthyotoxins are karlotoxins, produced by *Karlodinium veneficum*. Karlotoxins have been studied extensively in the last decades, with research revealing their lytic and antifungal properties[14,15]. Their hairpin-like structure (Figure 2) is believed to aid them in their toxicity. The novel toxin garnering the attention of researchers is karmitoxin, which is produced by the related species *Karlodinium armiger*[16,17]. Like karlotoxin, the structurally related karmitoxin (Figure 2) has shown lytic as well as ichthyotoxic properties[18]. So far, not much is known about the toxic properties of karmitoxin, although it is believed to exhibit similar effects as karlotoxins.

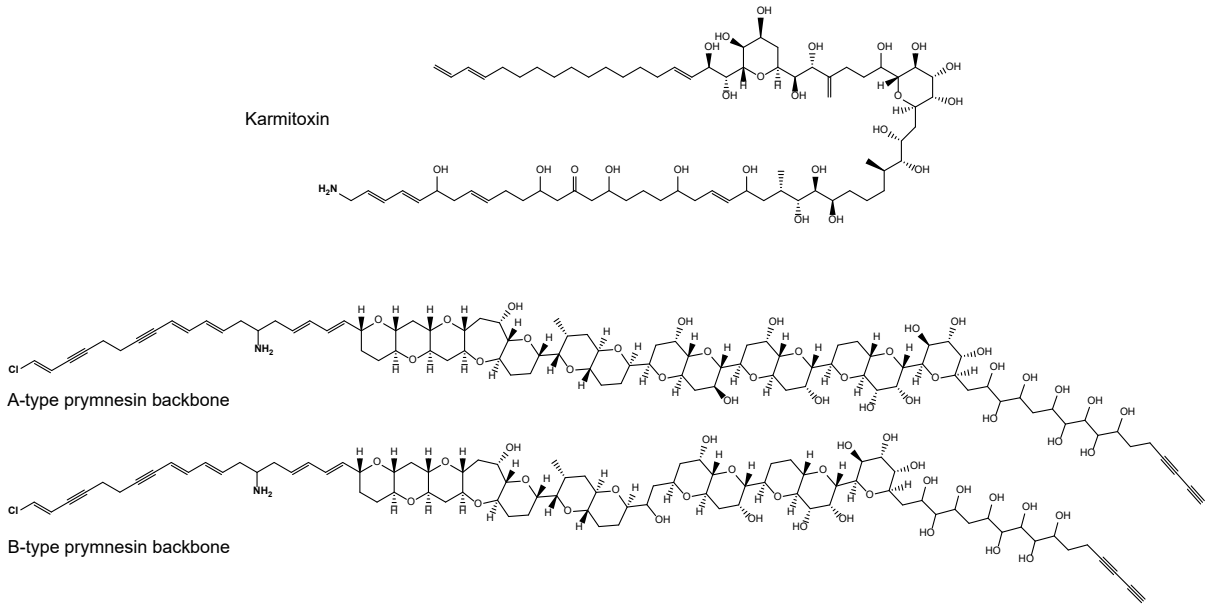

Figure 2 – Chemical structures of dinoflagellate toxin karmitoxin from Karlodinium armiger *and A- and B-type prymnesin backbone structures from the haptophyte* Prymnesium parvum.

A trait these allelopathic compounds share, is that to date their mode of action (MoA) remains unknown. Lytic properties have been observed for both prymnesins and karmitoxin, although it is unclear through which mechanism lysis is induced. They are believed to cause fish kills by disrupting the cellular membrane of gill cells, causing them to increase mucus production, and ultimately the fish die of suffocation[19,20]. Both karmitoxin and prymnesins are hypothesized to be highly lipophilic and therefore to interact with lipids of the membrane to induce lysis. In order to understand the severity of *P. parvum* and *K. armiger* HABs, it is essential to first understand the MoA and toxic mechanism of the allelochemical compounds.

2 Aims

In this study we focused on expanding the knowledge on the toxic potential of the allelochemicals produced by the haptophyte *Prymnesium parvum* and the dinoflagellate *Karlodinium armiger*. As their mode of actions are not yet fully understood, it is crucial to lay the foundation for future research on their toxicity, with the goal to ultimately characterize their relevance and risk in the eco-system.

Firstly, the cytotoxic and lytic potencies of prymnesins and karmitoxin were assessed to help complete the understanding of their toxic properties. For prymnesins, it was of particular interest to investigate the role of individual analogs to get an insight into their contribution to strain-specific toxicity. To this end, the fish gill cell line RTgill-W1 and the human cell line HCEC-1CT were used for the evaluation of cytotoxicity, and red blood cells of Atlantic salmon (*Salmo salar*) for hemolysis.

Secondly, emphasis was placed on how interactions with membrane components contribute to their toxic mechanism. Specifically, the interaction with cholesterol was examined, which is supposedly the point of contact for these ichthyotoxins. Whether prymnesins and karmitoxin can form complexes with selected sterols was tested via surface plasmon resonance and the addition of free sterols to the medium before cytotoxicity or lysis assays.

Lastly, the impact prymnesins have on cellular morphology was assessed using fluorescent imaging. The influence of selected ions on toxicity was evaluated based on cytotoxicity tests and changes in morphology.

By testing these theories, we want to provide new aspects of adverse effects of prymnesins and karmitoxin on the cellular level. This should aid future researchers in their approach to characterizing the interactions between these ichthyotoxins and the cell membrane. The overarching goal guiding this project is to hone in on the process of targeting the cell membrane and the subsequent pore-formation.

3 Theoretical Background

3.1 *Prymnesium parvum*

P. parvum is a species of haptophyte microalgae belonging to the class of Prymnesiophyceae. Typically, this species is found in brackish water but is also able to live in lower or higher salinities or temperatures, due to its euryhaline and eurythermal nature[1,12,21,22]. This species was first described in 1939 by Otterstrom & Nielsen[23]. *P. parvum* cells range in size from 6 to 10 µm (Figure 3), with differences recorded between the strains. Several fish kills ensuing from HAB events in which prymnesins are released have been recorded, the last massive fish killing taking place the Odra/Oder River in Poland/Germany[9]. *P. parvum* blooms are most likely to occur under suboptimal environmental conditions. Recent studies corroborated that prymnesin production increased when *P. parvum* cells were exposed to higher salinity or nutrient limitation[12,24–29].

Figure 3 – Prymnesium parvum N. Carter. *Picture copyright C.F. Carter. Algaebase. Retrieved 3rd February 2025 from www.algaebase.org.*

3.1.1 Prymnesins

Although *P. parvum* was first discovered and investigated before the mid-20th century[23], the term prymnesin for the ichthyotoxin responsible for fish kills was given only in 1961[30]. It took thirty more years for the A-type prymnesin structure to be elucidated by the group of Igarashi *et al*.. Two analogs were characterized by this group, which were then named prymnesin-1 and prymnesin-2[10]. Another twenty years later, Rasmussen *et al*. was able to elucidate the structure of B-type prymnesins (called prymnesin-B1 and -B2) and tentatively describe the structure of C-type prymnesins[11].

Prymnesins are currently grouped into three types; A-, B-, and C-types, based on the length of their carbon backbone (91, 85, 83 carbon atoms, respectively). A feature that distinguishes prymnesins from other phycotoxins is the large diversity within their group, with over 100 congeners detected. This is due to the variability in degree of chlorination, saturation, and glycosylation[31]. One important functional moiety shared by all analogs identified so far is a primary amine group in the lipophilic arm of the prymnesins[10,11,31,32]. A more defining nomenclature was proposed by Binzer and Svenssen *et al.* where the individual glycosylation and chlorination of each analog can be considered [31]. Therefore, the analog formerly known as prymnesin-1 for instance is called prymnesin-A (3 Cl) + 2 pentose + hexose. This nomenclature will be used throughout this entire dissertation. It is important to note that one strain of

P. parvum can only produce prymnesins of one type (A, B, or C), but various analogs within this type[31]. It has been well established that prymnesin analogs vary in their potency, yet another factor influencing the expected toxicity from a specific *P. parvum* strain is the amount of analog produced[11,31,33]. The analog mixture produced by strain K-0374 (B-type) is more ichthyotoxic than the mixture produced by strain K-0081 (B-type). Yet, K-0081 was found to have a significantly larger toxin per cell-quota, meaning that higher concentrations of toxins can be found in these cultures, possibly making them more potent in case of HABs[13,33].

Attempts to establish methods to isolate these toxins have not been as effective as hoped, due to their amphipathic nature causing sample loss and the relatively low toxin production[13,34]. Currently, the most common method to obtain prymnesins from a culture is a methanol (MeOH) extraction from algal cell pellet after removal of chlorophyll with acetone, as prymnesins are largely biomass associated (approximately 90 %)[13]. Another hurdle to overcome is the lack of analytical standards, rendering an absolute and reliable quantification nearly impossible. Svenssen *et al*. developed a method to quantify the sum of prymnesins in a sample, based on the derivatization of the primary amine group and subsequent fluorescent tagging thereof[13]. An apparent recovery of 60 % was reported for this indirect quantification. The mycotoxins fumonisins B_1 and B_2 are used as external calibrators.

3.1.2 Prymnesin toxicity

Prymnesins are considered lipophilic and amphipathic compounds, which can damage the cell membrane of fish gill cells, the primary physiological target[35,36]. This damage is believed to occur in the form of pore-formation in the membrane, which causes osmotic disbalance[19]. As a response, the fish gill cells increase their mucus production, and if this condition persists, the fish ultimately succumbs to suffocation[19,37]. Prymnesins also displayed hemolytic properties[10,30,38].

It is not fully understood how prymnesins are able to cause membrane damage. It was hypothesized that these microalgal toxins interact with lipids found in cellular membranes, of which sterols are the main targets of interest[38,39]. Previous studies recorded that prymnesins were more likely to target liposomes containing cholesterol than those not containing cholesterol[40].

Changes in the pH and salinity of the exposure environment were shown to influence prymnesin toxicity as well[36,38]. The presence of Ca^{2+} ions led to an increase in ichthyotoxicity, and fish exposed to $CaCl_2$ or $MgCl_2$ prior to prymnesin exposure were more susceptible to its toxicity[34,41].

3.2 *Karlodinium armiger*

The genus of *Karlodinium* describes unarmored dinoflagellates which have been associated with HAB events[15,16,42]. Of the *Karlodinium*, several species are currently considered toxic, among them *K. veneficum* and *K. armiger*[15,18,43,44]. At the time of writing, *K. veneficum* is one of the most studied *Karlodinium* species and has been associated with harmful effects on fish, mussels, and other microalgae[45–48]. *K. armiger* (Figure 4) was first discovered and isolated in the Mediterranean Sea[16,17]. Like *K. veneficum*, *K. armiger* is a mixotrophic alga and a peduncle feeder (tube feeder), immobilizing prey by extending a capture filament in order to access nutrients or pull the prey into food vacuoles for digestion[17,49,50].

Since it was shown that *K. armiger* grows poorly in common microalgal media such as f/2 or K-medium without addition of prey, they are typically cultured under mixotrophic conditions[18,49,51]. However, Binzer *et al*. showed that adding up to 50 µM ammonium to the culture medium is a good alternative to prey addition[51]. The ammonium can be used as a nitrogen source to perform autotrophic growth, while maintaining karmitoxin cell quotas[52].

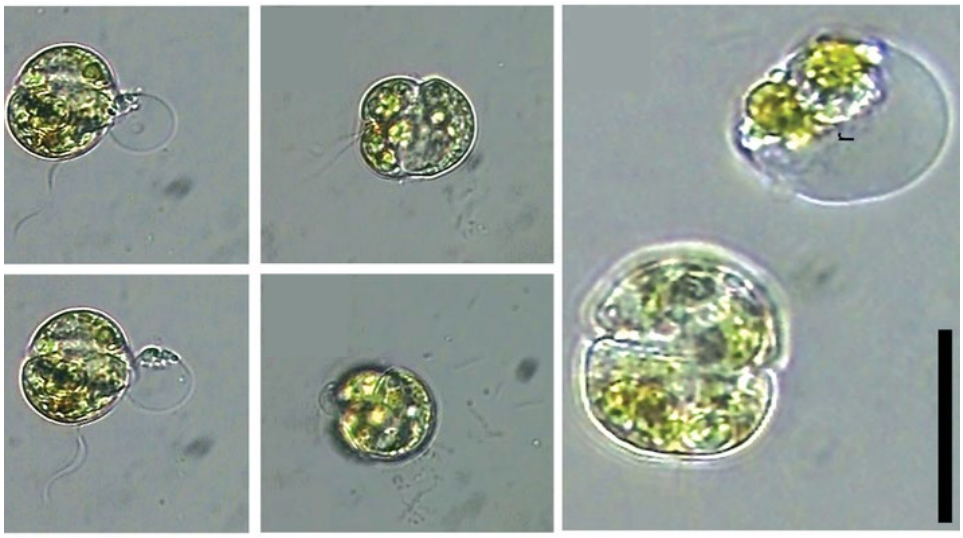

Figure 4 – Karlodinium armiger. *Scale bar = 20 µm. Adapted from Berge* et al.[49]

3.2.1 Karmitoxin

The structure of karmitoxin was elucidated by Rasmussen *et al.* and is strikingly similar to that of the already identified karlotoxins from *K. veneficum* and amphidinols of the dinoflagellate *Amphidinium klebsii*, with the difference that karmitoxin is longer (around 70 vs. 63-67 carbon atoms) and contains a primary amine group[18]. Like karlotoxins and amphidinols, karmitoxin conformation is that of a hairpin[53–56]. As for prymnesins, the lack of analytical standards hinders the proper quantification of this toxin. Thus, the indirect quantification using fumonisins B_1 and B_2 is applied for karmitoxin as well, which is only possible because of the presence of the aforementioned amine group[52].

3.2.2 Karmitoxin toxicity

Few studies on the adverse effects of karmitoxin exist, while the toxicity of karlotoxins is a much-investigated topic. Given their structural similarities, it can be assumed that karmitoxin exhibits similar

behavior when it comes in contact with a target cell. Evidence suggests that karlotoxins target fish gill cells via their affinity towards sterols[14,20,57]. Also amphidinols were shown to interact with membrane sterols such as ergosterol or cholesterol and cause pore-formation[58,59]. It is therefore likely that karmitoxin likewise exhibits high sterol affinity and antifungal activity. Rasmussen *et al*. showed that the cytotoxic and ichthyotoxic properties of karmitoxin were comparable to those of karlotoxin, with isolated karmitoxin in the nanomolar range achieving full cytotoxicity in RTgill-W1 cells and mortality of the copepod *Acartia tonsa*[18].

3.3 Cell lines

3.3.1 RTgill-W1

This cell line is derived from rainbow trout (*Oncorhynchus mykiss* (Walbaum)) gills. Primary cell cultures were cultivated with collagenase and sub-cultivated, to finally give rise to the new immortalized cell line RTgill-W1. These cells exhibit a polygonal shape and create a tightly packed monolayer, their nuclei are round to ellipsoid with patches of heterochromatin, while mitochondria are typically round and less abundant. RTgill-W1 cells show a high chromosomal variability yet have a dominant range from 105 to 120 chromosomes [60].

Cell lines such as RTgill-W1 are commonly used as an alternative to *in vivo* bioassays[61]. They offer a target-specific test system in which the MoA of ichthyotoxins can be investigated[61,62]. In June 2021, the Organisation for Economic Co-operation and Development (OECD) published a guideline for testing the acute toxicity of chemicals with the RTgill-W1 cell[63]. While the basic test principle is the same as those applied in the thesis, the exact procedure is different (e.g. 24 wells vs. 96 wells) due to limitation of available test material. Furthermore, for in-house comparability we stuck to our original protocols and did not switch to the OECD guideline for this project.

3.3.2 HCEC-1CT

This immortalized human epithelial cell line is derived from a healthy adult male donor. HCEC-1CT cells exhibit a cuboidal shape, and express colonic epithelial as well as stem cell markers, and retain the ability to differentiate into various epithelial lineages. Owing to their non-tumorigenic nature, HCEC-1CT cells can be applied for a multitude of investigations[64].

Some microalgal toxins are well known for their adverse effect on human health[1,5,65]. This cell line was selected for additional testing of prymnesins and karmitoxin as human exposure cannot be fully excluded. In the event of ingestion of water or aquatic food sources contaminated with these ichthyotoxins, however unlikely, it would be of interest to understand how the cells in the gastro-intestinal tract would respond. Moreover, this information can provide yet another puzzle piece to the toxicological profile of prymnesins and karmitoxin.

3.4 Cell membrane

The cell membrane consists of a bilayer (two leaflets) of phospholipids, embedded with glycolipids, sterols, and proteins[66–68]. Polar groups face the aqueous environments (intra- and extracellular compartments), whereas apolar groups make up the interior of the membrane. Due to this arrangement, membranes are deemed amphipathic[68–70]. The fluid nature of cell membranes was described by the mosaic model proposed by Singer and Nicolson, according to which membrane components can move laterally[70]. Depending on the type of membrane, cell, and species the constituents vary in their quantity. Cholesterol for instance is most abundant in the plasma membrane, followed by the Golgi, and least in the endoplasmic reticulum membrane, where it is synthesized. Another example is the protein-rich composition (75 %) of the inner membrane of mitochondria and bacterial membrane[68,69].

3.4.1 Lipids

The lipids found in biological membranes are sterols, phospholipids, and glycolipids. Importantly, the inner and outer leaflet compositions are not the same[68]. The exterior of the mammalian bilayer was found to be rich in the phospholipids sphingomyelin (a sphingophospholipid) and phosphatidyl-choline, while the interior contained more phosphatidylserine and phosphatidylethanolamine[67,68].

Typically, cell membranes possess a lipid domain, which is particularly rich in cholesterol and sphingolipids. These domains had been discovered for a while before receiving a proper definition in 2006[71]. Referred to as membrane rafts, these domains are usually between 10 and 200 nm large and are more tightly packed, dynamic, heterogeneous structures involved in membrane function[71,72]. The fluidity of the lipid domain is amongst others determined by the concentration and saturation of phospholipids[73].

Sterols are important for membrane structure as well as fluidity and permeability[74,75]. The major sterol of animal cells is cholesterol, while the main sterol found in fungi is ergosterol, which differs only slightly from cholesterol in its structure (Figure 5). In plants, sterol structures are usually more complex than their animal and fungal counterparts. Examples would be stigmasterol or brassicasterol[68,74,75]. Epicholesterol (Figure 5), the epimer of cholesterol with the C3 hydroxy group in α-position, does not occur naturally in membranes. Simply due to the orientation of this hydroxy group, epicholesterol does not exhibit the same behavior as cholesterol. When inserted into a synthetic membrane a 10-20 ° tilt was recorded, which limited its influence on membrane fluidity and disturbed the parallel packing of lipids in the bilayer[75].

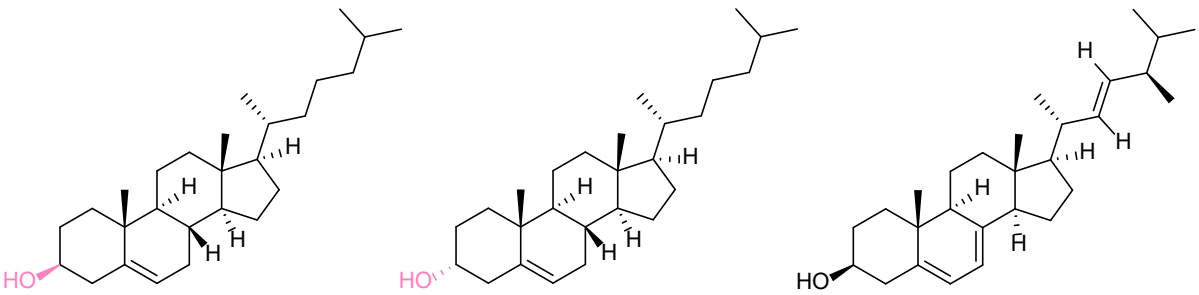

Figure 5 – Chemical structures of the animal cell sterol, cholesterol and its epimer epicholesterol, and the fungal sterol ergosterol.

Mammalian plasma membranes contain the majority of cellular cholesterol and sphingomyelin, and about half of the phospholipid content[76]. Human red blood cells (RBCs) have a particularly high cholesterol content as well as a larger amount of saturated lipids[66,67]. The cholesterol content in trout plasma membranes is dependent on temperature acclimation. The ratios of cholesterol to phospholipid in warm-acclimated fish were significantly higher than in cold-acclimated trout tissues, except in RBCs. Gill plasma membrane exhibited the highest cholesterol to phospholipid as well as cholesterol to protein-ratio[77].

3.4.2 Proteins

Membrane proteins are generally embedded in the membrane, often spanning from the cytoplasm to the extracellular side, and can exist within or outside the lipid rafts[70,72,73]. Lipid-protein and bilayer-protein interactions regulate membrane protein function, organization, and distribution. Their presence in the membrane allows for permeability, nutrient transport, and signaling[68,78].

Ion passage across the membrane is facilitated and regulated by ion channels and transporters, such as ATPases, cotransporters, or ion exchangers[79,80]. Passage through ion channels is generally considered to be of low energetic cost – passive – and dependent on external factors, while transport proteins are typically more selective and have to undergo conformational changes – at an energetic cost – in order to move ions across the membrane. This also enables transport against electrochemical gradients. Typically, hydrolysis of ATP is the main energy source for active transporters. Thus, transport capacities of ion channels are much larger than of transport proteins[79,81]. Some selective ion channels are voltage-gated, such as the Na^+, Ca^{2+}, and K^+ channels. These are essential for action potentials of neurons and other excitable cells[80–83]. For Na^+ and K^+ channels, permeating ions need to pass in a partially or completely dehydrated form, due to small pore sizes[80]. Non-selective channels, on the other hand, have larger pores allowing hydrated ions to pass[81].

3.5 Osmoregulation in fish gills

Maintaining cellular ion concentrations and water is fundamental to cell survival. For fish this means combating external osmotic pressures to preserve their internal homeostasis, which often comes with an energetic cost[84,85]. Freshwater teleost fishes, such as the rainbow trout (*O. mykiss*), for instance must counteract the influx of water and salt depletion, as their body fluids are hyperosmotic in comparison to their environment. The reverse is the case for marine teleosts, which live in a hyperosmotic environment and thus need to avoid salt loading[84,86–88]. Ion and water uptake occur primarily in the gills, which can be categorized into either pavement cells or mitochondria-rich ionocytes (or chloride cells)[85,88–91]. Pavement cells make up 90 % of epithelial cells in fish gills and are chiefly responsible for structural support. Ionocytes are the main site for ion transport, and house important transport proteins such as Na^+/K^+- and H^+-ATPases. Notably, studies have shown that ion regulation may also take place in pavement cells in freshwater teleosts. The exact mechanism of osmoregulation in these fishes is not fully understood and warrants further research[85,91–93]. Epithelial Ca^{2+} channels are proposed to be the main pathway for Ca^{2+} uptake. Na^+ uptake is likely facilitated by the H^+-ATPase linked to a Na^+ channel, or through the Na^+/H^+ exchanger. An NH_4^+-dependent Na^+ uptake was also suggested. Two models for Cl^- regulation were proposed, with the main pathway via Na^+/Cl^- cotransporters appearing more favorable, although a Cl^-/HCO_3^- exchange is still being debated[84,88,93].

The characteristic traits of pavement cells and ionocytes have not been detected in RTgill-W1 cells, probably because these derived from undifferentiated gill precursor stem cells[60,94]. Therefore, the osmoregulation of this cell line must inevitably differ to that of their *in-vivo* counterparts and should be kept in mind for interpreting results.

4 Overview of publications

Manuscript	*1*	*2*	*3*
Title	Cytotoxicity of *Prymnesium parvum* extracts and prymnesin analogs on epithelial fish gill cells RTgill-W1 and the human colon cell line HCEC-1CT	How relevant are sterols in the mode of action of prymnesins?	The cytotoxic and hemolytic potential of karmitoxin from *Karlodinium armiger* and how it interacts with sterols
Authors	Elisabeth Varga and **Hélène-Christine Prause**, Matthias Riepl, Nadine Hochmayr, Deniz Berk, Eva Attakpah, Endre Kiss, Nikola Medić, Giorgia Del Favero, Thomas Ostenfeld Larsen, Per Juel Hansen, Doris Marko	**Hélène-Christine Prause**, Deniz Berk, Catharina Alves-de-Souza, Per Juel Hansen, Thomas Ostenfeld Larsen, Doris Marko, Giorgia Del Favero, Allen Place, Elisabeth Varga	**Hélène-Christine Prause**, Nadine Hochmayr, Yanan Yu, Thomas Ostenfeld Larsen, Per Juel Hansen, Giorgia Del Favero, Doris Marko, Allen Place, Elisabeth Varga
Journal	Archives of Toxicology Volume 98, p. 999–1014	Aquatic Toxicology Volume 276, 107080	Harmful Algae Volume 143, 102817
Date received/submitted; accepted; published	27 October, 2023; 7 December 2023; 11 January, 2024	8 June, 2024; 2 September, 2024; 3 September, 2024	15 November, 2024; 7 February, 2025; 15 February, 2025
DOI	https://doi.org/10.1007/s00204-023-03663-5	https://doi.org/10.1016/j.aquatox.2024.107080	https://doi.org/10.1016/j.hal.2025.102817
Status	Published	Published	Published

4.1 Key findings of publications

4.1.1 Manuscript 1

In this study, *P. parvum* extracts and purified prymnesins were assessed for their cytotoxic effects on the RTgill-W1 and HCEC-1CT cells, and the potency of various analogs/prymnesin profiles was compared. Both cell lines exhibited a dose-dependent decrease in cell viability, which was highest for A-type prymnesins, followed by C-type, and lastly B-type prymnesins.

The concentrations were consistent in both cell lines, spanning from low (A- and C-type) to middle (B-type) nM ranges. This demonstrates that prymnesin toxicity is not limited to tissue derived from fish gills but could in theory also affect human health. The onset of cytotoxic effects was rapid, which could also be confirmed with live-cell imaging.

Moreover, the variability between toxicity of various extracts and the prymnesin analogs was emphasized. It was shown that the prymnesin profile expressed by strains of the same toxin-type can vary, ultimately affecting their toxic potential. It seems that the presence of specific analogs determines the potency to be expected. For instance, the analogs prymnesin-A (3 Cl) + 2 pentose + hexose and prymnesin-A (3 Cl) + pentose were considered responsible for the pronounced cytotoxicity of two different A-type prymnesin samples.

Lastly, it was highlighted that prymnesin toxicity is coupled with an osmotic imbalance caused in the target cell. Cl^- and Ca^{2+} seem to be particularly involved in this process in RTgill-W1 cells, as Ca^{2+} removal in the medium environment exacerbated the effects, while Cl^- removal was able to reduce the morphological changes caused by prymnesin exposure. Interestingly, toxicity on HCEC-1CT cells was not affected by the removal of neither Ca^{2+} nor Na^+, however, removal of Cl^- decreased the cytotoxic potential.

Overall, it was shown that the analog profile of *P. parvum* potentially dictates their toxicity, which seems to be intertwined with dysregulation of the cellular osmosis, particularly where Cl^- and Ca^{2+} are involved.

4.1.2 Manuscript 2

This project aimed at shedding light on the interactions between prymnesins and sterols present in the target cell membrane. It was hypothesized that prymnesins can cause cell lysis through binding with sterols, and thus creating a pore, destabilizing the cellular osmoregulation. Extracts from A-, B-, and C-type strains were evaluated for their cytotoxic and hemolytic potential in RTgill-W1 cells and red blood cells (RBCs) from Atlantic salmon (*Salmo salar*).

Also in this study, the relevance of specific prymnesin analogs was highlighted. The order of potency observed in cytotoxic studies could be reproduced in RBCs, however, the potency differences between these two cell types were significant. The HC_{50}[1] of the C-type extract was approximately 5-fold higher than the concentration needed for 50 % cytotoxicity in RTgill-W1 cells, and the HC_{50} of the B-type extract was 10-fold higher. Curiously, both tested A-type extracts were only 1.5- to 2-fold less potent in RBCs. This result warrants further research, specifically regarding the composition of cellular membranes of target cells. It has been shown previously that the origin of RBC can affect prymnesin potency, which seems to underline the importance of membrane structure for prymnesin toxicity. This outcome is also an indication of mechanical differences in the way in which A-, B-, or C-type prymnesins cause lysis.

It was shown that addition of sterols to the medium prior to starting the hemolysis assay could significantly reduce the expected hemolysis. This observation is hypothesized to be caused by prymnesins forming complexes with the free sterols, rendering the prymnesins unavailable to target the RBCs. Interestingly, the decrease in expected hemolysis was not dependent on the concentration of added sterol, and an additional drop in hemolysis was only observed for the A-type extracts. This outcome raises the important question of whether the interactions between target membrane and toxin are different between the three types of prymnesins.

A variance in sterol interactions was also confirmed by surface plasmon resonance (SPR) measurements, where the dissociation rate from complexes between A- and B-type extracts with selected sterols was evaluated. The curve fit was calculated using the 1:1 model, which the B-type extract seemed to follow much better, with lower Chi^2 (model fit) values, than the A-type prymnesin extract. This indicates that A-type prymnesins likely do not follow a single exponential decay from sterols. Importantly, cellular cholesterol modulation of RTgill-W1 cells showed that cholesterol, or at least the absolute cholesterol content of the target cells, is not the determining factor of prymnesin toxicity.

In summary, this study highlights the complexity of the prymnesin MoA. Cellular cholesterol may be crucial for targeting the cell, yet the ensuing cell lysis may be caused by different mechanisms. Importantly, A-, B-, and C-type prymnesins might not follow the same exact mode of action.

[1] Hemolytic concentration 50: Concentration at which 50 % of RBCs are lysed

4.1.3 Manuscript 3

The cytotoxic and hemolytic activity of karmitoxin was assessed in this project, using both the RTgill-W1 and the HCEC-1CT cell line, as well as RBCs of Atlantic salmon (*Salmo salar*). Incubation times of 3 and 24 h were tested, and lastly the role of sterols was assessed.

Karmitoxin exhibited rapid dose-dependent cytotoxicity in both cell lines, although the human HCEC-1CT cell line was less susceptible. Longer incubation times (24 h) showed that lower concentrations of karmitoxin likely trigger cell-repair mechanisms, which could overcome the adversity of the toxin. However, once a certain concentration threshold was passed, the potency was much more pronounced. This was also reflected in the lytic damage recorded for these cell lines, where lactate dehydrogenase (LDH) leakage only increased significantly at higher concentrations.

The hemolytic potential of karmitoxin proved to be comparable to that of karlotoxin, as well as its cytotoxic potency. The observed HC_{50} was about 160 nM. An addition of free cholesterol or epicholesterol prior to starting the hemolysis assay reduced the expected hemolysis to approximately 0 %. Modulation of cholesterol in RTgill-W1 cells, on the other hand, had no effect on the expected cytotoxicity.

SPR measurements for complex dissociation showed that karmitoxin formed the most stable complex with ergosterol, which indicates that karmitoxin most likely possesses antifungal properties. By comparing the model fit (1:1 model) for the dissociation rate, it could be argued that karmitoxin follows a 2-step dissociation from epicholesterol and ergosterol, but not from cholesterol.

To conclude, karmitoxin was shown to be a potent hemolysin and cytotoxic agent in RTgill-W1 and HCEC-1CT cells, with potencies comparable to the structurally related karlotoxins. Ther affinity for sterols is also in accordance with previous findings for karlotoxins and amphidinols. In order to provide a full picture of the toxic mechanism of karmitoxin, further research focusing on membrane interactions and cellular changes is necessary.

4.1.4 Summary of key findings and conclusions

Prymnesins and karmitoxin are potent cytotoxic and hemolytic microalgal allelochemicals. It was shown that their adverse effects are not limited to fish gill cells but can also affect human cells. Generally, their cytotoxic potential is similar to their hemolytic potency, however, for prymnesins the EC_{50} values increased significantly for B- and C-types. Both karmitoxin and prymnesins exhibited strong affinities towards cholesterol, epicholesterol, and ergosterol in SPR measurements. Complexing with sterols was seemingly also achieved during hemolytic assays adding free sterols to the ichthyotoxins. Nonetheless, modification of the cellular cholesterol content of RTgill-W1 cells did not impact cytotoxicity for the tested compounds.

To summarize, new aspects regarding prymnesin MoA could be uncovered. The importance of analog-type for the toxicity of a *P. parvum* strain was highlighted, and a distinction between the potency of A-, B-, or C-type prymnesins could be drawn. In addition, it was shown that the prymnesin types likely differ in the way in which they target cellular membranes. The dinoflagellate toxin karmitoxin was found to be highly cytotoxic and lytic, with a clear affinity for sterols. Sterol complex-formation with karmitoxin seems to be similar to that of karlotoxins and amphidinols.

5 Discussion

In order to fully appreciate the relevance of the ichthyotoxins of *P. parvum* and *K. armiger*, a comprehensive characterization of their MoAs, target organs, acute and chronic effects, and dose-response relationships is needed. With this work we aimed to provide insight into the MoA, specifically the interaction with the target cell membrane.

The results acquired in this project support previous findings. For one, the quick onset of adverse effects recorded in this study is in line with the suggested ecological purpose: Prymnesins can kill competing microalgae[95], and supposedly even aid *P. parvum* in its food uptake by immobilizing and lysing target cells[96]. In some *Karlodinium* spp. the production of allelochemicals provides protection against grazers[3,47,48,97–99] and karlotoxin can increase predation of *K. veneficum*[100]. It can be inferred that karmitoxin has a similar function for *K. armiger*.

Secondly, prymnesins and karmitoxin display a high affinity for sterols, including ergosterol, implying antifungal properties. The main membrane sterol of *K. veneficum* was discovered to be gymnodinosterol, to which karlotoxin showed no affinity[14]. This phenomenon is likely a protection system of the microalga against its own toxin. Considering the similarity of *K. veneficum* and *K. armiger*, it is likely that the latter also employs this protection method. Ghosh *et al.* reported very low sterol concentrations in *P. parvum* cells, which could likewise be interpreted as a protection against prymnesins[101]. Our findings together with previous data underline the importance of sterols in the toxic MoA of prymnesins and karmitoxin. When comparing the karmitoxin data acquired here to amphidinols, it can be speculated that the way in which karmitoxin forms complexes with membrane sterols is similar to the 2-step binding described for amphidinols[59]. Before debating the role of sterols in the prymnesin toxicity, it should be acknowledged that A-, B-, and C-type prymnesins probably follow distinct MoAs. This could be attributed to their structural differences. As an example, for the dinoflagellate toxins it is assumed that the hairpin formation is relevant to the MoA[55,102]. Considering that the stereochemistry for prymnesins has not been fully explored, especially in relation to characteristics of the three types, no conclusions can be drawn about their interaction with sterols. This area requires further research and would undoubtedly help comprehend the difference in cytotoxic and especially hemolytic potential. We speculate that sterol complexing between the three prymnesin types is responsible for type-specific potency.

Nonetheless, as evidenced by the modulation of RTgill-W1 cell cholesterol levels, sterol affinity seems to be only one aspect of membrane interaction, likely coupled with one or more additional factors. As observed for karmitoxin, the rapid onset of toxic effects *in-vitro* could apparently be counteracted by cellular repair mechanisms when given enough time. An increase in the EC_{50} indicates that the cells actively protected themselves against the adverse effects, possibly by modifying the cellular membrane, actively resisting lysis or upregulating their pathways. A modification of the membrane in order to protect from the toxin would only be useful if the toxin required specific membrane interactions. Again, since modulation of RTgill-W1 cholesterol did not change the cytotoxicity, we must look to other membrane constituents for answers. Assessing the lipid profile of the target cells before and after toxin-exposure may provide yet another puzzle piece. Membrane fluidity studies could also provide important insights into the bilayer integrity upon toxin exposure.

Other features to consider are the influence prymnesins and karmitoxin can have on cells at the molecular scale. Promising areas of research include cytoskeleton involvement, membrane repair, and especially ionoregulation. Understanding the connection to ionoregulation and disruption of cellular homeostasis presents an appropriate starting point for future analyses. The next question to answer is whether osmotic dysregulation is simply a consequence of the pore created or whether membrane proteins involved in osmoregulation are targeted specifically by these ichthyotoxins. As tentatively investigated for prymnesins here, dysregulation of cellular homeostasis through interference with ion channels or transporters seems a likely contender. It would be useful to assess the involvement of ion channels/transporters in the MoA, for instance by blocking specific transport regulators and subsequently measure ichthyotoxin potency.

To conclude, the MoA of prymnesins and karmitoxin is more intricate than hypothesized. Pore-formation and subsequent lysis are likely the result of a succession of steps in which sterol affinity is only one of the steps deciding the fate of the cell. Other mechanisms, either in combination with sterol complexion or as its consequence must therefore be equally relevant.

Future research should focus on the involvement of ion transporters and ionoregulation. Furthermore, assessing effects on the molecular level can greatly aid the understanding of prymnesin and karmitoxin toxicity. Important aspects to consider would be changes in cell signaling and repair mechanisms. An evaluation of the stereochemistry of A-, B-, and C-type prymnesins is essential for sterol interaction studies and could prove valuable for researching the MoA of prymnesins.

6 References

(1) Hallegraeff, G. M. A Review of Harmful Algal Blooms and Their Apparent Global Increase. *Phycologia* **1993**, *32* (2), 79–99. https://doi.org/10.2216/I0031-8884-32-2-79.1.

(2) Legrand, C.; Rengefors, K.; Fistarol, G. O.; Granéli, E. Allelopathy in Phytoplankton - Biochemical, Ecological and Evolutionary Aspects. *Phycologia* **2003**, *42* (4), 408–419. https://doi.org/10.2216/I0031-8884-42-4-406.1.

(3) Smayda, T. J. Harmful Algal Blooms: Their Ecophysiology and General Relevance to Phytoplankton Blooms in the Sea. *Limnol Oceanogr* **1997**, *42* (5part2), 1137–1153. https://doi.org/10.4319/LO.1997.42.5_PART_2.1137.

(4) Wolfe, G. V. The Chemical Defense Ecology of Marine Unicellular Plankton: Constraints, Mechanisms, and Impacts. *Biol Bull* **2000**, *198* (2), 225–244. https://doi.org/10.2307/1542526.

(5) Sanseverino, I.; Conduto, D.; Pozzoli, L.; Dobricic, S.; Lettieri, T. Algal Bloom and Its Economic Impact. *EUR 27905 EN* **2016**. https://doi.org/10.2788/660478.

(6) Daneshian, M.; Botana, L. M.; Bottein, M. Y. D.; Buckland, G.; Campàs, M.; Dennison, N.; Dickey, R. W.; Diogène, J.; Fessard, V.; Hartung, T.; Humpage, A.; Leist, M.; Molgó, J.; Quilliam, M. A.; Rovida, C.; Suarez-Isla, B. A.; Tubaro, A.; Wagner, K.; Zoller, O.; Dietrich, D. A Roadmap for Hazard Monitoring and Risk Assessment of Marine Biotoxins on the Basis of Chemical and Biological Test Systems. *ALTEX* **2013**, *30* (4), 487–545. https://doi.org/10.14573/ALTEX.2013.4.487.

(7) Hoagland, P.; Anderson, D. M.; Kaoru, Y.; White, A. W. The Economic Effects of Harmful Algal Blooms in the United States: Estimates, Assessment Issues, and Information Needs. *Estuaries* **2002**, *25* (4), 819–837. https://doi.org/10.1007/BF02804908.

(8) Granéli, E.; Hansen, P. J. Allelopathy in Harmf Algae: A Mechanism to Compete for Resources? *Ecol Harm Alg* **2006**, 189–201. https://doi.org/https://doi.org/10.1007/978-3-540-32210-8_15.

(9) Free, G.; Van de Bund, W.; Gawlik, B.; Van Wijk, L.; Wood, M.; Guagnini, E.; Koutelos, K.; Annunziato, A.; Grizzetti, B.; Vigiak, O.; Gnecchi, M.; Poikane, S.; Christiansen, T.; Whalley, C.; Antognazza, F.; Zerger, B.; Hoeve, R. J.; Stielstra, H. An EU Analysis of the Ecological Disaster in the Oder River of 2022. *Publications Office of the European Union: Luxembourg* **2023**. https://doi.org/10.2760/067386.

(10) Igarashi, T.; Satake, M.; Yasumoto, T. Prymnesin-2: A Potent Ichthyotoxic and Hemolytic Glycoside Isolated from the Red Tide Alga *Prymnesium parvum*. *JACS* **1996**, *118* (2), 479–480. https://doi.org/10.1021/ja9534112.

(11) Rasmussen, S. A.; Meier, S.; Andersen, N.; Blossom, H. E.; Duus, J. Ø.; Nielsen, K. F.; Hansen, P. J.; Larsen, T. O. Chemodiversity of Ladder-Frame Prymnesin Polyethers in *Prymnesium parvum*. *J Nat Prod* **2016**, *79* (9), 2250–2256. https://doi.org/10.1021/acs.jnatprod.6b00345.

(12) Manning, S. R.; La Claire, J. W. Prymnesins: Toxic Metabolites of the Golden Alga, *Prymnesium parvum* Carter (Haptophyta). *Mar Drugs* **2010**, *8* (3), 678–704. https://doi.org/10.3390/MD8030678.

(13) Svenssen, D. K.; Binzer, S. B.; Medić, N.; Hansen, P. J.; Larsen, T. O.; Varga, E. Development of an Indirect Quantitation Method to Assess Ichthyotoxic B-Type Prymnesins from *Prymnesium parvum*. *Toxins* **2019**, *11* (5), 251. https://doi.org/10.3390/toxins11050251.

(14) Deeds, J.; Place, A. Sterol-Specific Membrane Interactions with the Toxins from *Karlodinium Micrum* (Dinophyceae) – a Strategy for Self-Protection? *Afr J Mar Sci* **2006**, *28* (2), 421–425. https://doi.org/10.2989/18142320609504190.

(15) Deeds, J. R.; Terlizzi, D. E.; Adolf, J. E.; Stoecker, D. K.; Place, A. R. Toxic Activity from Cultures of *Karlodinium Micrum* (=*Gyrodinium Galatheanum*) (Dinophyceae)—a Dinoflagellate Associated with Fish Mortalities in an Estuarine Aquaculture Facility. *Harmf Algae* **2002**, *1* (2), 169–189. https://doi.org/10.1016/S1568-9883(02)00027-6.

(16) Garcés, E.; Fernandez, M.; Penna, A.; Van Lenning, K.; Gutierrez, A.; Camp, J.; Zapata, M. Characterization of Nw [New] Mediterranean *Karlodinium* Spp. (Dinophyceae) Strains Using Morphological, Chemical, and

Physiological Methodologies. *J Phycol* **2006**, *42* (5), 1096–1112. https://doi.org/10.1111/j.1529-8817.2006.00270.x.

(17) Bergholtz, T.; Daugbjerg, N.; Moestrup, Ø.; Fernández-Tejedor, M. On the Identity of *Karlodinium Veneficum* and Description of *Karlodinium Armiger* Sp. Nov. (Dinophyceae), Based on Light and Electron Microscopy, Nuclear-Encoded LSU RDNA, and Pigment Composition. *J Phycol* **2006**, *42* (1), 170–193. https://doi.org/10.1111/j.1529-8817.2006.00172.x.

(18) Rasmussen, S. A.; Binzer, S. B.; Hoeck, C.; Meier, S.; De Medeiros, L. S.; Andersen, N. G.; Place, A.; Nielsen, K. F.; Hansen, P. J.; Larsen, T. O. Karmitoxin: An Amine-Containing Polyhydroxy-Polyene Toxin from the Marine Dinoflagellate *Karlodinium Armiger*. *J Nat Prod* **2017**, *80* (5), 1287–1293. https://doi.org/10.1021/acs.jnatprod.6b00860.

(19) Tillmann, U. Kill and Eat Your Predator: A Winning Strategy of the Planktonic Flagellate *Prymnesium parvum*. *Aquat Microb Ecol* **2003**, *32* (1), 73–84. https://doi.org/10.3354/AME032073.

(20) Place, A. R.; Ramos-Franco, J.; Waters, A. L.; Peng, J.; Hamann, M. T. Sterolysin from a 1950s Culture of *Karlodinium Veneficum* (Aka *Gymnodinium Veneficum* Ballantine) Forms Lethal Sterol Dependent Membrane Pores. *Sci Rep* **2024**, *14* (1), 17998. https://doi.org/10.1038/s41598-024-68669-0.

(21) Kaartvedt, S.; Johnsen, T. M.; Aksnes, D. L.; Lie, U.; Svendsen, H. Occurrence of the Toxic Phytoflagellate *Prymnesium parvum* and Associated Fish Mortality in a Norwegian Fjord System. *Can J Fish Aquat Sci* **1991**, *48* (12), 2316–2323. https://doi.org/10.1139/f91-272.

(22) Roelke, D. L.; Grover, J. P.; Brooks, B. W.; Joanglass; Davidbuzan; Southard, G. M.; Lorainefries; Gable, G. M.; Schwierzke-Wade, L.; Meridithbyrd; Janetnelson. A Decade of Fish-Killing *Prymnesium parvum* Blooms in Texas: Roles of Inflow and Salinity. *J Plankton Res* **2011**, *33* (2), 243–253. https://doi.org/10.1093/PLANKT/FBQ079.

(23) Otterstrøm, C. V.; Nielsen, S. Two Cases of Extensive Mortality in Fishes Caused by the Flagellate *Prymnesium parvum*. *Rep Dan Biol* **1939**, *44*, 5–24.

(24) Granéli, E.; Salomon, P. S. Factors Influencing Allelopathy and Toxicity in *Prymnesium parvum*. *JAWRA* **2010**, *46* (1), 108–120. https://doi.org/10.1111/J.1752-1688.2009.00395.X.

(25) Shilo, M. Formation and Mode of Action of Algal Toxins. *Bacteriol Rev* **1967**, *31* (3), 180–193. https://doi.org/https://doi.org/10.1128/br.31.3.180-193.1967.

(26) Franco, M. E.; Hill, B. N.; Brooks, B. W.; Lavado, R. *Prymnesium parvum* Differentially Triggers Sublethal Fish Antioxidant Responses *in Vitro* among Salinity and Nutrient Conditions. *Aquat Toxicol* **2019**, *213*, 105214. https://doi.org/10.1016/j.aquatox.2019.05.016.

(27) Hill, B. N.; Saari, G. N.; Steele, W. B.; Corrales, J.; Brooks, B. W. Nutrients and Salinity Influence *Prymnesium parvum* (UTEX LB 2797) Elicited Sublethal Toxicity in *Pimephales Promelas* and *Danio Rerio*. *Harmf Algae* **2020**, *93*, 101795. https://doi.org/10.1016/j.hal.2020.101795.

(28) Taylor, R. B.; Hill, B. N.; Langan, L. M.; Chambliss, C. K.; Brooks, B. W. Sunlight Concurrently Reduces *Prymnesium parvum* Elicited Acute Toxicity to Fish and Prymnesins. *Chemosphere* **2021**, *263*, 127927. https://doi.org/10.1016/j.chemosphere.2020.127927.

(29) Valenti, T. W.; James, S. V.; Lahousse, M. J.; Schug, K. A.; Roelke, D. L.; Grover, J. P.; Brooks, B. W. A Mechanistic Explanation for PH-Dependent Ambient Aquatic Toxicity of *Prymnesium parvum* Carter. *Toxicon* **2010**, *55* (5), 990–998. https://doi.org/10.1016/j.toxicon.2009.09.014.

(30) Yariv, J.; Hestrin, S. Toxicity of the Extracellular Phase of *Prymnesium parvum* Cultures. *J Gen Microbiol* **1961**, *24* (2), 165–175. https://doi.org/10.1099/00221287-24-2-165.

(31) Binzer, S. B.; Svenssen, D. K.; Daugbjerg, N.; Alves-de-Souza, C.; Pinto, E.; Hansen, P. J.; Larsen, T. O.; Varga, E. A-, B- and C-Type Prymnesins Are Clade Specific Compounds and Chemotaxonomic Markers in *Prymnesium parvum*. *Harmf Algae* **2019**, *81*, 10–17. https://doi.org/10.1016/j.hal.2018.11.010.

(32) Igarashi, T.; Satake, M.; Yasumoto, T. Structures and Partial Stereochemical Assignments for Prymnesin-1 and Prymnesin-2: Potent Hemolytic and Ichthyotoxic Glycosides Isolated from the Red Tide Alga *Prymnesium parvum*. *JACS* **1999**, *121* (37), 8499–8511. https://doi.org/10.1021/ja991740e.

(33) Blossom, H. E.; Rasmussen, S. A.; Andersen, N. G.; Larsen, T. O.; Nielsen, K. F.; Hansen, P. J. *Prymnesium parvum* Revisited: Relationship between Allelopathy, Ichthyotoxicity, and Chemical Profiles in 5 Strains. *Aquat Toxicol* **2014**, *157*, 159–166. https://doi.org/10.1016/J.AQUATOX.2014.10.006.

(34) Shilo, M. The Toxic Principles of *Prymnesium parvum*. In *The Water Environment*; Springer US: Boston, MA, 1981; pp 37–47. https://doi.org/10.1007/978-1-4613-3267-1_4.

(35) Ulitzur, S. The Amphiphatic Nature of *Prymnesium parvum* Hemolysin. *Biochimica et Biophysica Acta (BBA) - Biomembranes* **1973**, *298* (3), 673–679. https://doi.org/10.1016/0005-2736(73)90083-7.

(36) Ulitzur, S.; Shilo, M. Mode of Action of *Prymnesium parvum* Ichthyotoxin. *J Protozool* **1966**, *13* (2), 332–336. https://doi.org/10.1111/J.1550-7408.1966.TB01915.X.

(37) Svendsen, M. B. S.; Andersen, N. R.; Hansen, P. J.; Steffensen, J. F. Effects of Harmful Algal Blooms on Fish: Insights from *Prymnesium parvum*. *Fishes* **2018**, *3* (1), 11. https://doi.org/10.3390/FISHES3010011.

(38) Igarashi, T.; Aritake, S.; Yasumoto, T. Biological Activities of Prymnesin-2 Isolated from a Red Tide Alga *Prymnesium parvum*. *Nat Tox* **1998**, *6* (1), 35–41. https://doi.org/10.1002/(SICI)1522-7189(199802)6:1<35::AID-NT7>3.0.CO;2-7.

(39) Moran, A.; Ilani, A. The Effect of Prymnesin on the Electric Conductivity of Thin Lipid Membranes. *J. Membrane Biol* **1974**, *16*, 237–256. https://doi.org/10.1007/BF01872417.

(40) Imai, M.; Inoue, K. The Mechanism of Action of *Prymnesium* Toxin on Membranes. *Biochim Biophys Acta* **1974**, *352*, 344–348. https://doi.org/10.1016/0005-2736(74)90226-0.

(41) Ulitzur, S.; Shilo, M. A Sensitive Assay System for Determination of the Ichthyotoxicity of *Prymnesium parvum*. *J Gen Microbial* **1964**, *36*, 161–169. https://doi.org/10.1099/00221287-36-2-161.

(42) Lim, H. C.; Leaw, C. P.; Tan, T. H.; Kon, N. F.; Yek, L. H.; Hii, K. S.; Teng, S. T.; Razali, R. M.; Usup, G.; Iwataki, M.; Lim, P. T. A Bloom of *Karlodinium Australe* (Gymnodiniales, Dinophyceae) Associated with Mass Mortality of Cage-Cultured Fishes in West Johor Strait, Malaysia. *Harmf Algae* **2014**, *40*, 51–62. https://doi.org/10.1016/j.hal.2014.10.005.

(43) Kempton, J. W.; Lewitus, A. J.; Deeds, J. R.; Law, J. M.; Place, A. R. Toxicity of *Karlodinium Micrum* (Dinophyceae) Associated with a Fish Kill in a South Carolina Brackish Retention Pond. *Harmf Algae* **2002**, *1* (2), 233–241. https://doi.org/10.1016/S1568-9883(02)00015-X.

(44) de Salas, M. F. de S.; Bolch, C. J. S.; Hallegraeff, G. M. *Karlodinium Australe* Sp. Nov. (Gymnodiniales, Dinophyceae), a New Potentially Ichthyotoxic Unarmoured Dinoflagellate from Lagoonal Habitats of South-Eastern Australia. *Phycologia* **2005**, *44* (6), 640–650. https://doi.org/10.2216/0031-8884(2005)44[640:KASNGD]2.0.CO;2.

(45) Abbott, B. C.; Ballantine, D. The Toxin from *Gymnodinium Veneficum* Ballantine. *J Mar Biol Assoc U.K.* **1957**, *36* (1), 169–189. https://doi.org/10.1017/S0025315400017173.

(46) Berge, T.; Poulsen, L. K.; Moldrup, M.; Daugbjerg, N.; Juel Hansen, P. Marine Microalgae Attack and Feed on Metazoans. *ISME* **2012**, *6* (10), 1926–1936. https://doi.org/10.1038/ismej.2012.29.

(47) Place, A. R.; Bowers, H. A.; Bachvaroff, T. R.; Adolf, J. E.; Deeds, J. R.; Sheng, J. *Karlodinium Veneficu*m—The Little Dinoflagellate with a Big Bite. *Harmf Algae* **2012**, *14*, 179–195. https://doi.org/10.1016/j.hal.2011.10.021.

(48) Adolf, J. E.; Krupatkina, D.; Bachvaroff, T.; Place, A. R. Karlotoxin Mediates Grazing by *Oxyrrhis Marina* on Strains of *Karlodinium Veneficum*. *Harmf Algae* **2007**, *6* (3), 400–412. https://doi.org/10.1016/j.hal.2006.12.003.

(49) Berge, T.; Hansen, P.; Moestrup, Ø. Feeding Mechanism, Prey Specificity and Growth in Light and Dark of the Plastidic Dinoflagellate *Karlodinium Armiger*. *Aquat Microb Ecol* **2008**, *50*, 279–288. https://doi.org/10.3354/ame01165.

(50) Li, A.; Stoecker, D.; Adolf, J. Feeding, Pigmentation, Photosynthesis and Growth of the Mixotrophic Dinoflagellate *Gyrodinium Galatheanum*. *Aquat Microb Ecol* **1999**, *19*, 163–176. https://doi.org/10.3354/ame019163.

(51) Binzer, S. B.; Varga, E.; Andersen, A. J. C.; Svenssen, D. K.; de Medeiros, L. S.; Rasmussen, S. A.; Larsen, T. O.; Hansen, P. J. Karmitoxin Production by *Karlodinium Armiger* and the Effects of *K. Armiger* and Karmitoxin towards Fish. *Harmf Algae* **2020**, *99*, 101905. https://doi.org/10.1016/j.hal.2020.101905.

(52) Andersen, A.; de Medeiros, L.; Binzer, S.; Rasmussen, S.; Hansen, P.; Nielsen, K.; Jørgensen, K.; Larsen, T. HPLC-HRMS Quantification of the Ichthyotoxin Karmitoxin from *Karlodinium Armiger*. *Mar Drugs* **2017**, *15* (9), 278. https://doi.org/10.3390/md15090278.

(53) Satake, M.; Murata, M.; Yasumoto, T.; Fujita, T.; Naoki, H. Amphidinol. a Polyhydroxypolyene Antifungal Agent with an Unprecedented Structure, from a Marine Dinoflagellate, *Amphidinium Klebsii*. *JACS* **1991**, *113* (26), 9859–9861. https://doi.org/10.1021/ja00026a027.

(54) Van Wagoner, R. M.; Deeds, J. R.; Satake, M.; Ribeiro, A. A.; Place, A. R.; Wright, J. L. C. Isolation and Characterization of Karlotoxin 1, a New Amphipathic Toxin from *Karlodinium Veneficum*. *Tetrahedron Lett* **2008**, *49* (45), 6457–6461. https://doi.org/10.1016/j.tetlet.2008.08.103.

(55) Waters, A. L.; Oh, J.; Place, A. R.; Hamann, M. T. Stereochemical Studies of the Karlotoxin Class Using NMR Spectroscopy and DP4 Chemical-Shift Analysis: Insights into Their Mechanism of Action. *Angew Chem* **2015**, *127* (52), 15931–15936. https://doi.org/10.1002/ange.201507418.

(56) Peng, J.; Place, A. R.; Yoshida, W.; Anklin, C.; Hamann, M. T. Structure and Absolute Configuration of Karlotoxin-2, an Ichthyotoxin from the Marine Dinoflagellate *Karlodinium Veneficum*. *JACS* **2010**, *132* (10), 3277–3279. https://doi.org/10.1021/ja9091853.

(57) Place, A. R.; Bai, X.; Kim, S.; Sengco, M. R.; Coats, D. W. Dinoflagellate Host-Parasite Sterol Profiles Dictate Karlotoxin Sensitivity. *J Phycol* **2009**, *45* (2), 375–385. https://doi.org/10.1111/J.1529-8817.2009.00649.X.

(58) Swasono, R. T.; Mouri, R.; Morsy, N.; Matsumori, N.; Oishi, T.; Murata, M. Sterol Effect on Interaction between Amphidinol 3 and Liposomal Membrane as Evidenced by Surface Plasmon Resonance. *Bioorg Med Chem Lett* **2010**, *20* (7), 2215–2218. https://doi.org/https://doi.org/10.1016/J.BMCL.2010.02.025.

(59) Matsumori, N.; Hieda, M.; Morito, M.; Wakamiya, Y.; Oishi, T. Truncated Derivatives of Amphidinol 3 Reveal the Functional Role of Polyol Chain in Sterol-Recognition and Pore Formation. *Bioorg Med Chem Lett* **2024**, *98*, 129594. https://doi.org/https://doi.org/10.1016/j.bmcl.2023.129594.

(60) Bols, N. C.; Barlian, A.; Chirino-Trejo, M.; Caldwell, S. J.; Goegan, P.; Lee, L. E. J. Development of a Cell Line from Primary Cultures of Rainbow Trout, *Oncorhynchus Mykiss (Walbaum)*, Gills. *J Fish Dis* **1994**, *17* (6), 601–611. https://doi.org/10.1111/j.1365-2761.1994.tb00258.x.

(61) Segner, H. Fish Cell Lines as a Tool in Aquatic Toxicology. In *Fish Ecotoxicology*; EXS: Birkhäuser, Basel, 1998; Vol. 86, pp 1–38. https://doi.org/https://doi.org/10.1007/978-3-0348-8853-0_1.

(62) Fischer, M.; Belanger, S. E.; Berckmans, P.; Bernhard, M. J.; Bláha, L.; Coman Schmid, D. E.; Dyer, S. D.; Haupt, T.; Hermens, J. L. M.; Hultman, M. T.; Laue, H.; Lillicrap, A.; Mlnaříková, M.; Natsch, A.; Novák, J.; Sinnige, T. L.; Tollefsen, K. E.; von Niederhäusern, V.; Witters, H.; Županič, A.; Schirmer, K. Repeatability and Reproducibility of the RTgill-W1 Cell Line Assay for Predicting Fish Acute Toxicity. *Toxicol Sci* **2019**, *169* (2), 353–364. https://doi.org/10.1093/toxsci/kfz057.

(63) OECD. *Test No. 249: Fish Cell Line Acute Toxicity-The RTgill-W1 Cell Line Assay.*; 2021. https://doi.org/https://doi.org/10.1787/c66d5190-en.

(64) Roig, A. I.; Eskiocak, U.; Hight, S. K.; Kim, S. B.; Delgado, O.; Souza, R. F.; Spechler, S. J.; Wright, W. E.; Shay, J. W. Immortalized Epithelial Cells Derived From Human Colon Biopsies Express Stem Cell Markers and Differentiate In Vitro. *J Gastroenterol* **2010**, *138* (3), 1012-1021.e5. https://doi.org/https://doi.org/10.1053/j.gastro.2009.11.052.

(65) Benson, J. M.; Tischler, D. L. Uptake, Tissue Distribution, and Excretion of Brevetoxin 3 Administered to Rats by Intratracheal Instillation. *J Toxicol Environ Health A* **1999**, *57* (5), 345–355. https://doi.org/https://doi.org/10.1080/009841099157656.

(66) O'Brien, J. S. Cell Membranes—Composition: Structure: Function. *J Theor Biol* **1967**, *15* (3), 307–324. https://doi.org/10.1016/0022-5193(67)90140-3.

(67) Bretscher, M. S. Asymmetrical Lipid Bilayer Structure for Biological Membranes. *Nat New Biol* **1972**, *236* (61), 11–12. https://doi.org/10.1038/newbio236011a0.

(68) Watson, H. Biological Membranes. *Essays Biochem* **2015**, *59*, 43–69. https://doi.org/10.1042/bse0590043.

(69) Guidotti, G. Membrane Proteins. *Annu Rev Biochem* **1972**, *41* (1), 731–752. https://doi.org/10.1146/annurev.bi.41.070172.003503.

(70) Singer, S. J.; Nicolson, G. L. The Fluid Mosaic Model of the Structure of Cell Membranes. *Science* **1972**, *175* (4023), 720–731. https://doi.org/10.1126/science.175.4023.720.

(71) Pike, L. J. Rafts Defined: A Report on the Keystone Symposium on Lipid Rafts and Cell Function. *J Lipid Res* **2006**, *47* (7), 1597–1598. https://doi.org/10.1194/jlr.E600002-JLR200.

(72) Simons, K.; Ehehalt, R. Cholesterol, Lipid Rafts, and Disease. *J Clin Investig* **2002**, *110* (5), 597–603. https://doi.org/10.1172/JCI16390.

(73) Smith, J. E. Erythrocyte Membrane: Structure, Function, and Pathophysiology. *Vet Pathol* **1987**, *24* (6), 471–476. https://doi.org/10.1177/030098588702400601.

(74) Schaller, H. The Role of Sterols in Plant Growth and Development. *Prog Lipid Res* **2003**, *42* (3), 163–175. https://doi.org/10.1016/S0163-7827(02)00047-4.

(75) Dufourc, E. J. Sterols and Membrane Dynamics. *J Chem Biol* **2008**, *1* (1–4), 63–77. https://doi.org/10.1007/s12154-008-0010-6.

(76) Lange, Y.; Swaisgood, M. H.; Ramos, B. V; Steck, T. L. Plasma Membranes Contain Half the Phospholipid and 90% of the Cholesterol and Sphingomyelin in Cultured Human Fibroblasts. *J Biol Chem* **1989**, *264* (7), 3786–3793. https://doi.org/10.1016/S0021-9258(19)84918-9.

(77) Robertson, J. C.; Hazel, J. R. Cholesterol Content of Trout Plasma Membranes Varies with Acclimation Temperature. *Am J Physiol Regul Integr Comp Physiol* **1995**, *269* (5), 1113–1119. https://doi.org/10.1152/ajpregu.1995.269.5.R1113.

(78) Andersen, O. S.; Koeppe, R. E. Bilayer Thickness and Membrane Protein Function: An Energetic Perspective. *Annu Rev Biophys Biomol Struct* **2007**, *36* (1), 107–130. https://doi.org/10.1146/annurev.biophys.36.040306.132643.

(79) Dubyak, G. R. Ion Homeostasis, Channels, and Transporters: An Update on Cellular Mechanisms. *Adv Physiol Educ* **2004**, *28* (4), 143–154. https://doi.org/10.1152/advan.00046.2004.

(80) Roux, B. Ion Channels and Ion Selectivity. *Essays Biochem* **2017**, *61* (2), 201–209. https://doi.org/10.1042/EBC20160074.

(81) Vinothkumar, K. R.; Henderson, R. Structures of Membrane Proteins. *Q Rev Biophys* **2010**, *43* (1), 65–158. https://doi.org/10.1017/S0033583510000041.

(82) Hodgkin, A. L.; Huxley, A. F. A Quantitative Description of Membrane Current and Its Application to Conduction and Excitation in Nerve. *J Physiol* **1952**, *117* (4), 500–544. https://doi.org/10.1113/jphysiol.1952.sp004764.

(83) Catterall, W. A. Structure and Function of Voltage-Gated Ion Channels. *Annu Rev Biochem* **1995**, *64* (1), 493–531. https://doi.org/10.1146/annurev.bi.64.070195.002425.

(84) Greenwell, M. G.; Sherrill, J.; Clayton, L. A. Osmoregulation in Fish. *Vet Clin N Am - Exot Anim Pract* **2003**, *6* (1), 169–189. https://doi.org/10.1016/S1094-9194(02)00021-X.

(85) Hwang, P. P.; Lee, T. H.; Lin, L. Y. Ion Regulation in Fish Gills: Recent Progress in the Cellular and Molecular Mechanisms. *Am J Physiol Regul Integr Comp Physiol* **2011**, *301* (1), 28–47. https://doi.org/10.1152/AJPREGU.00047.2011/ASSET/IMAGES/LARGE/ZH60061175900004.JPEG.

(86) Hughes, G. M. General Anatomy of the Gills. In *Fish Physiology*; 2023; Vol. 40, pp 9–78. https://doi.org/10.1016/bs.fp.2023.09.001.

(87) Karnaky, K. J. Ion-Secreting Epithelia: Chloride Cells in the Head Region of *Fundulus Heteroclitus*. *Am J Physiol Regul Integr Comp Physiol* **1980**, *238* (3), 185–198. https://doi.org/10.1152/ajpregu.1980.238.3.R185.

(88) McCormick, S. D. Endocrine Control of Osmoregulation in Teleost Fish. *Am Zool* **2001**, *41* (4), 781–794. https://doi.org/10.1093/icb/41.4.781.

(89) Flik, G.; Kaneko, T.; Greco, A. M.; Li, J.; Fenwick, J. C. Sodium Dependent Ion Transporters in Trout Gills. *Fish Physiol Biochem* **1997**, *17* (1/6), 385–396. https://doi.org/10.1023/A:1007768825043.

(90) Goss, G.; Perry, S.; Laurent, P. 10 Ultrastructural and Morphometric Studies on Ion and Acid-Base Transport Processes in Freshwater Fish. *Fish Physiol* **1995**, *14*, 257–284. https://doi.org/10.1016/S1546-5098(08)60249-6.

(91) Wilson, J. M.; Laurent, P. Fish Gill Morphology: Inside Out. *J Exp Zool* **2002**, *293* (3), 192–213. https://doi.org/https://doi.org/10.1002/jez.1012410.1002/jez.10124.

(92) Hwang, P.-P.; Lee, T.-H. New Insights into Fish Ion Regulation and Mitochondrion-Rich Cells. *Comp Biochem Physiol A Mol Integr Physiol* **2007**, *148* (3), 479–497. https://doi.org/https://doi.org/10.1016/j.cbpa.2007.06.416.

(93) Marshall, W. S. Na^+, Cl^-, Ca^{2+} and Zn^{2+} Transport by Fish Gills: Retrospective Review and Prospective Synthesis. *J Exp Zool* **2002**, *293* (3), 264–283. https://doi.org/10.1002/jez.10127.

(94) Lee, L. E. J.; Dayeh, V. R.; Schirmer, K.; Bols, N. C. Applications and Potential Uses of Fish Gill Cell Lines: Examples with RTgill-W1. *In Vitro Cell Dev Biol-Animal* **2009**, *45*, 127–134. https://doi.org/10.1007/s11626-008-9173-2.

(95) Fistarol, G.; Legrand, C.; Granéli, E. Allelopathic Effect of *Prymnesium parvum* on a Natural Plankton Community. *Mar Ecol Prog Ser* **2003**, *255*, 115–125. https://doi.org/10.3354/meps255115.

(96) Skovgaard, A.; Hansen, P. J. Food Uptake in the Harmful Alga *Prymnesium parvum* Mediated by Excreted Toxins. *Limnol Oceanogr* **2003**, *48* (3), 1161–1166. https://doi.org/10.4319/lo.2003.48.3.1161.

(97) Vaqué, D.; Felipe, J.; Sala, M. M.; Calbet, A.; Estrada, M.; Alcaraz, M. Effects of the Toxic Dinoflagellate *Karlodinium Sp*. (Cultured at Different N/P Ratios) on Micro and Mesozooplankton. *Sci Mar* **2006**, *70* (1), 59–65. https://doi.org/10.3989/scimar.2006.70n159.

(98) Brownlee, E. F.; Sellner, S. G.; Sellner, K. G.; Nonogaki, H.; Adolf, J. E.; Bachvaroff, T. R.; Place, A. R. Responses of *Crassostrea Virgini*a (Gmelin) and *C. Ariakensis* (Fujita) To Bloom-Forming Phytoplankton Including Ichthyotoxic *Karlodinium Veneficum* (Ballantine). *J Shellfish Res* **2008**, *27* (3), 581–591. https://doi.org/10.2983/0730-8000(2008)27[581:ROCVGA]2.0.CO;2.

(99) Gilbert, P. M.; Alexander, J.; Meritt, D. W.; North, E. W.; Stoecker, D. K. Harmf Algae Pose Additional Challenges for Oyster Restoration: Impacts of the Harmf Algae *Karlodinium Veneficum* and *Prorocentrum Minimum* on Early Life Stages of the Oysters *Crassostrea Virginica* and *Crassostrea Ariakensis*. *J Shellfish Res* **2007**, *26* (4), 919–925. https://doi.org/10.2983/0730-8000(2007)26[919:HAPACF]2.0.CO;2.

(100) Adolf, J.; Bachvaroff, T.; Krupatkina, D.; Nonogaki, H.; Brown, P.; Lewitus, A.; Harvey, H.; Place, A. Species Specificity and Potential Roles of *Karlodinium Micrum* Toxin. *Afr J Mar Sci* **2006**, *28* (2), 415–419. https://doi.org/10.2989/18142320609504189.

(101) Ghosh, P.; Patterson, G. W.; Wikfors, G. H. Sterols of Some Marine Prymnesiophyceae. *J Phycol* **1998**, *34* (3), 511–514. https://doi.org/10.1046/j.1529-8817.1998.340511.x.

(102) Houdai, T.; Matsuoka, S.; Morsy, N.; Matsumori, N.; Satake, M.; Murata, M. Hairpin Conformation of Amphidinols Possibly Accounting for Potent Membrane Permeabilizing Activities. *Tetrahedron* **2005**, *61* (11), 2795–2802. https://doi.org/https://doi.org/10.1016/j.tet.2005.01.069.

7 Publications

7.1 Manuscript 1 – “Cytotoxicity of *Prymnesium parvum* extracts and prymnesin analogs on epithelial fish gill cells RTgill-W1 and the human colon cell line HCEC-1CT”

Published in Archives of Toxicology, Volume 98, in January 2024. https://doi.org/10.1007/s00204-023-03663-5

Author contributions: conceptualization, E.V., G.D.F, D.M.; methodology, E.V., G.D.F., T.O.L., P.J.H. and D.M.; formal analysis, investigation, data curation and visualization, E.V., **H.C.P**., M.R., N.H., D.B., N.M.; resources, E.V., N.M., G.D.F., T.O.L., P.J.H. and D.M.; writing—original draft preparation, E.V., **H.C.P**.; writing—review and editing, all co-authors; supervision, E.V., and D.M.; project administration, E.V.; funding acquisition, E.V., T.O.L. and P.J.H.; all authors have read and agreed to the published version of the manuscript.

This is a shared first co-authorship article, for which the practical work was divided between several parties. Nicola Medić supervised by Per Juel Hansen and Thomas Ostenfeld Larsen was responsible for *P. parvum* cultivation and the provision of biomass. The master student Matthias Riepl performed the toxin extraction and conducted cytotoxicity tests (CTB, LDH, and SRB), including comparative assays of B-type toxicity and 3 vs. 24 h exposure. Eva Attakpah assisted Matthias Riepl in performing the live-cell imaging in HCEC-1CT cells for B-type prymnesins. The master student Nadine Hochmayr performed cytotoxicity assays (CTB and LDH) in RTgill-W1 cells for A- and B-type prymnesins. Deniz Berk assisted the author of the thesis in the optimization of ion free medium for the RTgill-W1 cells. Exposure of RTgill-W1 cells to C-type prymnesins and imaging of RTgill-W1 cells exposed to A-type prymnesins in ion-free media were performed by this author. Data evaluation and visualization, manuscript drafting and writing were the sole responsibility of Hélène-Christine Prause. Endre Kiss and Giorgia Del Favero were of invaluable help and introduced the author of this thesis to the fluorescence microscope and data evaluation thereof. Elisabeth Varga was the principal investigator of this project and co-supervisor of the master students (Matthias Riepl, Nadine Hochmayr, Deniz Berk), as well as responsible for prymnesin analysis, and editing of the initial manuscript. Doris Marko served as supervisor of this work, provided resources and the basis for this work at the Department of Food Chemistry and Toxicology.

Archives of Toxicology (2024) 98:999–1014
https://doi.org/10.1007/s00204-023-03663-5

BIOLOGICS

Cytotoxicity of *Prymnesium parvum* extracts and prymnesin analogs on epithelial fish gill cells RTgill-W1 and the human colon cell line HCEC-1CT

Elisabeth Varga[1,2] · Hélène-Christine Prause[1,3] · Matthias Riepl[1] · Nadine Hochmayr[1] · Deniz Berk[1] · Eva Attakpah[1] · Endre Kiss[1,4] · Nikola Medić[5,6] · Giorgia Del Favero[1,4] · Thomas Ostenfeld Larsen[7] · Per Juel Hansen[5] · Doris Marko[1]

Received: 27 October 2023 / Accepted: 7 December 2023 / Published online: 11 January 2024

Abstract

Harmful algal blooms kill fish populations worldwide, as exemplified by the haptophyte microalga *Prymnesium parvum*. The suspected causative agents are prymnesins, categorized as A-, B-, and C-types based on backbone carbon atoms. Impacts of *P. parvum* extracts and purified prymnesins were tested on the epithelial rainbow trout fish gill cell line RTgill-W1 and on the human colon epithelial cells HCEC-1CT. Cytotoxic potencies ranked A > C > B-type with concentrations spanning from low (A- and C-type) to middle (B-type) nM ranges. Although RTgill-W1 cells were about twofold more sensitive than HCEC-1CT, the cytotoxicity of prymnesins is not limited to fish gills. Both cell lines responded rapidly to prymnesins; with EC_{50} values for B-types in RTgill-W1 cells of 110 ± 11 nM and 41.5 ± 0.6 nM after incubations times of 3 and 24 h. Results of fluorescence imaging and measured lytic effects suggest plasma membrane interactions. Postulating an osmotic imbalance as mechanisms of toxicity, incubations with prymnesins in media lacking either Cl^-, Na^+, or Ca^{2+} were performed. Cl^- removal reduced morphometric rearrangements observed in RTgill-W1 and cytotoxicity in HCEC-1CT cells. Ca^{2+}-free medium in RTgill-W1 cells exacerbated effects on the cell nuclei. Prymnesin composition of different *P. parvum* strains showed that analog composition within one type scarcely influenced the cytotoxic potential, while analog type potentially dictate potency. Overall, A-type prymnesins were the most potent ones in both cell lines followed by the C-types, and lastly B-types. Disturbance of Ca^{2+} and Cl^- ionoregulation may be integral to prymnesin toxicity.

Keywords Microalgae · Ichthyotoxin · UHPLC · MS · Fluorescence microscopy · Ionoregulation

Elisabeth Varga and Hélène-Christine Prause authors contributed equally.

✉ Elisabeth Varga
elisabeth.varga@vetmeduni.ac.at

1 Department of Food Chemistry and Toxicology, Faculty of Chemistry, University of Vienna, Währinger Str. 38-40, 1090 Vienna, Austria

2 Unit Food Hygiene and Technology, Institute of Food Safety, Food Technology and Veterinary Public Health, University of Veterinary Medicine, Vienna, Veterinärplatz 1, 1210 Vienna, Austria

3 Vienna Doctoral School in Chemistry, Faculty of Chemistry, University of Vienna, Währinger Str. 42, 1090 Vienna, Austria

4 Core Facility Multimodal Imaging, Faculty of Chemistry, University of Vienna, Währinger Str. 38-42, 1090 Vienna, Austria

5 Marine Biological Section, Department of Biology, University of Copenhagen, Strandpromenaden 5, 3000 Helsingør, Denmark

6 Center for Bioresources, Division for Food and Production, Danish Technological Institute, Gregersensvej 8, 2630 Taastrup, Denmark

7 Department of Biotechnology and Biomedicine, Technical University of Denmark, Søltofts Plads 221, 2800 Kgs Lyngby, Denmark

Introduction

Microalgae play an important role in the marine ecosystem, i.e., the production of oxygen, uptake of carbon dioxide (CO_2) and inorganic nutrients and provide food for the entire aquatic food web (Tsai et al. 2012). In general, they can be divided into macroalgae, which are visible to the naked eye, and microalgae, which are one-cell organisms and can be of prokaryotic or eukaryotic nature. Microalgae can on the one hand produce nutrient-rich and beneficial biomolecules like fatty acids, lipids, and vitamins, and on the other hand, produce harmful toxins. Among the most important harmful algal bloom (HAB)-forming microalga worldwide is the haptophyte *Prymnesium parvum* (Hallegraeff 1993; Manning and La Claire 2010). These HABs are characterized by a rapid proliferation of the microalgae, and can have huge economic and ecological impacts, lasting from several days to months, depending on the given environmental conditions (Ryan et al. 2017; Vasas et al. 2012). HABs can lead to massive fish kills (Manning and La Claire 2010) by lowering oxygen levels in the water, damaging the inhabitants of the marine life by toxin production or causing direct damage to fish gills as well as clogging (Hallett et al. 2016). Just last summer (August 2022), 360 t of fish died in the Oder River in Poland/Germany due to this alga (Free et al. 2023).

In case of *P. parvum*, the prymnesins (PRMs) have been identified as causative ichthyotoxic agents and possess cytotoxic and hemolytic properties (Binzer et al. 2019; Igarashi et al. 1996). The height of the blooms often occurs when the environmental conditions are suboptimal (Granéli and Salomon 2010; Manning and La Claire 2010; Shilo 1967; Svenssen et al. 2019). PRMs are supersized (1600–2300 Da) ladder-frame polyethers (Fig. 1), currently grouped into three categories A-, B-, and C-type PRMs (Igarashi et al. 1996, 1999; Rasmussen et al. 2016b). They differ in the length of their aglycon backbone, the longest being A-type with 91, followed by B- and C-type, with 85 and 83 carbon atoms, respectively (Binzer et al. 2019). While the backbone structure of two A- (prymnesin-1 and prymnesin-2, Igarashi et al. 1996, 1999) and one B-type (prymnesin B1, Rasmussen et al. 2016a) were fully characterized by NMR, the exact structure of C-type PRMs remains unclear. Within each category exists a large diversity in terms of degree of saturation, chlorination, and attached sugar moieties (Binzer et al. 2019). One feature the three groups share is a primary amine located in the lipophilic part of the ladder-frame (Fig. 1) (Igarashi et al. 1996, 1999; Rasmussen et al. 2016a). One strain of *P. parvum* produces exclusively one type of toxin, but different analogs thereof, and the toxic potential varies between the types (Binzer et al. 2019; Rasmussen et al. 2016a). Overall, identifying the strain and thus category of PRM produced is essential for understanding *P. parvum* toxicity. Whether the type of PRM analog influences the potency, however, remains unclear.

Fish mortality due to these toxins is caused by gill damage, typically manifesting as increased permeability, ultimately leading to internal oxygen deficiency (Svendsen et al. 2018; Ulitzur and Shilo 1966; Yariv and Hestrin 1961). This is seemingly achieved through pore formation in gill cells, resulting in disruption of the ionic balance and increased mucus production (Otterstrom and Nielsen 1939; Ulitzur and Shilo 1964, 1966; Tillmann 2003). When investigating HAB-forming microalgae, scientists typically resort to fish bioassays for acute or sublethal toxicity in brine shrimp, larval or juvenile fish (Segner 1998; Svendsen et al. 2018; McKim et al. 1987). These bioassays have been widely criticized especially for ethical reasons,

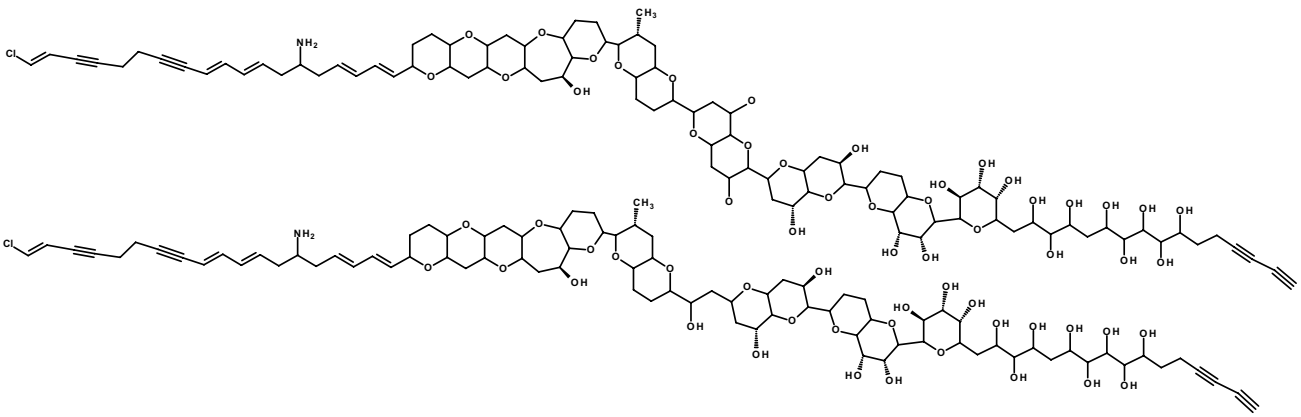

Fig. 1 Backbone structure of **A**- (top) and **B**-type (bottom) prymnesins according to Igarashi et al. (1996) and Rasmussen et al. (2016a), respectively. The main difference is the length of the carbon backbone, further modifications of prymnesin analogs are attached sugar moieties, the degree of saturation and the number of incorporated chloride and oxygen atoms

given the large number of animals that are required, and the severe harm imposed on them. Also, acute fish toxicity assays only reflect a relative toxicity where no specific mode-of action is investigated (Fischer et al. 2019; Segner et al. 1998). The use of cell lines such as the epithelial rainbow trout (*Oncorhynchus mykiss* (Walbaum)) fish gill cell line RTgill-W1 as an alternative represents a target-specific test system, that does not require the sacrifice of live animals (Bols et al. 1994; Segner 1998). By the same token, it allows for the investigation of the mode of action of ichthyotoxins, with the possibility to select various endpoints (Fischer et al. 2019; Segner 1998). Since June 2021, a guideline for testing the acute toxicity of chemicals with the RTgill-W1 cell line is available from the Organisation for Economic Co-operation and Development (OECD 2021).

The exact mechanism through which PRMs exhibit their toxicity remains unclear, although evidence points to a direct interaction with the cell membrane (Igarashi et al. 1998; Shilo 1967). Brevetoxins which share a similar ladder-frame core structure as PRM were found to bind to voltage-sensitive Na^+-channels. A similar mode of action was hypothesized for PRMs (Baden 1989; Rasmussen et al. 2016b). Moreover, the presence or absence of ions in the medium has been shown to affect PRM toxicity in fish, further hinting at the involvement of ions (Shilo 1967; Ulitzur and Shilo 1966; Yariv and Hestrin 1961). PRM toxicity was observed also in short-term exposure of fish, which indicates a fast interaction with their physiological target (Svendsen et al. 2018).

Given the current state of knowledge, the aim of this study was to assess the toxic potential of A-, B-, and C-type PRMs. We hypothesize that different prymnesin types and different prymnesin analogs influence toxicity. To provide answers cell viability and membrane integrity of RTgill-W1 cells and the human epithelial colon cell line HCEC-1CT were assessed. The HCEC-1CT cell line was selected, because it cannot be excluded that humans will be exposed to PRMs. Other phycotoxins, such as brevetoxin aerosols, are known to have adverse effects on humans (Benson et al. 1999; Hallegraeff 1993; Sanseverino et al. 2016). Furthermore, a better understanding may be gained from comparing the response of cell lines derived from different species to PRM cytotoxicity. For evaluating the rapidity with which PRMs act, toxicity tests were performed for two incubation times (3 h vs. 24 h). Furthermore, we hypothesize that PRMs interact with ion channels and ionoregulation is a relevant factor for toxicity. Morphological changes upon exposure to PRMs were captured using fluorescent dyes during live-cell imaging. Additionally, the effect selected ions may have on the potency of PRMs was investigated and a possible influence of two RTgill-W1 media on the cell viability and morphology after exposure to PRMs was assessed.

Materials and methods

Chemicals and reagents

HPLC-grade acetone, methanol and acetonitrile (ACN) as well as absolute ethanol (99.8%) were purchased at Fisher Chemical (Loughborough, UK). HPLC grade formic acid was obtained from Carl Roth GmbH + Co. KG (Karlsruhe, Germany) and LC–MS grade water was from VWR (Vienna, Austria).

Samples

The non-axenic microalgal strains were previously obtained from the Scandinavian Culture Collection of Algae and Protozoa (SCCAP, now incorporated in the Norwegian Culture Collection of Algae, NORCCA, strain K-0081), the Roscoff Culture Collection (RCC, strain RCC-191 and RCC-1436) or the Culture Collection of Algae of the University of Texas (UTEX, strain UTEX-2797). The strains were maintained in F/2 growth medium prepared from filtered (Whatman® glass microfiber filters, grade GF/F, Sigma Aldrich, St. Louis, MO/USA) and pasteurized (95 °C, 95 min) natural seawater off the coast of Helsingør at around 30 salinity (Guillard 1975). They were kept at 15 °C and an irradiance of 450–500 µmol photons/(m^2 s) on a 14:10 h light–dark cycle. *P. parvum* cultures used for the bioassays were inoculated and kept in exponential growth in 10 L glass bottles with gentle aeration to prevent elevation of pH due to photosynthesis. During the cultivation period, the cell concentrations were determined every 2–3 days using a flow cytometer (CytoFLEX flow cytometer, Beckman Coulter, Copenhagen, Denmark). Cells were distinguished from the background using pigment fluorescence (PC5.5) and forward scatter (FSC). The microalgal biomass was harvested in the late exponential growth using the Avanti J-26 XP, JFC-Z continues centrifuge (Beckmann Coulter) with flow rates between 15 and 20 mL/min at 4 °C and 3500 rounds per minutes (rpm, ca. 1111 relative centrifugal force, rcf). The biomass was transferred into falcon tubes and centrifuged again at 4000 rcf for 15 min to discard as much supernatant as possible. The biomass pellets were stored at − 80 °C until further extraction. The inorganic carbon in the culture was measured using the total organic carbon analyzer (TOC-L, Shimadzu Europe GmbH, Duisburg, Germany). The extraction of PRMs followed the procedure described in (Rasmussen et al. 2016a; Binzer et al. 2019). First, the biomass was thawed and centrifuged at 4000 rcf for 5 min using a Z326-K centrifuge (Hermle Labortechnik GmbH, Wehingen, Germany) and then the aqueous supernatant

was removed. The algal biomass samples were extracted several times with ice-cold acetone to remove the chlorophyll followed by extractions with methanol to obtain the PRMs. In-between the extraction steps, the samples were centrifuged, and the extracts of the same solvent were combined. The solvent was removed by a rotavapor (R-114, Büchi Labortechnik AG, Flawil, Switzerland) or a CentriVap Benchtop Vacuum Concentrator coupled to a CentriVap Coldtrap (both Labconco Corporation, Kansas City, MO/USA). The samples were reconstituted in absolute ethanol, treated in the ultrasonic bath for several minutes, centrifuged again and the particle free supernatant was transferred to HPLC vials.

The two extracts from UTEX-2797 will henceforward be called A1 and A2, and B-type extracts, all from strain K-0081, as B1-B4. Two C-type PRM extracts, C1 and C2, from strains RCC-1436 and RCC-191, respectively, were tested as well. Single compound solutions were previously purified by means of liquid chromatography and are referred to as sA1, sB1 and sB2. One A-type solution (A3) which was previously available from Sigma Aldrich as lysis standard (No. P-1389), was provided by Tom Shier (Department of Medicinal Chemistry, College of Pharmacy, University of Minnesota, Minneapolis/MN, USA).

Chemical analysis

Quantitative analysis

For cell-based assays, it was essential to have analytical information about the investigated *P. parvum* samples. Hence, PRM concentrations were semi-quantified via high-performance liquid chromatography using a fluorescence detector (HPLC-FLD), with an indirect method previously described by Svenssen et al. (2019) with slight modifications. Fluorescence derivatization of the primary amine of the PRMs was performed using the AccQ-Tag Fluor Reagent Kit from Waters Corporation (Milford/MA, USA). Due to the lack of standards, a mixture of fumonisins B_1 and B_2 (Romer Labs, Tulln, Austria) was used as external calibrant. The chromatographic separation was performed on a 1200 HPLC system (Agilent Technologies, Waldbronn, DE), using an Agilent Poroshell C18 column (2.1 × 50 mm 2.7 µm) at 40 °C and a flow rate of 0.4 mL/min. The eluents were water (eluent A) and ACN (eluent B) and both contained 0.1% formic acid. A linear gradient was applied starting with 20% B for 1 min, increasing to 100% B over 7 min, and held for 2 min before returning to the start conditions. Injection volumes varied between 1 µL and 20 µL. The PRMs were detected by fluorescence using an excitation wavelength of 250 nm and an emission wavelength of 395 nm. Data were evaluated using ChemStation for LC Rev. B.04.01 SP1 from Agilent Technologies.

Qualitative analysis

The composition of PRM analogs in the samples was analyzed via ultra-high performance liquid chromatography coupled with high resolution mass spectrometry (UHPLC-HRMS). Here, a 1290 UHPLC system was coupled to a 6550 iFunnel Q-TOF LC/MS equipped with a dual Agilent Jet Stream (AJS) operated in the electrospray ionization mode (all Agilent Technologies, Waldbronn, DE). A Kinetex F5 column (100 × 2.1 mm, 2.6 µm, Agilent Technologies, Waldbronn, DE) was used at 30 °C with a flow rate of 0.4 mL/min. Eluent A was water, and eluent B was ACN:H_2O (90:10, *v/v*) and both eluents contained 0.1% formic acid and 1 mM ammonium formate. The following gradient was applied: the starting conditions were 20% eluent B for 30 s, followed by a linear gradient reaching 67% B over 15.5 min. Thereafter the column was flushed for 3 min using 100% eluent B before returning to the starting conditions. Injection volumes ranged between 1 and 10 µL. The capillary voltage was set to 4000 V and the nozzle voltage to 500 V. The gas temperature was 130 °C and the drying gas flow was 14 L/min. The sheath gas temperature was set to 300 °C and a flow rate of 10 L/min. The nebulizer pressure was held at 2.07 bar ($2.07*10^5$ Pa). The mass spectrometer was operated in full-scan positive ionization mode scanning *m/z* 50 to 1700 with 3 scans per second. Reference masses of *m/z* 121.05087 and *m/z* 922.00 were constantly infused into the ion source via a second nebulizer to ensure mass accuracy. The examined masses were adopted from Binzer et al. (2019). Data were acquired using MassHunter Workstation LC/MS Data Acquisition version B.06.01 and data evaluation was performed using Agilent MassHunter Qualitative Analysis B.10.00.

Cell culture

Cytotoxicity assays were performed with the rainbow trout (*Oncorhynchus mykiss*) gill cell line RTgill-W1 obtained from Kristin Schirmer (Department of Environmental Toxicology, EAWAG, Dübendorf, CH). This cell line was cultured at 19 °C and sub-cultured every week, by first rinsing the flask with Versene (Thermo Fisher Scientific, Waltham, MA, US) and subsequent trypsinization using 0.25% trypsin/0.02% ethylenediaminetetraacetic acid in phosphate buffered saline (PAN Biotech, Aidenbach, Germany). The cells were centrifuged at 50 rcf and 21 °C for 3 min, the supernatant discarded, and the cells suspended in fresh medium prior to further usage. Two cultivation media were compared and tested, that differed both in their composition and the supplementation (supplementary information (SI) Table 1). The fully supplemented media are referred to as L-15 complete.

The human epithelial colon cell line HCEC-1CT was kindly provided by Jerry W. Shay, UT Southwestern Medical Center, Dallas, Texas, USA, and was used for cytotoxicity tests and live-cell imaging as previously described (Del Favero et al. 2018; Rebhahn et al. 2022). The cells were cultivated in Dulbecco's Modified Eagle's Medium (DMEM (Thermo Fisher Scientific, Waltham, USA)), supplemented with essential nutrients and growth media, at 37 °C and 5% CO_2. For 500 mL DMEM 10 mL Medium 199 (10x), 10 mL HEPES buffer solution 1 M, 5.2 mL Insulin-Transferrin-Selenium-G Supplement (Thermo Fisher Scientific, Waltham, USA), 10 mL HyClone™ Cosmic Calf™ Serum (GE Healthcare Life Sciences HyClone Laboratories, South Logan, USA), 0.6 mL gentamycin solution (Sigma Aldrich GmbH, St. Louis, USA), 100 µL recombinant human epidermal growth factor (100 µg/mL, Szabo-Scandic HandelsgmbH & Co KG, Vienna, Austria) and 100 µL hydrocortisone (5 mg/mL, Merck KGaA, Darmstadt, Germany) were added. Cells were passaged every 2–3 days when a confluence of 80% was reached. HCEC-1CT cells were first rinsed with phosphate buffered saline and then detached with Accutase® (Corning, Manassas, USA).

Both cell lines were cultured in cell culture flasks using the "cell + surface" (Sarstedt AG & Co KG, Nürnbrecht, Germany) of various sizes (T-25 to T-175). Cytotoxicity assays were performed in 96-well polystyrene cell culture plates (cell + surface, flat base, order number 83.3924.300; Sarstedt AG & Co. KG, Nürnbrecht, Germany), whereas live-cell-imaging assays were performed with 96-well flat clear bottom black polystyrene TC-treated microplates from Corning® (order number: 3603, Corning, USA).

Cytotoxicity testing

RTgill-W1 cells were seeded at a density of $2*10^4$ cells/well and HCEC-1CT cells at $5*10^3$ cells/well in 96-well plates and grown for 48 h. PRM samples in EtOH were diluted 1:200 in culture medium to achieve a final EtOH concentration of 0.5%. Since PRM are light labile exposure to sun light was avoided and the exposure time to artificial light were kept to a minimum. Cells were exposed to 100 µL of different concentrations thereof, for 3 or 24 h in the dark. The CellTiter-Blue® (CTB) assay was performed to measure the metabolic activity of the cells, according to the manufacturer's instructions. The CTB dye was diluted 1:10 (v/v) in cell culture medium and applied to the cells for 1 h in the dark.

Where applicable, prior to starting the CTB assay, the lytic potential of PRMs was analyzed with the lactate dehydrogenase (LDH) assay (Thermo Fisher Scientific, Waltham, USA). The measurements were performed according to the manufacturer's protocol.

Additionally, cell protein content was assessed for 24 h incubations, using the sulforhodamine B (SRB) assay. In short, the cells were rinsed with Dulbecco's Phosphate Buffered Saline (Thermo Fisher Scientific, Waltham USA)), fixed with trichloroacetic acid and incubated for 1 h at 4 °C. The plate was then washed four times with distilled water and dried overnight. The fixed cells were stained with SRB reagent for 1 h at room temperature, after which it was discarded, and the plate was rinsed with water followed by 1% acetic acid in water. The plate was again dried overnight, and finally, Tris base was used to dissolve the stained proteins. After shaking the plate for 5 min, the absorbance was taken at 570 nm.

For PRM toxicity in ion-free media, crystal violet (CV) dye was used instead of CTB. Cells were seeded and exposed to test solutions as described before. After incubation, wells were aspirated, and the cells fixed with ice-cold EtOH for 10 min at 4 °C. This was discarded, and 0.1%-CV solution (in EtOH) was used to stain the cells for 5 min. Subsequently cells were rinsed with water and dried overnight. De-staining solution (1% acetic acid in EtOH) was added to each well and absorbance was measured at 595 nm.

Live-cell imaging

The cell nuclei and membranes were visualized using Hoechst 33,258 and Cell Mask™ Deep Red plasma membrane stain (Fisher Chemical, Loughborough, UK), diluted 1000-fold in Live Cell Imaging Solution (LCIS; Thermo Fisher Scientific, Waltham, USA). After staining for 30 min at room temperature (RTgill-W1) or at 37 °C and 5% CO_2 (HCEC-1CT), cells were rinsed first with the respective media, and images were taken right before adding the substances (t_0), and again 1.5 h (t_1) and 3 h (t_2) after starting the exposure to PRMs. Sample dilutions were prepared in LCIS, normal external solution (NES), and the ion-free media. Images were acquired using a BioTek Lionheart FX (Agilent, Santa Clara, CA, United States) automated microscope. Data evaluation was performed with ImageJ Software and BioTek Gen5 Software for imaging and microscopy.

Ion-free media

Specific ions (Na^+, Ca^{2+} or Cl^-) were chosen to be omitted entirely for cytotoxicity testing and fluorescence microscopy, adapting protocols previously described (Del Favero et al. 2012). The composition of each medium can be found in SI Table 2. Additionally, LDH and CV assays in HCEC-1CT were performed for different concentrations of B-type PRM in the selected ion-free media, as well as NES, LCIS, and HCEC-1CT culture medium.

Statistics

CTB and LDH results were tested for normality via the Shapiro–Wilk Test, significance (* = $p < 0.05$; ** = $p < 0.01$; *** = $p < 0.001$) was calculated with One Way ANOVA, followed by the post hoc Fisher´s least significant difference test using OriginLab.

Results

Chemical analysis

The PRM content was analyzed semi-quantitatively, and qualitatively. The mycotoxins fumonisin B_1 and B_2 were used as external calibration standards due to the lack of PRM standards, as these also contain a primary amine, for which individual calibration curves were created. A-type PRM eluded at a retention time of 7.6 min, B-type between 6.75 and 7.65, and C-type PRMs had a retention time between 6.1 and 7.4 min. PRM analogs could not be distinguished in this method. Peaks with an area larger than 50 were excluded, and the samples were diluted for repeated measurements. From the external calibration, approximate concentrations of the ichthyotoxins could be calculated, and those are provided in SI Table 3. SI Table 4 states the PRM profiles that were determined using UHPLC-HRMS analysis. This was also performed to estimate the purity of the solutions. The most common ion species observed were the double charged ions $[M+2H]^{+2}$, $[M+NH_4+H]^{+2}$ and $[M+Na+H]^{+2}$. In case of B-type PRMs also, the single charged $[M+H]^{+}$ was observed. Beside the exact masses, also the quite distinctive isotopic patterns were taken into consideration to confirm the presence of PRMs. The isotope distribution of PRMs is very specific due to the high number of C-atoms and the occurrence of Cl-atoms. For one of the two UTEX-2797 extracts, A2, no more than four analogs could be identified, with the majority, 81%, attributed to the A-type prymnesin with 3 Cl-atoms incorporated and one pentose moiety (short form: PRM-A (3 Cl) + pentose). For extract A1, on the other hand, ten analogs were identified. The highest concentration was 41% for PRM-A (3 Cl) + pentose. We currently have no explanation for the difference in the PRM-pattern of the same strain which was cultivated years apart. Sample A3, from unknown strain origin (Sigma Aldrich), was found to consist of seven different analogs, with PRM-A (3 Cl) + 2 pentose + hexose being the most abundant, at 63%. The PRM profiles for the B-type extracts of K-0081 consisted of eight different analogs. Approximately half of the PRM content, though, was comprised of PRM-B (1 Cl) + hexose. Generally, PRM compositions matched perfectly between extraction replicates of each B-type *P. parvum* strain. Only for sample B4, which was harvested from K-0081 3 years prior to the other B-type extracts, differed slightly from its counterparts. Lastly, sample C1 of the strain RCC-1436 was found to contain at least seven analogs, while for C2 from strain RCC-191, more than ten analogs of C-type PRMs could be identified. Interestingly, PRM-C (4 Cl + DB) + pentose appeared to be the most abundant in both cases.

In order to identify whether potencies differ between PRM analogs, purified solutions were also analyzed and subsequently tested for cytotoxicity. Both, the A-type single substance solution from the UTEX-2797 strain, sA1, and a purified B-type sample harvested from strain K-0081, sB1, consisted of only two analogs. One of which was significantly more dominant than the other, for both samples, respectively. For sB2, three analogs could be identified, where PRM-B (1 Cl) + 2 hexose made up for 79%. An overview of the identified PRM analogs is provided in SI Table 4.

Cytotoxicity

The cytotoxic potential of *P. parvum* extracts and PRM single compounds was tested in a CTB cell viability assay, for which the optimal incubation time of 60 min was determined. A final EtOH concentration of 0.5% was applied as solvent control, which was the point of reference for SRB and CTB calculations. For LDH analyses, a maximum LDH release (maximum lysis) of the cells was determined, which was ultimately used as reference for potency analyses. Triton™ X-100 (short Triton X, Sigma-Aldrich, St. Louis, MO, USA) served as positive control. For CTB assays, 0.05% (v/v) in medium were applied to the RTgill-W1 cells and 0.1% (v/v) to HCEC-1CT, and in LDH assays, 0.1% (v/v) Triton X was used. The setup for the 24 h incubation was the same as for 3 h, only Triton X concentrations were changed to 0.025% in RTgill-W1 cells, and 0.075% (v/v) for HCEC-1CT cells.

RTgill-W1

The fish gill cell line RTgill-W1 was exposed to A-, B, and C-type PRM samples and also the impact of two culture media compositions (recipe 1 and recipe 2) was assessed. Toxin potencies did not differ significantly in the two media (SI Fig. 1). Incubation times of 3 h and 24 h were compared, and the effective concentration 50 (EC_{50}) values differed only by a factor of around 2.2 (SI Table 5). Given the small differences, a 3 h incubation was chosen for the remaining experiments.

Cells were exposed to the A-type PRM solution from Sigma Aldrich (A3), B-type extract of the K-0081 strain (B3), and a C-type PRM extract of RCC-191 (C2) diluted in medium following recipe 2. A cytotoxic effect could be measured for all the tested samples, some of which

are shown in Fig. 2. The A-type sample, A3, showed a clear increase in cytotoxicity with increasing concentrations (Fig. 3A). Yet, at the lowest concentrations an elevation of RTgill-W1 metabolic activity was observed. Cell viability was decreased to about 50% at a concentration of 127 nM of the B-type PRM extract B3. Extract C2, from the C-type producing strain RCC-191, already reduced cell viability to 75% at 5 nM, and had an EC_{50} of 9.8 ± 0.8 nM. The effects of PRMs in the fish gill cell line were compared to the human-derived HCEC-1CT cells (SI Table 3) and RTgill-W1 cells were about twofold more sensitive to the ichthyotoxins than the human cell line.

HCEC-1CT

P. parvum extracts were tested on non-tumorigenic human colon epithelial cells. HCEC-1CT cells were exposed to the B-type extract B1 of *P. parvum* strain K-0081 (Fig. 3). CTB and LDH assays were performed for 3 h incubations, and CTB and SRB for 24 h incubations (Fig. 3A). CTB measurements after 3 h exposure showed very low viability for the highest concentrations, while the lowest seemingly did not alter cell viability. An EC_{50} of 170 ± 9 nM was calculated with RStudio (packages "drc", "ggplot2"). For the 24 h incubation, the EC_{50} was calculated to be around 145 ± 7 nM. These findings were mirrored in the corresponding LDH data obtained for the 3 h incubations (Fig. 3B), and SRB results (Fig. 3C) for the 24 h incubation. Based on the cytotoxicity results obtained for B-type PRMs, all following exposures

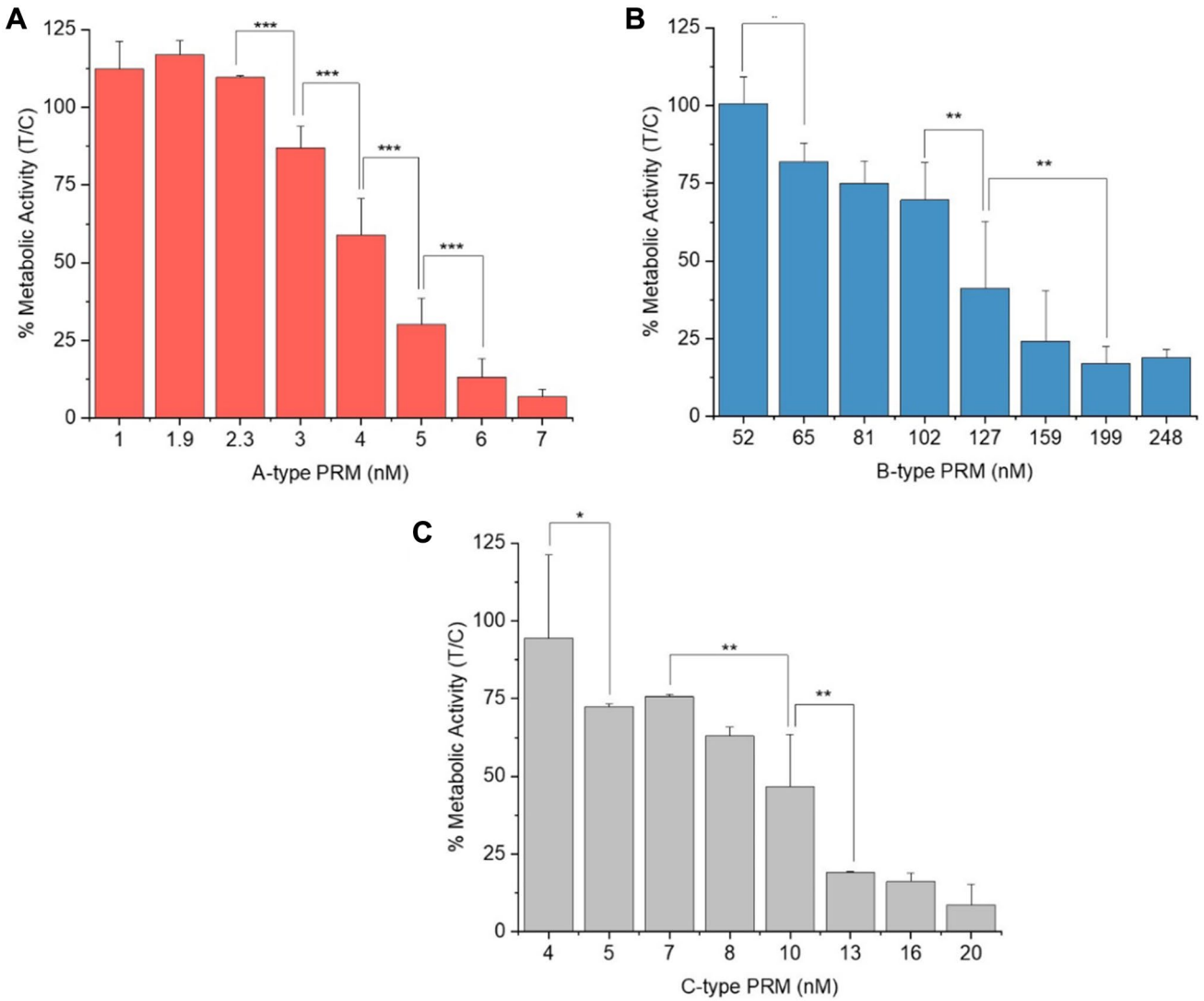

Fig. 2 RTgill-W1 cell viability after 3-h exposure to prymnesins (PRM). **A** shows data of the A-type solution A3 from an unknown strain, **B** results for the K-0081 extract B3, and **C** the RCC-191 extract C2. Data are represented as mean ± SD, n ≥ 3

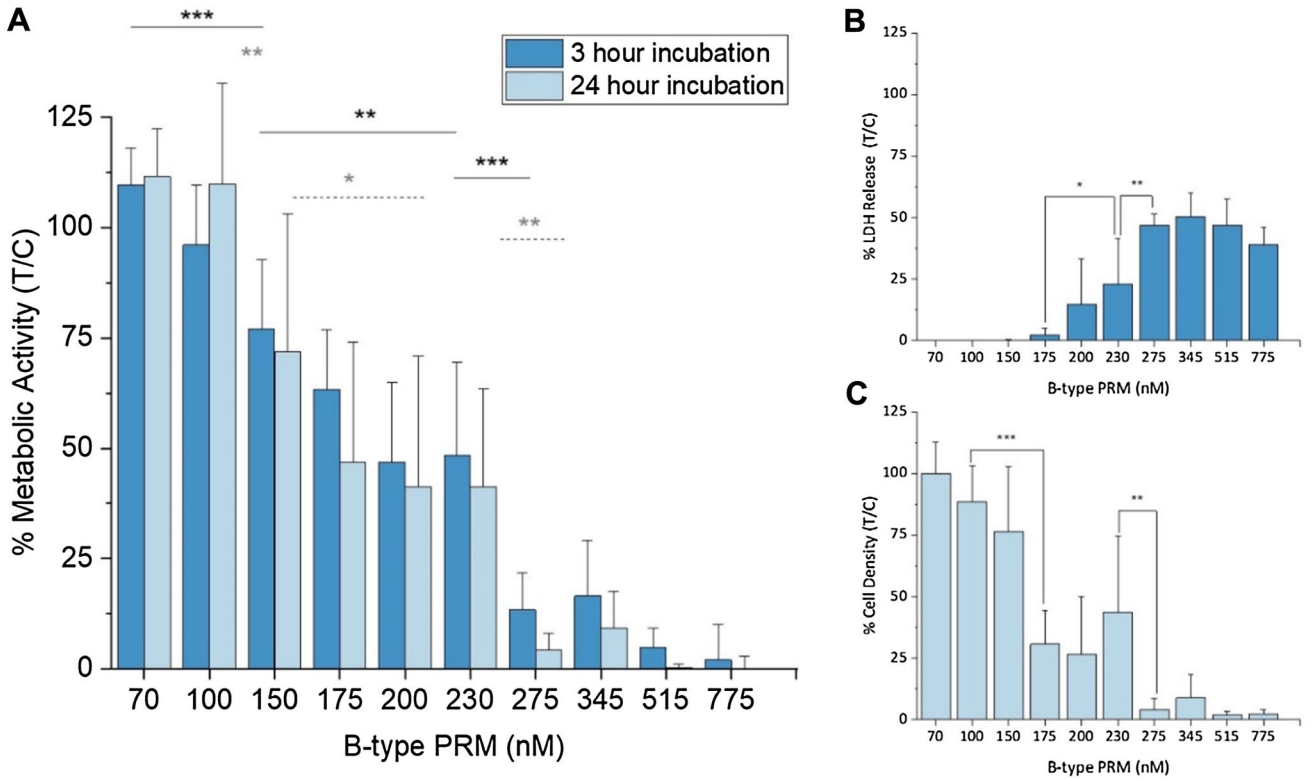

Fig. 3 Comparison between HCEC-1CT cell viability after incubation with B-type prymnesin (PRM) extract B1 obtained from *Prymnesium parvum* strain K-0081 for 3 h and 24 h (significances displayed with straight and dotted lines) (**A**). **B** shows the cell lysis corresponding *to* a 3-h incubation measured in the lactate dehydrogenase (LDH) assay, and **C** the protein/cell density after 24-h exposure to PRMs, using the sulforhodamine B assay. Data are represented as mean ± SD of n ≥ 3

were limited to 3 h. Extract A1 from strain UTEX-2797 was applied in concentrations ranging from 5 to 40 nM (SI Fig. 2A), and a strong cytotoxic potential could be observed. An EC_{50} of 12.7 ± 0.3 nM was calculated. The C-type PRM extract of the *P. parvum* strain RCC-191 was also tested for their cytotoxic potential towards HCEC-1CT cells (SI Fig. 2B). A continuous decrease in cell viability could be observed, although 100% cell death was not reached.

The single compound samples, two B-type (sB1 and sB2) and one A-type (sA1), were also assessed for their effects on cell viability (Fig. 4). An EC_{50} value was estimated at 76 ± 34 nM for sA1 (Fig. 4A). Exposure to sB1 and sB2 also resulted in a continuous decline of cell viability, an EC_{50} values of 220 ± 30 nM and 270 ± 160 nM were calculated, respectively. In the LDH assay, however, cell damage could not be detected until a viability of ≤ 45% was attained in the CTB. For better comparison, the EC_{50} values obtained from CTB assays were translated into the sum of PRM analogs in µg/L (SI Table 3 and SI Formula 1).

Finally, a comparative assessment was performed between *P. parvum* extracts obtained at different dates. This was performed to measure possible variabilities between extractions, as well as influences of storage time on toxicity (SI Fig. 3). Both extracts of the UTEX-2797 strain, harvested 3 years apart, showed a distinct positive correlation between PRM concentration and cytotoxic effects. Nonetheless, extract A1 was significantly more potent than A2; 16 nM of A1 reduced cell viability to 15%, whereas exposure to the same concentration of A2 only achieved a decrease to 73%. Interestingly, this considerable difference in potency could no longer be observed for the highest concentration. It was striking that the prymnesin profile differed between these two strains as previously mentioned (SI Table 4). Similarly, four B-type PRM extracts derived from strain K-0081 were tested for biological variance (Fig. 3B). Unlike the results for the A-type extracts, the responses of HCEC-1CT cell exposure to the B-type samples were nearly identical and also the prymnesin profile was quite similar (SI Table 4).

Cytotoxicity in ion-free media—fluorescence microscopy

RTgill-W1 cells and HCEC-1CT cells were stained with Hoechst and CellMask™ for live-cell imaging to visualize the cell nuclei and the cell membrane. A concentration of 6 nM of A-type sample A3 was applied to RTgill-W1, and

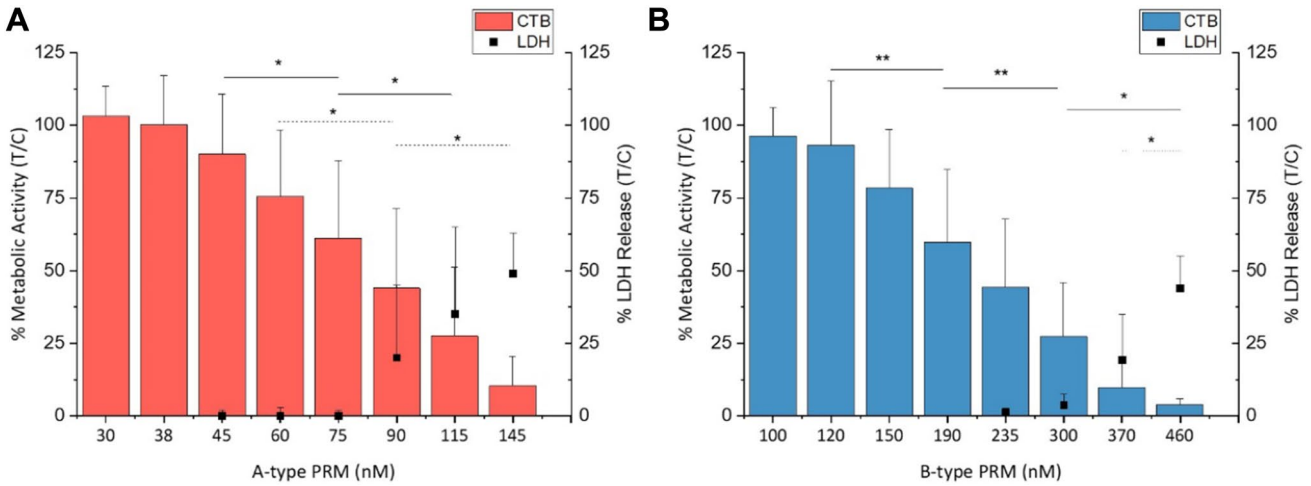

Fig. 4 Cell viability and membrane integrity of HCEC-1CT cells after 3-h incubation with single compounds of A-type prymnesin (PRM) sA1 derived from UTEX-2784 (**A**). In **B** the same can be seen for B-type PRM single substance solution of sB1. Cell titer blue (CTB) (straight line) and lactate dehydrogenase (LDH) (dotted line) assay data are represented as mean ± SD of n = 5

three concentrations of B-type PRM extract B1 were applied to the HCEC-1CT cells. Toxin solutions were prepared in LCIS (only for HCEC-1CT), NES, Na^+-free, Cl^--free, and Ca^{2+}-free medium.

Image analyses for RTgill-W1 cells were performed with the aid of Gen5 Software as well as the ImageJ Software. The time point t_2 (3 h) was chosen for analysis of the effects of the treatment on the RTgill-W1 cells. The nuclear morphometric parameters like area and circularity were evaluated as indicators of the osmotic stress (Finan and Guilak 2009) for each cell that was counted within one image using Gen5. All data points for these two parameters, gathered throughout several biological replicates, were plotted for each medium (Fig. 5). Additionally, the ratio between cellular and nuclear area was assessed, by random manual selection of twelve cells per image using ImageJ (Fig. 5). Exposure of RTgill-W1 cells to PRMs lead to an increase in nuclear circularity in the control medium (NES). This effect was just as pronounced in Ca^{2+}-free and Na^+-free medium (Fig. 5). The impact on nuclear circularity of RTgill-W1 cells exposed to PRMs in Cl^--free medium could also be observed, albeit not as evident. Although Cl^--free medium in general caused a slight increase in circularity, as can be seen in the solvent control in Fig. 5A, which was not observed for the other media. Example images for fluorescent staining are provided in SI Fig. 4 and phase contrast images are shown in SI Fig. 5.

Interestingly, incubation of RTgill-W1 cells in Cl^--free medium also resulted in a slightly larger nuclear area, compared to in NES medium. This could indicate that the change in nuclear morphology observed in medium lacking Cl^- ions may be due to the medium itself, as opposed to the exposure to PRMs. It is worth mentioning that PRM-exposure in Ca^{2+}-free medium had an effect on the nuclear area as well (Fig. 5). Here, however, the change in area was not observed in the solvent control. The ratio of the cell area versus the nucleus area is provided in SI Fig. 6.

For analysis of the HCEC-1CT cells, the total cellular area per well was divided by the number of nuclei detected to obtain the average area per cell. This value was used for comparison between the different testing conditions and time points. Each timepoint was related to LCIS without PRMs at t_0 (before incubation). Images were taken after 1.5 h (t_1) and 3 h (t_2). At t_1, the mean cellular area decreased after exposure to PRMs in all media but the Cl^--free (SI Table 6). A further decline was observed when the incubation time was extended for another 1.5 h (total of 3 h). For PRMs in the Cl^--free medium, a slight increase in area of about 14% was observed. SI Figs. 7, 8, 9, 10, 11 provide representative images of the solvent control in the different media at t_0 and t_3 and the two higher PRM-concentrations tested (t_3).

Building on the assumption that Cl^- could be relevant for PRM toxicity, the impact of the lack thereof was assessed in cell viability analyses for HCEC-1CT cells, as the effect was more pronounced in this cell line. Since the CTB dye solution contains NaCl, alternative cell viability assays were required, and it was found out that neither the LDH- nor the CV-assay interfere with the cellular osmotic equilibrium. The B-type PRM extract was prepared in HCEC-1CT culture medium, LCIS, and Cl^--free medium (SI Table 7). Three PRM concentrations were tested per condition. The LDH assay showed a clear lytic effect for the highest concentration of PRMs in culture medium and in LCIS, albeit to a much lower extent. No significant toxicity was measured for the Cl^--free medium, which is in accordance with the live imaging data. The influence of ions was also tested for

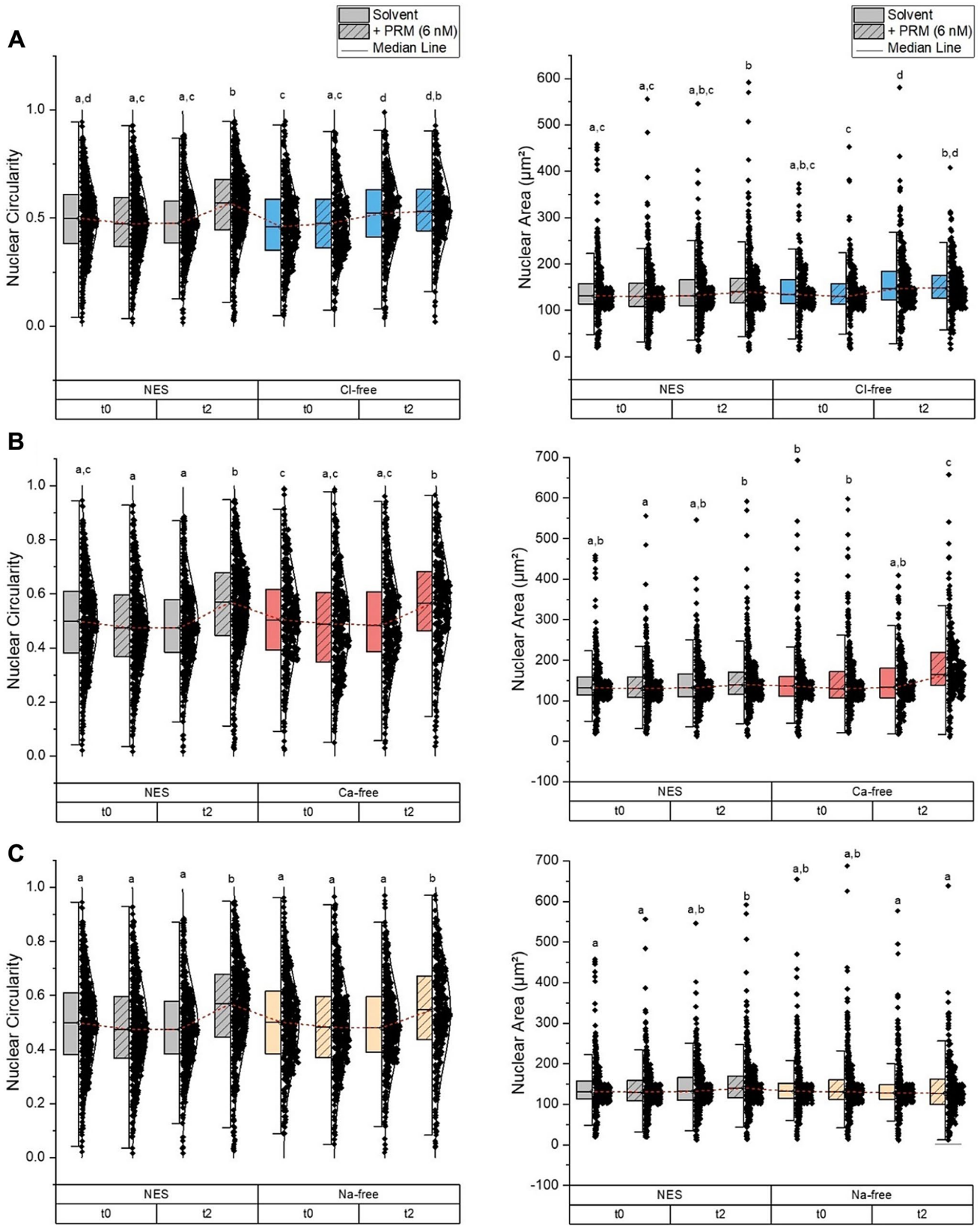

Fig. 5 Nuclear circularity and nuclear area of RTgill-W1 cells after 3-h exposure to A-type prymnesins (PRMs) of solution A3 in normal external solution (NES), Cl^--free medium (**A**), Ca^{2+}-free medium (**B**), and Na^+-free medium (**C**). Graphs show all data points collected from biological replicates of $n \geq 3$

A-type PRMs. The solution A3 of unknown strain origin was tested for its toxicity in NES, Na^+-free, Ca^{2+}-free, and Cl^--free medium. As expected, a high cytotoxic potential was measured for all media except for the medium containing no Cl^-. Cellular changes upon exposure were captured with bright field images (SI Fig. 12).

Discussion

All prymnesin extracts of *P. parvum* tested in this project were cytotoxic. Only minimal differences in the potency were observed between the two exposure times (3 h and 24 h), indicating that PRMs act quickly. For instance, the EC_{50} values of the K-0081 extract B1 only differed by 25 nM between the two incubation times in HCEC-1CT (170 ± 9 nM and 145 ± 7 nM for 3 and 24 h, respectively) and for 68 nM in RTgill-W1 (see SI Table 5). This similarity indicates that even a short-term interaction with PRMs can cause substantial adverse effects, and that longer exposure would not significantly increase the effect in vitro. This theory was highlighted during fluorescence live-cell imaging, where cells visibly changed their morphology after a 1.5-h exposure to PRMs already. These findings are supported by the observations made by Svendsen et al. (2018), who found that short-term exposure to *P. parvum* microalgae had considerable negative effects on rainbow trout fish, which were not reversible.

Generally, the fish gill cell line was more susceptible to the PRMs than HCEC-1CT cells, albeit to a small degree. This observation also withstood when compared to the data described by Rasmussen et al. (2016a), where RTgill-W1 cells were exposed to A- and B-type PRMs for three hours. Either way, the experiments here showed that *P. parvum* toxins can be just as effective towards human-derived cells. This should be kept in mind for future HAB episodes although no human incident has been reported to this day. In the *P. parvum* bloom in the Oder River in August 2022, beside 360 t of dead fish, also the death of freshwater bivalves, other mollusks as well as birds, ducks, beavers and other wildlife was reported, but could not be directly linked to the HAB (Free et al. 2023). Nonetheless, algal toxins often accumulate in bivalves and shellfish (not shown for PRMs yet), which are then consumed by humans (Hallegraeff 1993; Rasmussen et al. 2016b). Thus, it is not entirely inconceivable that humans can be exposed to toxic PRMs as well (Manning & La Claire 2010; Vasas et al. 2012). Should humans consume contaminated shellfish, PRMs may pass through the gastrointestinal tract, where the pH is naturally low; pH 1.3–1.7, in the stomach (Dressman et al. 1990; Russel et al. 1993). How PRMs would behave in this environment is debatable. Higher hemolytic potential has been described for PRMs at lower pH, yet maximum ichthyotoxicity was observed at pH 9 (Igarashi et al. 1998; Manning & la Claire 2010; Ulitzur and Shilo 1964). Another possibility for humans to get in touch with PRMs is through bathing in contaminated water. Thus, assessing an impact of PRMs on skin/skin cells would be the next step towards understanding their hazard to humans.

A clear order of potency was observed in both HCEC-1CT and RTgill-W1 cells, with A-type PRMs being the most potent, and B-type the least. These findings are in accordance with the previously published results by Rasmussen et al. (2016a). For A-type PRM samples, concentrations were usually in the low nmol/L region, and C-type PRM concentrations were in a similar range. Meanwhile to achieve an equivalent cytotoxic effect, B-type PRM had to be applied in much larger molarities. Identifying the *P. parvum* strain is thus a crucial detail for assessing the risk of a *P. parvum* bloom. In yet another study, acute ichthyotoxicity of five strains of *P. parvum* in rainbow trout fish was analyzed, in which strains UTEX-2797 and K-0081 were found to be the two most potent (Blossom et al. 2014). This unexpected outcome, with a B-type strain being among the most toxic, is contrary to what has been known about PRM toxicity so far. This led to further investigations, and the studies showed that the cellular content of PRMs differs substantially among the *P. parvum* strains (Binzer et al. 2019; Svenssen et al. 2019). As an example for B-type PRM, cells of the strain K-0081 could contain up to 30 times more toxin than K-0374 (Medić et al. 2022; Svenssen et al. 2019).

A number of environmental factors such as pH, irradiance/sunlight, temperature, salinity, and nutrient availability have an impact on the growth of *P. parvum*, toxin content and toxin production (Hill et al. 2020; Manning and La Claire 2010; Medić et al. 2022; Svenssen et al. 2019; Taylor et al. 2021). However, many more studies are required to understand the production and release of PRMs. For instance, Medić et al. (2022) observed that the production of PRMs was directly coupled to the growth rate in the strain K-0081 grown at different irradiances, while this was not the case of the K-0734 strain (Medić et al. 2022).

Little is understood of the biosynthesis of marine secondary metabolites, yet, given their polyketide structure, the involvement of polyketide synthases is highly plausible (Anestis et al. 2021; Manning and La Claire 2010). The analyses of Anestis et al. (2021), showed a large number of polyketide synthase genes in nine *P. parvum* strains, although no clear connection to cellular PRM content could be found. Nonetheless, it was implied that toxin production in *P. parvum* comes at a metabolic cost (Anestis et al. 2021). Environmental conditions not only affect PRM synthesis and release, but also its stability, as shown for culture filtrates that lost acute toxicity towards fish after exposure to sunlight (Blossom et al. 2014; Taylor et al. 2021). Regarding these environmental factors, uniformity is needed for microalgal

cell culture conditions, as they can significantly affect the toxin production itself and consequently toxicological investigation (Brooks et al. 2010; Hill et al. 2020; Manning and La Claire 2010).

Considering the above, toxin quantification prior to toxicological research is just as crucial. One challenge for quantification, however, is posed by the extraction process, among other reasons due to low natural production and amphipathic properties of the compounds (Andersen et al. 2017; Svenssen et al. 2019; Tillmann 2003). A lack of reliable and commercially available standards combined with missing standardized isolation methods are the limiting factors for proper quantification of ichthyotoxins (Brooks et al. 2010; Manning et al. 2013; Svenssen et al. 2019). The method applied in this project was described by Svenssen et al. (2019), who reported an apparent recovery of 58%, which highlights the need for further improvement of ichthyotoxin extraction from biomass (Andersen et al. 2017; Svenssen et al. 2019). Loss during sample preparation can even hinder the applicability of those extracts in cytotoxicity assays, as the obtained concentrations might be too low, particularly when natural toxin production is already low (Svenssen et al. 2019). Taking this information into account, all given concentrations throughout this study should be interpreted as estimates. It is thus difficult to directly translate the results from the assays performed here into their potency in vivo. What can be done, though, is to draw relations between the strains and the PRM analogs produced, i.e. fish exposed to the RCC-191 strain could be expected to suffer less than when exposed to RCC-1436 under the condition that PRMs are produced in the same quantities.

When different strains producing the same type of PRM were compared, the identified PRM profiles differed greatly. This variability was mirrored in the cytotoxic potential. Extracting PRMs from the same microalgal biomass at different times in case of strain K-0081 had effectively no impact on the PRM profile and consequently the toxic properties (SI Table 4 and SI Fig. 3B). Although, when the relative amount of the same analog between samples differed in 10% or more (e.g., extract A1 vs. A2, SI Table 4), significant changes in toxicity were observed (SI Fig. 3A). Apparently, the kind of analogs produced by *P. parvum* are essential when it comes to their cytotoxic potential. Whether this toxicity depends on a particular type of analog and its relative quantity or a specific combination of several analogs could not be discerned. The most toxic sample used in this study was the A-type solution from unknown strain origin, with only 4.0 ± 0.2 nM PRMs to achieve a 50% effect. The second most potent A-type sample was a UTEX-2797 extract (A1). What both of these samples had in common, was the relatively high amount of PRM-A (3 Cl) + 2 pentose + hexose, with 23 and 63% for the extract and the single compound solution respectively. The second most abundant analog in both samples was PRM-A (3 Cl) + pentose. Whether it is a combination of these two that influences potency or the analogs themselves that are more cytotoxic than others remain unclear. By looking at the PRM profiles of the tested samples, cytotoxicity was not related to the sheer number of analogs produced. Which could be seen in the C-type extracts from RCC-1436 and RCC-191. Seven kinds of analogs were identified for the former, and fourteen for the latter, yet the higher number did not cause higher cytotoxic effects. Likewise, all single compound solutions consisted of fewer PRM analogs than the *P. parvum* extracts, yet in general, extracts were more potent. This phenomenon may not be explained by the number of analogs, but by the presence of other potentially toxic undetected compounds in the extracts. It can be assumed that *P. parvum* extracts contain molecules that are not identified as PRMs, which may or may not enhance the toxic potential of PRMs. Nevertheless, assessing the single compound solutions showed that even purified PRMs are cytotoxic, and thus the harmful effects observed during HAB events can be, at least in part, attributed to the presence of these ichthyotoxins. Further cytotoxicity evaluations of PRMs should focus on the individual analogs, in order to obtain information about the role they play in overall toxicity. Ideally, single analogs can be tested, followed by combinatorial assessments. With these results, it can be interpreted that the harmfulness of *P. parvum* strains is connected to (1) the type of PRM (A, B, or C), (2) the PRM profile and (3) PRM abundance (for HAB episodes).

The impact of PRM extracts and single compound solutions could be observed via live-cell imaging experiments, with visible effects on their morphology, probably related to their viability. As already established previously, PRMs cause pore formation in the cell membrane, through a yet unknown mechanism, which increases their permeability (Ulitzur and Shilo 1966; Yariv and Hestrin 1961). Higher ichthyotoxicity of PRMs in the presence of Ca^{2+} and Mg^{2+} had been observed previously, and it was postulated that these cations act as cofactors or activators for these ichthyotoxins (Shilo 1981; Ulitzur and Shilo 1964; Yariv and Hestrin 1961). In RTgill-W1 cells, however, the absence of Ca^{2+} seemed to exacerbate the effects caused by PRMs. As this was a cell culture experiment, it should be noted that Ca^{2+} plays a crucial role in cell–cell adhesion as well as adhesion to the plate surface (Takeichi and Okada 1972; Weiss 1960). Removing Ca^{2+} from the medium could therefore impact the attachment of RTgill-W1 cells to the well bottom. The effect observed for PRMs in Ca^{2+}-free medium may thus be at least partially attributed to this fact. Considering that no significant difference for the nuclear parameters was measured between the Ca^{2+}-free solvent control and the control medium NES, it can be assumed that the condition "PRM-Ca^{2+}" was indeed responsible for the observed outcome. It appears that HCEC-1CT cells were

affected differently by PRMs than RTgill-W1 cells, not only because of differences on a structural level, but potentially because of differences in regulatory processes of these cell lines. For HCEC-1CT cells, the absence of Na^+ or Ca^{2+} had no impact on PRM cytotoxicity. Removing Cl^- from the medium, however, decreased cytotoxicity in HCEC-1CT cells. As for the RTgill-W1 cells, the changes in the nuclear parameters upon incubation in Cl^--free medium were possibly caused by the medium itself, as the same changes could be observed in the Cl^--free solvent control. During preparation of the most promising recipe for the Cl^--free medium, it could be observed that the viability of RTgill-W1 cells is strongly affected by the absence of Cl^- ions, making it difficult to assess the impact of PRMs in a medium lacking this essential ion. Evidently, PRM toxicity is achieved through creating an osmotic imbalance after damaging the plasma membrane (Ulitzur and Shilo 1966). One explanation could be that PRMs interfere with Cl^- channels, which can regulate cell volume, control the ionic composition of cell plasma, or cellular pH (Jentsch et al. 2002; Verkman and Galietta 2009). Given that the presence of Ca^{2+} ions increased the toxicity in fish and their absence in this in vitro assay strengthened the toxic effects, it can also be suggested that PRM toxicity is intertwined with the Ca^{2+} regulation of gill cells (Shilo 1981; Ulitzur and Shilo 1964; Yariv and Hestrin 1961).

Fish are particularly dependent on osmoregulation and have evolved highly efficient ionoregulation systems in which gills are a key figure (Hwang et al. 2011). The osmoregulatory systems in fish are highly intricate and surpass the scope of this paper. To give a brief description though, fish gill cells can roughly be divided into two major cell types, ionocytes and pavement cells (Flik et al. 1997; Goss et al. 1995; Hwang et al. 2011). Active ion transport happens mainly in ionocytes, where Na^+ and Cl^- uptake is regulated via the Na^+/K^+-ATPase (Lin et al. 1994; Marshall 1995, 2002). The vacuolar-type H^+-ATPase, supports the transport of ions through maintaining the cellular pH, generating electrochemical gradients, and indirectly contributing to ion exchangers (Hwang and Lee 2007; Hwang et al. 2011; Marshall 2002). This H^+-ATPase is activated by external Ca^{2+} and can be downregulated by high external Na^+ content (Lin et al. 1994). Ca^{2+} uptake involves a Ca^{2+} channel and is linked to Na^+ transport (Flik et al. 1997; Hwang et al. 2011; Marshall 2002). Gills are the main site for Ca^{2+} uptake in freshwater fish, and Ca^{2+} channels have been found in both pavement cells as well as ionocytes (Hwang et al. 2011; Shahsavarani et al. 2006).

Importantly, RTgill-W1 cells lack the characteristics of pavement cells and ionocytes, for they are apparently derived from undifferentiated gill precursor stem cells (Bols et al. 1994; Lee et al. 2009). The ion regulation of this cell line must thereby differ, at least to a certain degree, from the physiological functions described for rainbow trout gill cells. It can be reasonably expected that Na^+/K^+-ATPase is expressed in RTgill-W1 cells, as this pump is present in nearly all animal cells (Marshall 2002). Whether the functions of this pump are coupled with other ATPases relevant in *in-vivo* models remains to be elucidated. Clearly, in vivo as well as in vitro, PRMs seem to interfere with the Cl^- and Ca^{2+} homeostasis of the cells, ultimately leading to complete ionodysregulation should the toxin persist in the environment. It is interesting, how Na^+ elimination from the cell culture medium had no effect on the PRM toxicity in both RTgill-W1 as well as in HCEC-1CT cells. Specifically, because Na^+ and Cl^- regulation is often strongly interspersed (Hwang et al. 2011; Marshall 2002). Seeing how gills are vital organs for osmoregulation, the effect PRMs have on the ionoregulation is either a result of PRM toxicity or integral to the toxic mode of action or PRMs (Hwang et al. 2011; Lee et al. 2009). Further studies are needed to better understand this correlation.

In conclusion, it was shown that toxicity of *P. parvum* extracts is indeed caused by PRMs, although a combined effect with other unidentified compounds cannot be ruled out. Furthermore, the results clearly show that toxicity of PRMs is not limited to fish cells, but human cells as exemplified for HCEC-1CT, are affected in comparable concentration ranges. Strains producing the same type of PRM do not necessarily synthesize the same PRM analogs, and apparently, the kind and relative amount of analog used for toxicity testing impacts the overall toxicity. Studying the cytotoxicity of single analogs could paint a clearer picture of the mode of action of PRMs. Comparing the potency and the structure of each may reveal which structural and functional moieties are more prominent in highly toxic strains. Visible changes in the plasma membrane and nuclei resulted from exposure to PRMs, but so far it remains unclear how these ichthyotoxins induce that change. The effects in RTgill-W1 cells resulting from PRM exposure could be impacted by the absence of Cl^- and Ca^{2+} ions. It would be advisable to further investigate the impact of these ions on the PRM toxicity. For a complete picture, the role ion channels and regulators for osmotic balance play should be examined. As Cl^- lowered cytotoxic activity towards HCEC-1CT and in part towards RTgill-W1 cells, it would be of particular interest to study the involvement of Cl^--channels on a molecular level. Other membrane structures, such as cholesterol, sphingomyelins or phospholipids could also be relevant in PRM toxicity and interactions with those are worth exploring as well.

Electronic supplementary material The online version of this article (https://doi.org/10.1007/s00204-023-03663-5) contains supplementary material, which is available to authorized users.

Acknowledgements The authors want to acknowledge the initial work of prymnesin purification by Silas Anselm Rasmussen, Sofie Bjørnholt Binzer, Daniel Killerup Svenssen and Kristian Fog Nielsen in the HABFISH and/or SAFEFISH project conducted at the University of Copenhagen and the Technical University of Denmark. Tom Shier from the Department of Medicinal Chemistry, College of Pharmacy, University of Minnesota gratefully provided the A-type prymnesin solution previously available from Sigma Aldrich. Kristin Schirmer from the Department of Environmental Toxicology, EAWAG and Jerry W. Shay from the UT Southwestern Medical Center are acknowledged for the provision of the RTgill-W1 and the HCEC-1CT cell line, respectively. Imaging workflows were supported by the Core Facility Multimodal Imaging (Faculty of Chemistry, University of Vienna) member of the VLSI (Vienna Life Science Instruments). Maximilian Jobst and Janice A. Bergen are acknowledged for their input to data evaluation of imaging data. Peter Frühauf and the Department of Analytical Chemistry at the University of Vienna is acknowledged for the provision of the fluorescence detector and Franz Berthiller of the University of Natural Resources and Life Sciences, Vienna (BOKU) for the opportunity to perform LC-HRMS measurements on the 6550 iFunnel Q-TOF LC-MS system.

Author contributions Conceptualization, E.V., G.D.F, D.M.; methodology, E.V., G.D.F., T.O.L., P.J.H. and D.M.; formal analysis, investigation, data curation and visualization, E.V., H.C.P., M.R., N.H., D.B., N.M.; resources, E.V., N.M., G.D.F., T.O.L., P.J.H. and D.M.; writing—original draft preparation, E.V., H.C.P.; writing—review and editing, all co-authors; supervision, E.V., and D.M.; project administration, E.V.; funding acquisition, E.V., T.O.L. and P.J.H.; all authors have read and agreed to the published version of the manuscript. The authors have no relevant financial or non-financial interests to disclose.

Funding Open access funding provided by University of Veterinary Medicine Vienna. This research was funded in whole or in part by the Austrian Science Fund (FWF) [grant DOI:10.55776/I5707]. For open access purposes, the author has applied a CC BY public copyright license to any author accepted manuscript version arising from this submission. FWF-funding through the Erwin-Schrödinger fellowship [J3895-N28] awarded to Elisabeth Varga and the FWF-French National Research Agency (ANR) joint international project [I-5707] was received. Furthermore, the research was supported by the University of Vienna, Faculty of Chemistry, Department of Food Chemistry and Toxicology. The presented work is based on knowledge obtained through the Innovation Fund Denmark projects, SAFEFISH [project No. 4097-00007B] and HABFISH [project No 0603-00449B)]. Nikola Medić was funded by the European Union's Horizon 2020 research and innovation program under the Marie Skłodowska-Curie grant agreement number [766327] (MixITiN).

Data availability The authors declare that the data supporting the findings of this study are available within the paper and its Supplementary Information files. Should any raw data files be needed in another format they are available from the corresponding author upon reasonable request.

Declarations

Competing interests The authors have no competing interests to declare that are relevant to the content of this article. The funders had no role in the design of the study; in the collection, analyses, or interpretation of data; in the writing of the manuscript, or in the decision to publish the results.

References

Andersen AJC, De Medeiros LS, Binzer SB, Rasmussen SA, Hansen PJ, Nielsen KF, Jorgensen K, Larsen TO (2017) HPLC-HRMS quantification of the Ichthyotoxin Karmitoxin from *Karlodinium armiger*. Mar Drugs 15(9):278. https://doi.org/10.3390/md15090278

Anestis K, Kohli GS, Wohlrab S, Varga E, Larsen TO, Hansen PJ, John U (2021) Polyketide synthase genes and molecular trade-offs in the ichthyotoxic species *Prymnesium parvum*. Sci Total Environ 795:148878. https://doi.org/10.1016/j.scitotenv.2021.148878

Baden DG (1989) Brevetoxins: unique polyether dinoflagellate toxins. FASEB J 3:1807–1817. https://doi.org/10.1096/fasebj.3.7.2565840

Benson JM, Tischler DL, Baden DG (1999) Uptake, tissue distribution, and excretion of brevetoxin 3 administered to rats by intratracheal instillation. J Toxicol Environ Part A 57(5):345–355. https://doi.org/10.1080/009841099157656

Binzer SB, Svenssen DK, Daugbjerg N, Alves-de-Souza C, Pinto E, Hansen PJ, Larsen TO, Varga E (2019) A-, B-and C-type prymnesins are clade specific compounds and chemotaxonomic markers in *Prymnesium parvum*. Harmful Algae 81:10–17. https://doi.org/10.1016/j.hal.2018.11.010

Blossom HE, Rasmussen SA, Andersen NG, Larsen TO, Nielsen KF, Hansen PJ (2014) *Prymnesium parvum* revisited: Relationship between allelopathy, ichthyotoxicity, and chemical profiles in 5 strains. Aquat Toxicol 157:159–166. https://doi.org/10.1016/J.AQUATOX.2014.10.006

Bols NC, Barlian A, Chirino-Trejo M, Caldwell SJ, Goegan P, Lee LEJ (1994) Development of a cell line from primary cultures of rainbow trout, *Oncorhynchus mykiss* (Walbaum), gills. J Fish Dis 17(6):601–611. https://doi.org/10.1111/j.1365-2761.1994.tb00258.x

Brooks BW, James SV, Valenti TW Jr, Urena-Boeck F, Serrano C, Berninger JP, Schwierzke L, Mydlarz LD, Grover JP, Roelke DL (2010) Comparative toxicity of *Prymnesium parvum* in inland waters. JAWRA 46(1):45–62. https://doi.org/10.1111/J.1752-1688.2009.00390.X

Del Favero G, Florio C, Codan B, Sosa S, Poli M, Sbaizero O, Molgó J, Tubaro A, Lorenzon P (2012) The stretch-activated channel blocker Gd^{3+} reduces palytoxin toxicity in primary cultures of skeletal muscle cells. Chem Res Toxicol 25(9):1912–1920. https://doi.org/10.1021/tx300203x

Del Favero G, Zaharescu R, Marko D (2018) Functional impairment triggered by altertoxin II (ATXII) in intestinal cells *in vitro*: crosstalk between cytotoxicity and mechanotransduction. Arch Toxicol 92:3535–3547. https://doi.org/10.1007/s00204-018-2317-6

Dressman JB, Berardi RR, Dermentzoglou LC, Russell TL, Schmaltz SP, Barnett JL, Jarvenpaa KM (1990) Upper gastrointestinal (GI) pH in young, healthy men and women. Pharm Res 7(7):756–761. https://doi.org/10.1023/A:1015827908309

Finan JD, Guilak F (2009) The effects of osmotic stress on the structure and function of the cell nucleus. J Cell Biochem 109(3):460–467. https://doi.org/10.1002/jcb.22437

Fischer M, Belanger SE, Berckmans P, Bernhard MJ, Bláha L, Coman Schmid DE, Dyer SC, Haupt T, Hermens JLM, Hultman MT, Laue H, Lillicrap A, Mlnarikova M, Natsch A, Novak J, Sinnige TL, Tollefsen KE, van Niederhäusern V, Witters H, Zupanic A, Schirmer K (2019) Repeatability and reproducibility of the RTgill-W1 cell line assay for predicting fish acute toxicity. Toxicol Sci 169(2):353–364. https://doi.org/10.1093/toxsci/kfz057

Flik G, Kaneko T, Greco AM, Li J, Fenwick JC (1997) Sodium dependent ion transporters in trout gills. Fish Physiol Biochem 17:385–396. https://doi.org/10.1023/A:1007768825043

Free G, Van de Bund W, Gawlik B, Van Wijk L, Wood M, Guagnini E, Koutelos K, Annunziato A, Grizzetti B, Vigiak O, Gnecchi M, Poikane S, Christiansen T, Whalley C, Antognazza F, Zerger B, Hoeve R, Stielstra H. (2023) An EU analysis of the ecological disaster in the Oder River of 2022. Publications Office of the European Union, EUR 31418 EN, 1–44. https://doi.org/10.2760/067386, JRC132271

Goss G, Perry S, Laurent P (1995) 10 ultrastructural and morphometric studies on ion and acid-base transport processes in freshwater fish. Fish Physiol 14:257–284. https://doi.org/10.1016/S1546-5098(08)60249-6

Granéli E, Salomon PS (2010) Factors influencing allelopathy and toxicity in *Prymnesium parvum*. JAWRA 46(1):108–120. https://doi.org/10.1111/j.1752-1688.2009.00395.x

Guillard RR (1975) Culture of phytoplankton for feeding marine invertebrates. In: Smith WL, Chanley MH (eds) Culture of Marine Invertebrate Animals. Springer, Boston pp 29–60. https://doi.org/10.1007/978-1-4615-8714-9_3

Hallegraeff GM (1993) A review of harmful algal blooms and their apparent global increase. Phycologia 32(2):79–99. https://doi.org/10.2216/I0031-8884-32-2-79.1

Hallett CS, Valesini FJ, Clarke KR, Hoeksema SD (2016) Effects of a harmful algal bloom on the community ecology, movements and spatial distributions of fishes in a microtidal estuary. Hydrobiologia 763(1):267–284. https://doi.org/10.1007/s10750-015-2383-1

Hill BN, Saari GN, Steele WB, Corrales J, Brooks BW (2020) Nutrients and salinity influence *Prymnesium parvum* (UTEX LB 2797) elicited sublethal toxicity in *Pimephales promelas* and *Danio rerio*. Harmful Algae 93:101795. https://doi.org/10.1016/j.hal.2020.101795

Hwang PP, Lee TH (2007) New insights into fish ion regulation and mitochondrion-rich cells. Comp Biochem Physiol A Mol Integr Physiol 148(3):479–497. https://doi.org/10.1016/j.cbpa.2007.06.416

Hwang PP, Lee TH, Lin LY (2011) Ion regulation in fish gills: recent progress in the cellular and molecular mechanisms. Am J Physiol - Regul 301(1):R28–R47. https://doi.org/10.1152/ajpregu.00047.2011

Igarashi T, Satake M, Yasumoto T (1996) Prymnesin-2: a potent ichthyotoxic and hemolytic glycoside isolated from the red tide alga *Prymnesium parvum*. J Am Chem Soc 118(2):479–480. https://doi.org/10.1021/ja9534112

Igarashi T, Aritake S, Yasumoto T (1998) Biological activities of prymnesin-2 isolated from a red tide alga *Prymnesium parvum*. Nat Toxins 6(1):35–41. https://doi.org/10.1002/(SICI)1522-7189(199802)6:13.0.CO;2-7

Igarashi T, Satake M, Yasumoto T (1999) Structures and partial stereochemical assignments for prymnesin-1 and prymnesin-2: potent hemolytic and ichthyotoxic glycosides isolated from the red tide alga *Prymnesium parvum*. J Am Chem Soc 121(37):8499–8511. https://doi.org/10.1021/ja991740e

Jentsch TJ, Stein V, Weinreich F, Zdebik AA (2002) Molecular structure and physiological function of chloride channels. Physiol Rev 82(2):503–568. https://doi.org/10.1152/physrev.00029.2001

Lee LEJ, Dayeh VR, Schirmer K, Bols NC (2009) Applications and potential uses of fish gill cell lines: examples with RTgill-W1. In Vitro Cell Dev Biol 45(3):127–134. https://doi.org/10.1007/s11626-008-9173-2

Lin H, Pfeiffer DC, Vogl AW, Pan J, Randall DJ (1994) Immunolocalization of H^+-ATPase in the gill epithelia of rainbow trout. J Exp Biol 195(1):169–183. https://doi.org/10.1242/JEB.195.1.169

Manning SR, La Claire JW (2010) Prymnesins: toxic metabolites of the golden alga, *Prymnesium parvum* Carter (Haptophyta). Mar Drugs 8(3):678–704. https://doi.org/10.3390/md8030678

Manning SR, La Claire JW II (2013) Isolation of polyketides from *Prymnesium parvum* (Haptophyta) and their detection by liquid chromatography/mass spectrometry metabolic fingerprint analysis. Anal Biochem 442(2):189–195. https://doi.org/10.1016/j.ab.2013.07.034

Marshall WS (1995) 1 transport processes in isolated teleost epithelia: opercular epithelium and urinary bladder. Fish Physiol 14:1–23. https://doi.org/10.1016/S1546-5098(08)60240-X

Marshall WS (2002) Na^+, Cl^-, Ca^{2+} and Zn^{2+} transport by fish gills: retrospective review and prospective synthesis. J Exp Zool 293(3):264–283. https://doi.org/10.1002/jez.10127

McKim JM, Bradbury SP, Niemi GJ (1987) Fish acute toxicity syndromes and their use in the QSAR approach to hazard assessment. Environ Health Perspect 71:171–186. https://doi.org/10.1289/ehp.8771171

Medić N, Varga E, Van de Waal DB, Larsen TO, Hansen PJ (2022) The coupling between irradiance, growth, photosynthesis and prymnesin cell quota and production in two strains of the bloom-forming haptophyte *Prymnesium parvum*. Harmful Algae 112:102173. https://doi.org/10.1016/j.hal.2022.102173

OECD (2021) Test No. 249: fish cell line acute toxicity – The RTgill-W1 cell line assay. Organisation for Economic Co-operation and Development (OECD) Guidelines for the Testing of Chemicals, Section 2, OECD Publishing, Paris, https://doi.org/10.1787/c66d5190-en.

Otterstrom CV, Steemann-Nielsen E (1939) Two cases of extensive mortality in fishes caused by the flagellate *Pryrnnesium parvum* Carter. Report Danish Biol St 44:5–24

Rasmussen SA, Meier S, Andersen NG, Blossom HE, Duus JØ, Nielsen KF, Hansen PJ, Larsen TO (2016a) Chemodiversity of ladder-frame prymnesin polyethers in *Prymnesium parvum*. J Nat Prod 79(9):2250–2256. https://doi.org/10.1021/acs.jnatprod.6b00345

Rasmussen SA, Andersen AJC, Andersen NG, Nielsen KF, Hansen PJ, Larsen TO (2016b) Chemical diversity, origin, and analysis of phycotoxins. J Nat Prod 79(3):662–673. https://doi.org/10.1021/ACS.JNATPROD.5B01066

Rebhahn VIC, Kiss E, Marko D, Del Favero G (2022) Foodborne compounds that alter plasma membrane architecture can modify the response of intestinal cells to shear stress *in vitro*. Toxicol Appl Pharmacol 446:116034. https://doi.org/10.1016/j.taap.2022.116034

Russell TL, Berardi RR, Barnett JL, Dermentzoglou LC, Jarvenpaa KM, Schmaltz SP, Dressman JB (1993) Upper gastrointestinal pH in seventy-nine healthy, elderly, North American men and women. Pharm Res 10(2):187–196. https://doi.org/10.1023/A:1018970323716

Ryan JP, Kudela RM, Birch JM, Blum M, Bowers HA, Chavez FP, Doucette GJ, Hayashi K, Marin R III, Mikulski CM, Pennington JT, Scholin CA, Smith GJ, Woods A, Zhang Y (2017) Causality of an extreme harmful algal bloom in Monterey Bay, California, during the 2014–2016 northeast Pacific warm anomaly. Geophys Res Lett 44(11):5571–5579. https://doi.org/10.1002/2017GL072637

Sanseverino I, Conduto D, Pozzoli L, Dobricic S, Lettieri T (2016) Algal bloom and its economic impact. JRC Technical Reports. EUR 27905 EN. https://doi.org/10.2788/660478

Segner H (1998) Fish cell lines as a tool in aquatic toxicology. Fish Ecotoxicol 86:1–38. https://doi.org/10.1007/978-3-0348-8853-0_1

Shahsavarani A, McNeill B, Galvez F, Wood CM, Goss GG, Hwang PP, Perry SF (2006) Characterization of a branchial epithelial calcium channel (ECaC) in freshwater rainbow trout (*Oncorhynchus mykiss*). J Exp Biol 209(10):1928–1943. https://doi.org/10.1242/jeb.02190

Shilo M (1967) Formation and mode of action of algal toxins. Bacteriol Rev 31(3):180–193. https://doi.org/10.1128/br.31.3.180-193.1967

Shilo M (1981) The toxic principles of *Prymnesium parvum*. In: The water environment: Algal toxins and health. Boston, MA: Springer US, pp 37–47 https://doi.org/10.1007/978-1-4613-3267-1_4

Svendsen MBS, Andersen NR, Hansen PJ, Steffensen JF (2018) Effects of harmful algal blooms on fish: Insights from *Prymnesium parvum*. Fishes 3(1):11. https://doi.org/10.3390/FISHES3010011

Svenssen DK, Binzer SB, Medić N, Hansen PJ, Larsen TO, Varga E (2019) Development of an indirect quantitation method to assess ichthyotoxic B-type prymnesins from *Prymnesium parvum*. Toxins 11(5):251. https://doi.org/10.3390/toxins11050251

Takeichi M, Okada TS (1972) Roles of magnesium and calcium ions in cell-to-substrate adhesion. Exp Cell Res 74(1):51–60. https://doi.org/10.1016/0014-4827(72)90480-6

Taylor RB, Hill BN, Langan LM, Chambliss CK, Brooks BW (2021) Sunlight concurrently reduces *Prymnesium parvum* elicited acute toxicity to fish and prymnesins. Chemosphere 263:127927. https://doi.org/10.1016/J.CHEMOSPHERE.2020.127927

Tillmann U (2003) Kill and eat your predator: A winning strategy of the planktonic flagellate *Prymnesium parvum*. Aquat Microb Ecol 32:73–84. https://doi.org/10.3354/ame032073

Tsai DD-W, Ramaraj R, Chen PH (2012) Growth condition study of algae function in ecosystem for CO_2 bio-fixation. J Photochem Photobiol b, Biol 107:27–34. https://doi.org/10.1016/j.jphotobiol.2011.11.005

Ulitzur S, Shilo M (1964) A sensitive assay system for determination of the ichthyotoxicity of *Prymnesium parvum*. Microbiol 36(2):161–169. https://doi.org/10.1099/00221287-36-2-161

Ulitzur S, Shilo M (1966) Mode of action of *Prymnesium parvum* ichthyotoxin. J Protoz 13(2):332–336. https://doi.org/10.1111/J.1550-7408.1966.TB01915.X

Vasas G, Márta M, Borics G, Gonda S, Máthé C, Jámbrik K, Nagy ZL (2012) Occurrence of toxic *Prymnesium parvum* blooms with high protease activity is related to fish mortality in Hungarian ponds. Harmful Algae 17:102–110. https://doi.org/10.1016/j.hal.2012.03.007

Verkman AS, Galietta LJ (2009) Chloride channels as drug targets. Nat Rev Drug Discov 8(2):153–171. https://doi.org/10.1038/nrd2780

Weiss L (1960) Studies on cellular adhesion in tissue culture: III. Some effects of calcium. Exp Cell Res 21(1):71–77. https://doi.org/10.1016/0014-4827(60)90347-5

Yariv J, Hestrin S (1961) Toxicity of the extracellular phase of *Prymnesium parvum* cultures. Microbiol 24(2):165–175. https://doi.org/10.1099/00221287-24-2-165

Cytotoxicity of *Prymnesium parvum* extracts and prymnesin analogs on epithelial fish gill cells RTgill-W1 and the human colon cell line HCEC-1CT

Elisabeth Varga[1,2,#,*] and Hélène-Christine Prause[1,3,#], Matthias Riepl[1], Nadine Hochmayr[1], Deniz Berk[1], Eva Attakpah[1], Endre Kiss[1,4], Nikola Medić[5,6], Giorgia Del Favero[1,4], Thomas Ostenfeld Larsen[7], Per Juel Hansen[5], Doris Marko[1]

1 Department of Food Chemistry and Toxicology, Faculty of Chemistry, University of Vienna, Währinger Str. 38-40, 1090 Vienna, Austria.
2 Unit Food Hygiene and Technology, Institute of Food Safety, Food Technology and Veterinary Public Health, University of Veterinary Medicine, Vienna, Veterinärplatz 1, 1210 Vienna, Austria.
3 Vienna Doctoral School in Chemistry, Faculty of Chemistry, University of Vienna, Währinger Str. 42, 1090 Vienna, Austria.
4 Core Facility Multimodal Imaging, Faculty of Chemistry, University of Vienna, Währinger Str. 38-42, 1090 Vienna, Austria.
5 Marine Biological Section, Department of Biology, University of Copenhagen, Strandpromenaden 5, 3000 Helsingør, Denmark.
6 Center for Bioresources, Division for Food and Production, Danish Technological Institute, Gregersensvej 8, 2630 Taastrup, Denmark
7 Department of Biotechnology and Biomedicine, Technical University of Denmark, Søltofts Plads 221, 2800 Kgs. Lyngby, Denmark.

# Both authors contributed equally.

*Correspondence: elisabeth.varga@vetmeduni.ac.at; Tel.: +43 1 25077-3302

SI Table 1 Information on main differences of two RTgill-W1 cultivation media.

L-15 complete media	*Leibovitz's 15 media information*		*Complemented with (%)*		
	Reference and manufacturer	**Phenol red**	**L-glutamine (*v/v*)**	**FCS[#] (v/v)**	**P/S[#] (v/v)**
Recipe 1	21083027, Thermo Fisher Scientific	no	1 (included)	10	1
Recipe 2	L5520, Sigma-Aldrich	yes	1*	10	1

FCS Fetal calf serum; P/S; penicillin/streptomycin

*added separately from Thermo Fisher Scientific, Waltham, MA, USA

[#]Thermo Fisher Scientific, Waltham, MA, USA

SI Table 2 Media composition of ion-free media and media used for live-cell imaging.

Media for HCEC-1CT cells	*Desired concentration (mM)*	*Media for RTgill-W1 cells*	*Desired concentration (mM)*
Normal External Solution (NES)		**NES**	
NaCl	140.0	NaCl	140.0
KCl	2.8	KCl	5.6
$CaCl_2$	2.0	$CaCl_2$	1.3
$MgCl_2$	2.0	$MgCl_2$	1.7
HEPES	10.0	HEPES	10.0
Glucose	10.0	Galactose	5.0
pH adjusted to 7.3 with NaOH		pH adjusted to 7.3 with NaOH	
Na^+ free medium		**Na^+ free medium**	
N-methyl-D-glucamine	140.0	N-methyl-D-glucamine	140.0
KCl	2.8	KCl	5.6
$CaCl_2$	2.0	$CaCl_2$	1.3
$MgCl_2$	2.0	$MgCl_2$	1.7
HEPES	10.0	HEPES	10.0
Glucose	10.0	Galactose	5.0
pH adjusted to 7.3 with KOH		pH adjusted to 7.3 with KOH	
Ca^{2+} free medium		**Ca^{2+} free medium**	
NaCl	140.0	NaCl	140.0
KCl	2.8	KCl	5.6
$MgCl_2$	5.0	$MgCl_2$	1.7
EGTA	2.0	EGTA	/

HEPES	10.0	HEPES	10.0
Glucose	10.0	Galactose	5.0
pH adjusted to 7.3 with NaOH		pH adjusted to 7.3 with NaOH	
Cl^- free medium		**Cl^- free medium**	
Na_2SO_4	140.0	Na-acetate	140.0
K-gluconate	2.5	K-gluconate	17.4
$MgSO_4$ x 7 H_2O	1.0	$Mg(CH_3COO)_2$ x 4 H_2O	3.7
EGTA	2.0	HEPES	10.0
$CaSO_4$ x 2 H_2O	2.0	$CaSO_4$ x 2 H_2O	2.0
Glucose	10.0	Galactose	5.0
		Na-pyruvate	50.0
pH adjusted to 7.3 with NaOH		pH adjusted to 7.3 with NaOH	

SI Table 3 Description and composition of all used samples, including some single compound prymnesin (PRM) solutions. The identified analogs in the extracts are provided in SI Table 4. EC_{50} values were translated to the molar sum of all PRMs present, calculated using formula 1.

Strain	*ID*	*Characteristics*	*Stock concentration*	*EC_{50}*			
		Analogs identified via UHPLC/HRMS	**Semi-quantified (µM)**	**RTgill-W1**		**HCEC-1CT**	
				(nM)	**Sum_{PRM} (µg/L) [1]**	**(nM)**	**Sum_{PRM} (µg/L) [1)]**
UTEX-2797	A1	A-type biomass extract	20 ± 2	/		12.7 ± 0.3	26 ± <1
	A2	A-type biomass extract	20 ± 2	10.3± 0.3	20 ± <1	22.1 ± 5.6	43 ± 11
	sA1	PRM-A (3Cl) + pentose (purified)	58 ± 6	/		76 ± 34	149 ± 65
n.d. (Sig	A3	mixture of A-type prymnesins	3.6 ± 0.3	4.0 ± 0.2	8.7 ± 0.4	6.2 ± 0.1	13 ± <1
K-0081	B1	B-type biomass extract	348 ± 39	/		170 ± 9	307 ± 16
	B2	B-type biomass extract	145 ± 15	/		285 ± 21	506 ±37
	B3	B-type biomass extract	204 ± 13/ 139 ± 18	110 ± 11	200 ± 20	258 ± 126	460 ± 230
	B4	B-type biomass extract	393 ± 50	/		300*	560*
	sB1	PRM-B (1 Cl) + pentose; PRM-B (1 Cl) + hexose (purified)	92 ± 9	/		220 ± 30	395 ± 55
	sB2	PRM-B (1Cl) + 2 hexose; PRM-B (1Cl)	60 ± 7	/		270 ± 160	527 ± 312

		hexose + pentose (purified)					
RCC-1436	C1	C-type biomass extract	17 ± 2	13.9 ± 0.4	26.0 ± 0.7	ca 14**	ca 26**
RCC-191	C2	C-type biomass extract	40 ± 8	9.8 ± 0.8	19.3 ± 1.6	ca 33**	ca 65**

/ not conducted

* no standard deviation is provided since the EC_{50}-value is based on only one biological replicate

** not possible to calculate an EC_{50}-value with Rstudio since 0% metabolic activity is not reached and a high variability is observed around the EC_{50}-value

SI Table 4 Prymnesin (PRM) composition of *Prymnesium parvum* extracts in %. Analogs were identified via UHPLC/MS.

A-type PRM	***UTEX-2797***			***Sigma solution***
	A1	**A2**	**sA1**	**A3**
PRM-A (2 Cl)	2	-	-	-
PRM-A (2 Cl + DB)	1	-	-	-
PRM-A (2 Cl) + pentose	2	-	-	2
PRM-A (2 Cl + DB) + pentose	17	5	-	-
PRM-A (2 Cl) + 2 pentose + hexose	-	-	-	4
PRM-A (3Cl)	5	8	8	-
PRM-A (3 Cl) + pentose	41	81	92	18
PRM-A (3 Cl) + pentose + hexose	-	-	-	9
PRM-A (3 Cl) + hexose	1	-	-	-
PRM-A (3 Cl) + 2 pentose	2	-	-	3
PRM-A (3 Cl) + 2 hexose	6	-	-	-
PRM-A (3 Cl) + 2 pentose + hexose	23	6	-	63

B-type PRM	***K-0081***					
	B1	**B2**	**B3**	**B4**	**sB1**	**sB2**
PRM-B (1 Cl)	21	22	24	8	-	-
PRM-B (1 Cl) + pentose	17	19	18	9	87	-
PRM-B (1 Cl) + hexose	52	42	41	52	13	16
PRM-B (1 Cl) + pentose + hexose	1	2	2	2	-	5
PRM-B (1 Cl) + 2 hexose	5	9	10	25	-	79
PRM-B (2 Cl)	1	1	1	-	-	-
PRM-B (2 Cl) + pentose	1	1	1	4	-	-
PRM-B (2 Cl) + hexose	2	2	2	1	-	-
PRM-B (2 Cl) + 2 hexose	< 1	1	1	1	-	-

C-type PRM	***RCC-1436***	***RCC-191***
	C1	**C2**
PRM-C (2 Cl + DB) + pentose	4	-

PRM-C (2 Cl) + pentose + 2 hexose	-	*
PRM-C (3 Cl)	-	5
PRM-C (3 Cl + DB)	8	1
PRM-C (3 Cl + DB) + pentose	17	5
PRM-C (3 Cl + DB) + pentose + hexose	1	2
PRM-C (3 Cl + DB) + 2 pentose + hexose	-	2
PRM-C (3 Cl) + pentose	8	12
PRM-C (3 Cl) + 2 pentose + hexose	-	2
PRM-C (4 Cl + DB)	28	14
PRM-C (4 Cl + DB) + pentose	36	42
PRM-C (4 Cl + DB) + pentose + hexose	-	8
PRM-C (4 Cl + DB) + 2 pentose + hexose	-	4
PRM-C (4 Cl + 3 =O)	-	1
PRM-C (4 Cl + 3 =O) + pentose	-	2

"-" not detected; DB double bond; =O additional ketogroup;

* traces of PRM-C (2 Cl) + pentose + 2 hexose with the ion $[M + Na + H]^{+2}$ can neither be excluded nor confirmed due to overlay with PRM-C (3 Cl + DB) + hexose + 2 pentose with the ion $[M + NH_4 + H]^{+2}$ (*m/z* 1086.4)

SI Table 5 Effective concentration 50 (EC_{50}) values in nM for *Prymnesium parvum* extracts in RTgill-W1 cells after a 3 h and 24 h incubation period using the L-15 complete culture medium according to recipe 2.

Prymnesin type	***Strain***	***ID***	***3 hours***	***24 hours***	***Factor difference***
A-type	Unknown (Sigma)	A3	4.0 ± 0.2	2.4 ± 0.2	1.7
B-type	K-0081	B1	110 ± 11	41.5 ± 0.6	2.6
C-type	RCC-191	C2	9.8 ± 0.8	4.5 ± 0.1	2.2

SI Table 6 Mean cellular area of HCEC-1CT cells per well in % after 1.5 hours (t_1) and 3-hours (t_2) of incubation with K-0081 extract B1. All values are related to the control (live cell imaging solution (LCIS)) before the incubation (t_0) set to 100%. Data are provide as the mean of n=2. NES: normal external solution.

t_1	***LCIS***	***Cl^- free***	***Na^+ free***	***Ca^{2+} free***	***NES***
Solvent	100	111	106	106	105
165 nM	91	104	74	89	76
325 nM	96	106	79	95	77
645 nM	84	103	78	89	76
t_2	**LCIS**	**Cl^- free**	**Na^+ free**	**Ca^{2+} free**	**NES**

Solvent	96	114	104	105	104
165 nM	78	105	66	84	67
325 nM	92	107	74	89	71
645 nM	77	102	70	78	65

SI Table 7 Cytotoxic potential of B-type prymnesin extract B2 assessed in the HCEC-1CT complete medium (complete medium), live cell imaging solution (LCIS) and chlorine free medium after an incubation time of 3 hours. In case of the lactate dehydrogenase (LDH) assay the results are provided in percent relative to the LDH maximum control (treatment with lysis buffer) and the positive control (PC) was provided with the assay kit. In case of crystal violet (CV) the results are provided as cell viability in percent and are related to the respective solvent control (0.5 % ethanol). As positive control (PC), 0.075% (HCEC-1CT complete medium) or 0.05 % Triton X-100 (LCIS and Cl^- free medium) was applied. The data are shown as means ± standard deviations of at least three biological replicates, each performed in technical triplicates. The Shapiro-Wilk-Test was used for testing normality. Significant differences (* = $p < 0.05$) were calculated by One Way ANOVA, followed by the posthoc Fisher´s least significant difference (LSD) test.

	LDH			**CV**		
Extract B2	**complete medium**	**LCIS**	**Cl^- free**	**complete medium**	**LCIS**	**Cl^- free**
80 nM	0 ± 1 %	1 ± 1 %	1 ± 1 %	113 ± 9 %	119 ± 25 %	109 ± 10 %
325 nM	1 ± 2 %	* 7 ± 1 %	0 ± 1 %	* 75 ± 14 %	90 ± 16 %	111 ± 11 %
645 nM	* 71 ± 1 %	* 8 ± 2 %	2 ± 1 %	* 19 ± 4 %	92 ± 16 %	97 ± 5 %
PC	28 ± 2 %	39 ± 5 %	34 ± 6 %	54 ± 13 %	80 ± 15 %	75 ± 13 %

$$PRManalog\ \left(\frac{\mu g}{L}\right) = \frac{\left(\left(EC50\ \left(\frac{nmol}{L}\right) * \%\ PRManalog\right) * M\ PRManalog\left(\frac{ng}{nmol}\right)\right)}{1000}$$

SI Formula 1 Calculation for the sum of prymnesins (PRMs) in the single substance solutions based on their molecular weight

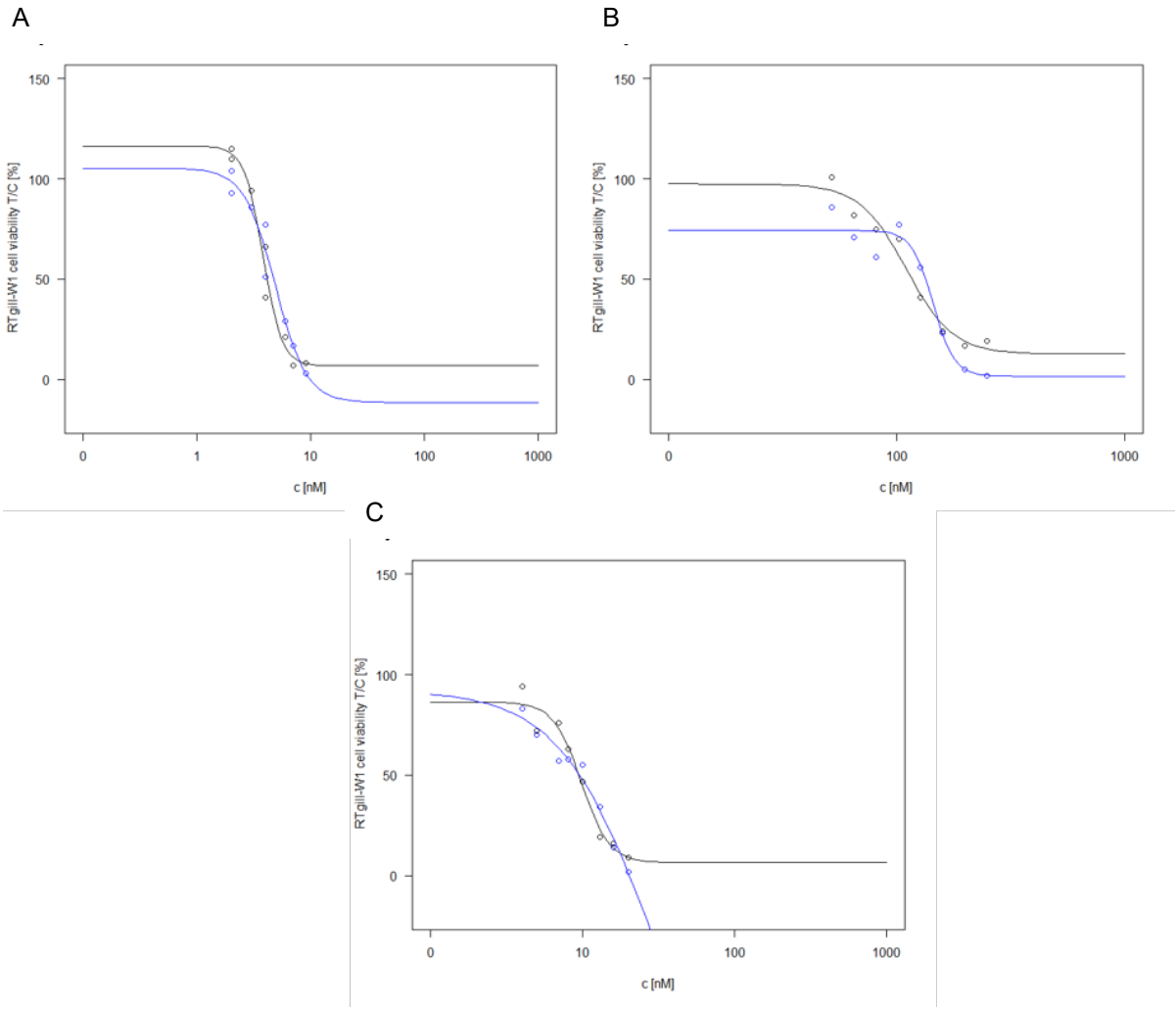

SI Fig. 1 Cytotoxic potency of prymnesins (PRM) in two RTgill-W1 culture media compared after a 3-hour exposure. The blue line represents the results in medium according to recipe 1 and the black line represents those in medium according to recipe 2. Dose response-curves are provided for the A-type PRM solution A3 (A), B shows the B-type PRM extract B3 from strain K-0081, and the C-type prymnesin extract C2 from strain RCC-191 is shown in C.

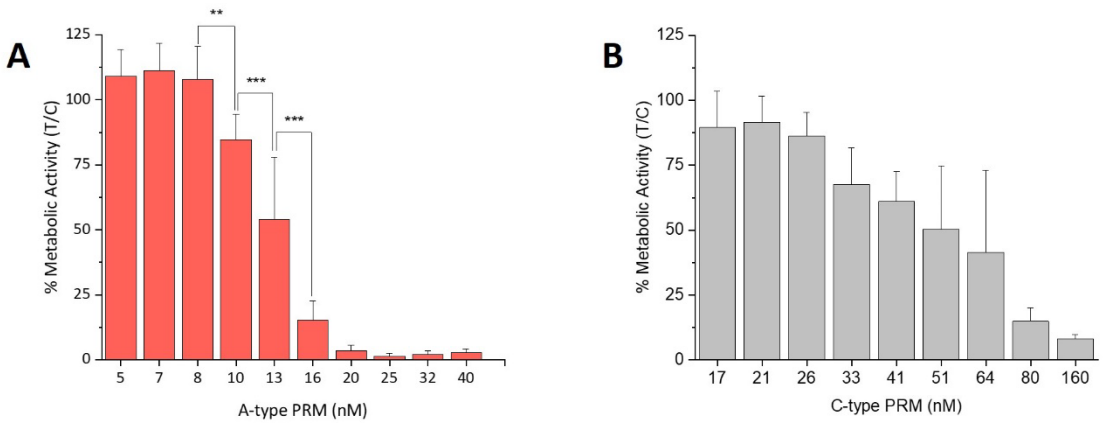

SI Fig. 2 Cell viability and membrane integrity of HCEC-1CT cells after 3-hour incubation with A-type prymnesin (PRM) extracts A1 obtained from the UTEX-2797 strain (A). Data are represented as mean ± SD of n = 4 for CellTiter blue (CTB), and n= 3 for data obtained through lactate dehydrogenase (LDH) measurements (dotted line). CTB results for C-type the PRM extract from RCC-191 are shown in B as mean ± SD of n ≥ 3.

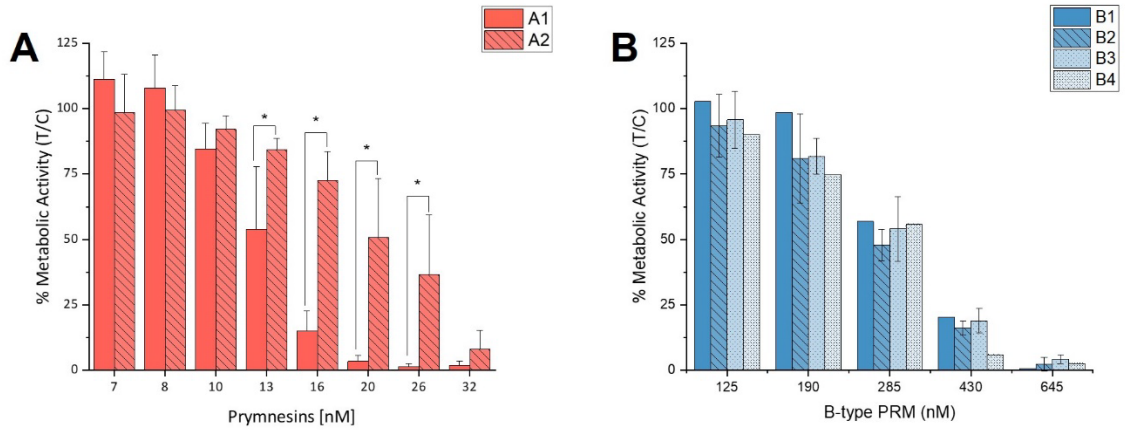

SI Fig. 3 Comparison between prymnesin (PRM) extracts taken from of the same *Prymnesium parvum* strain culture at different times. Data show the cell viability of HCEC-1CT cells after exposure to A UTEX-2797 PRM samples A1 and A2 and B to K-0081 PRM samples B1, B2, B3, and B4. Data show mean ± SD of n ≥ 3. If no standard deviation is displayed (B1 und B4) only one biological replicate was performed. Please notice that in case of B1 further replicates were tested but applying different dilutions and hence concentrations (see Fig. 3 of the main manuscript).

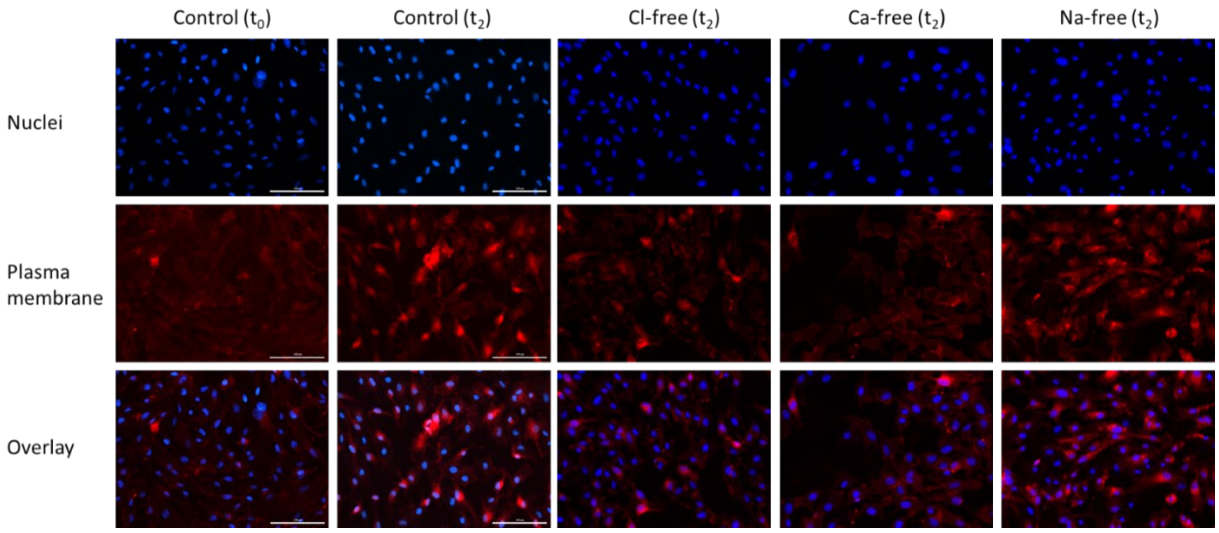

SI Fig. 4 Live cell images of RTgill-W1 cells in the control medium (normal external solution (NES)) before (t_0) and after a 3-hour (t_2) exposure to the A-type prymnesin (PRM) sample A3 in different media. Scale bar measures 100 µm. Brightness has been adjusted for images of the control for better visualization.

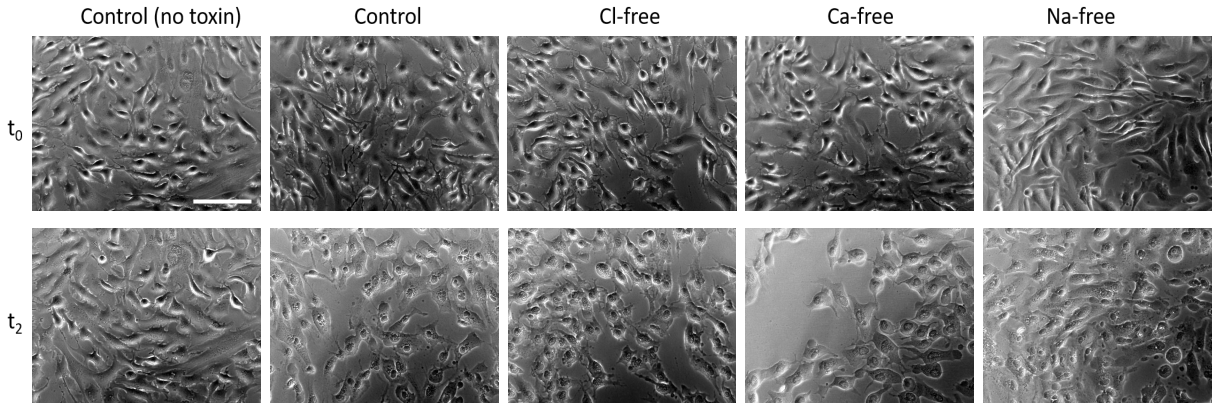

SI Fig. 5 Phase contrast images of RTgill-W1 cells before and after 3-hour exposure to the A-type prymnesin (PRM) sample A3 in different ion-free media. Scale bar represents 100 µm.

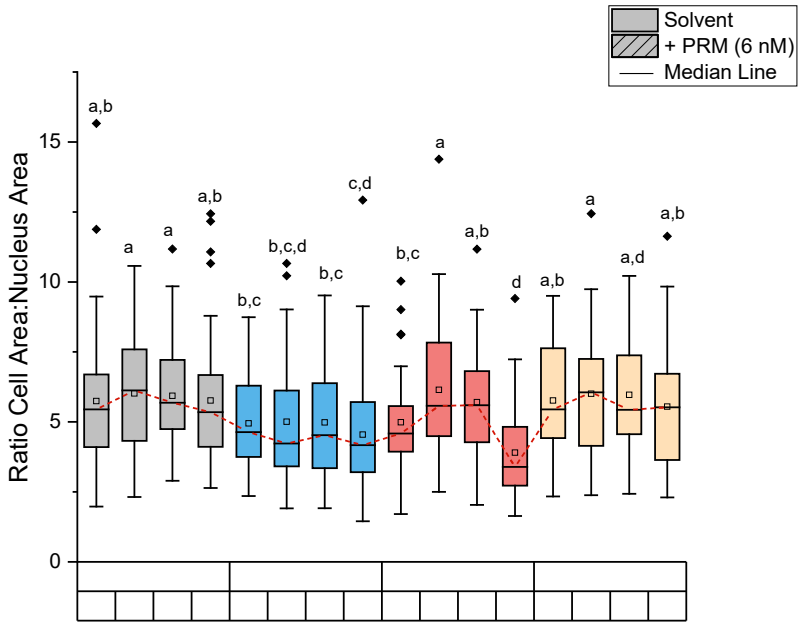

SI Fig. 6 Ratio of the cellular area of manually selected RTgill-W1 cells after exposure to prymnesins (PRMs) to the corresponding area of the cell nuclei. Data are provided as mean ± SD of n ≥ 36.

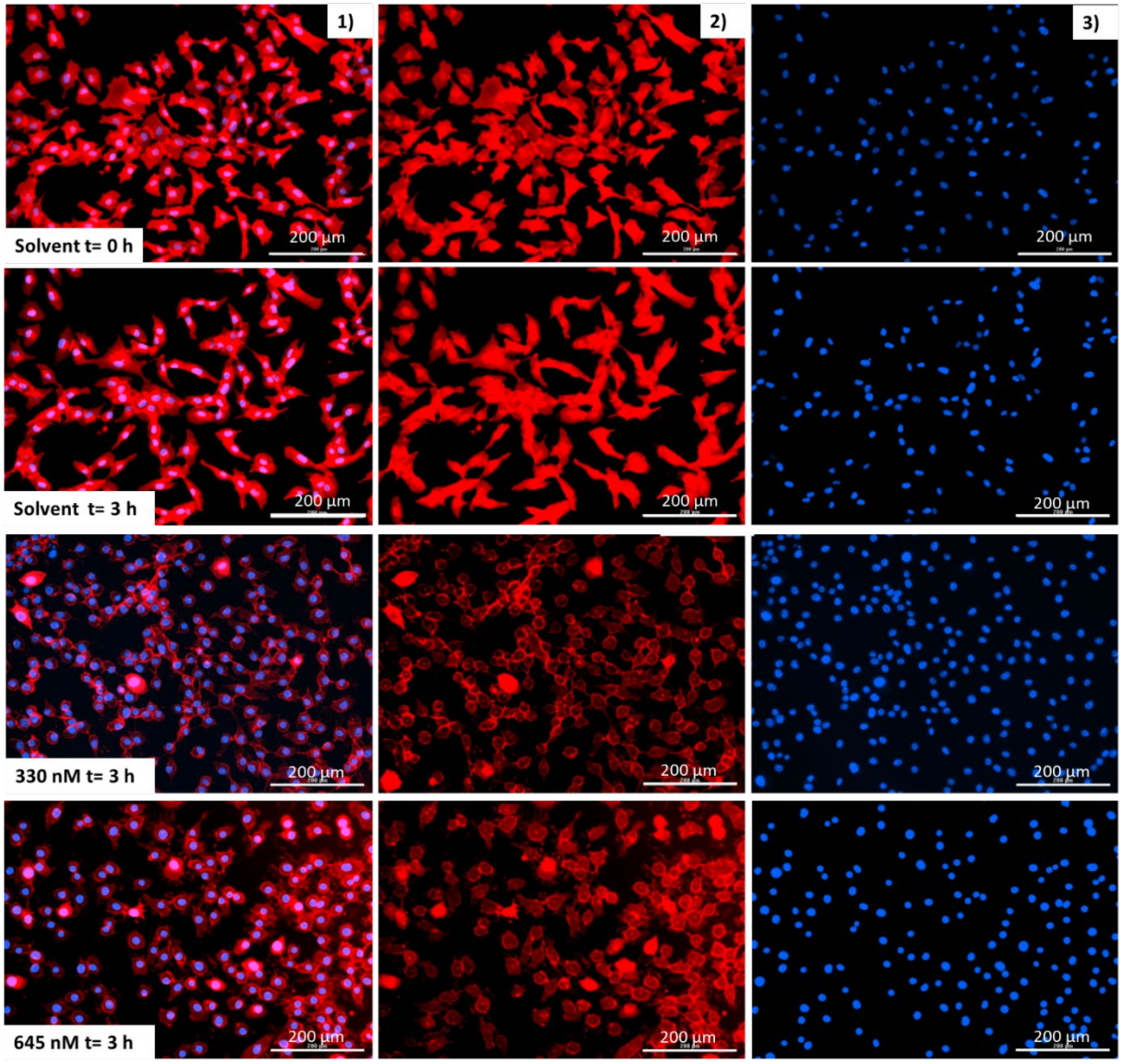

SI Fig. 7 Live cell images of HCEC-1CT cells treated with a K-0081 extract (extract B2) in live cell imaging solution. The figure illustrates the cell morphology at the very start of the incubation period and after a 3-hour treatment with the solvent control (0.5% ethanol) or the toxic extract respectively. In column 1), the overlay of cell mask and cell nuclei are shown. The cell membrane staining is provided in column 2) and the cell nuclei in column 3).

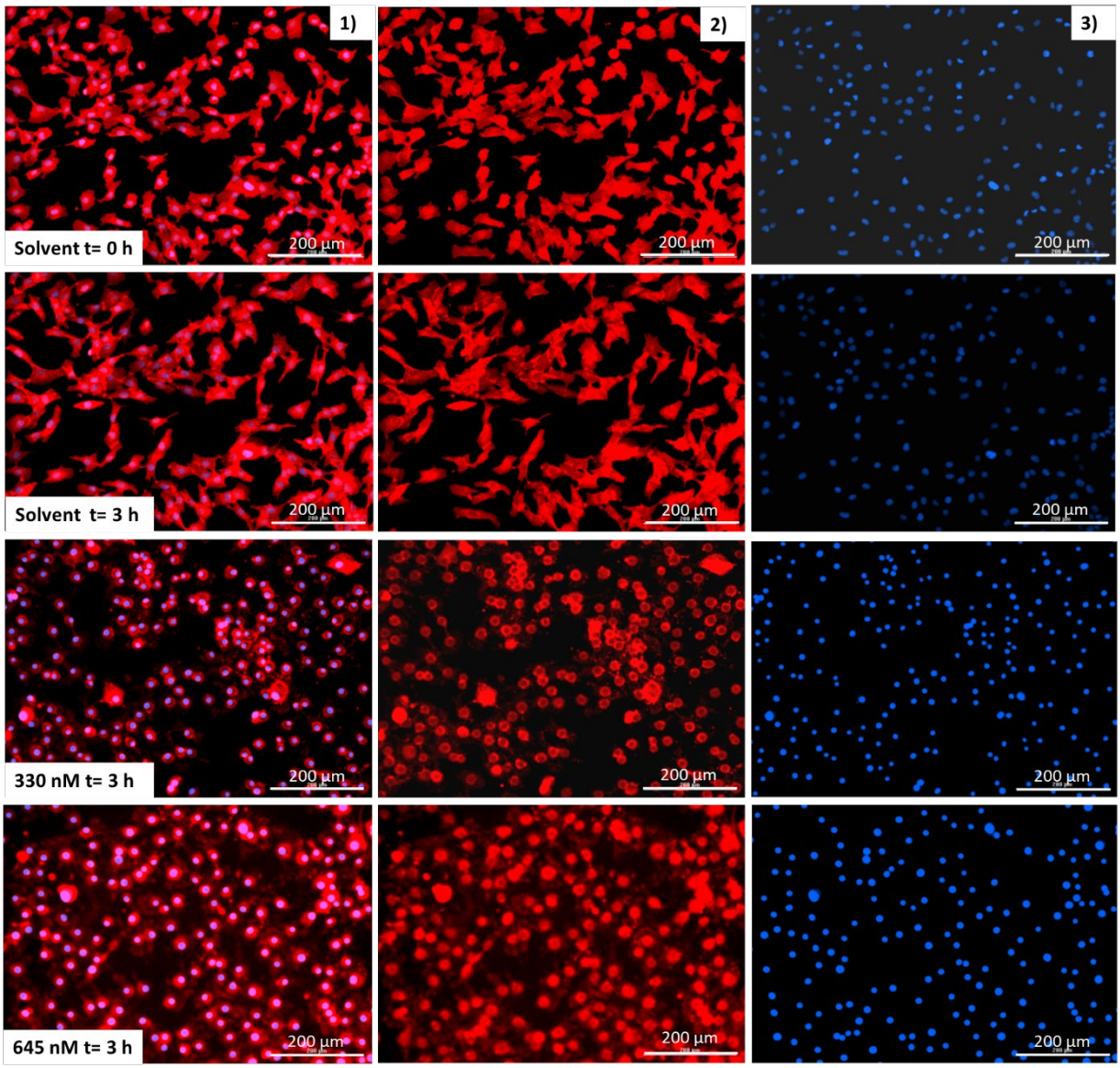

SI Fig. 8 Live cell images of HCEC-1CT cells treated with a K-0081 extract (extract B2) in Na^+ free medium. The figure illustrates the cell morphology at the very start of the incubation period and after a 3-hour treatment with the solvent control (0.5% ethanol) or the toxic extract, respectively. In column 1), the overlay of cell mask and cell nuclei are shown. The cell membrane staining is provided in column 2) and the cell nuclei in column 3).

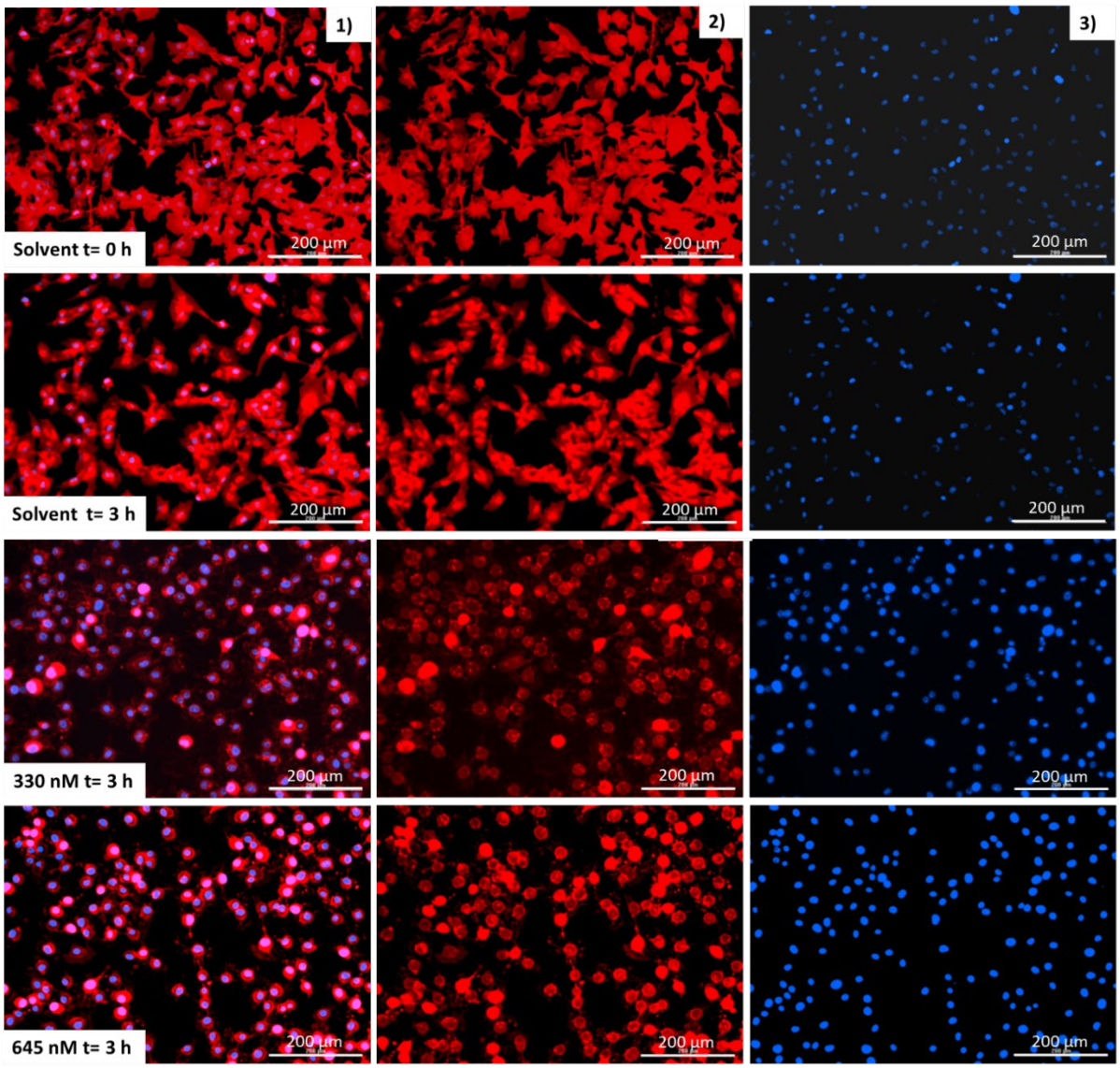

SI Fig. 9 Live cell images of HCEC-1CT cells treated with a K-0081 extract (extract B2) in Ca^{2+} free medium. The figure illustrates the cell morphology at the very start of the incubation period and after a 3-hour treatment with the solvent control (0.5% ethanol) or the toxic extract, respectively. In column 1), the overlay of cell mask and cell nuclei are shown. The cell membrane staining is provided in column 2) and the cell nuclei in column 3).

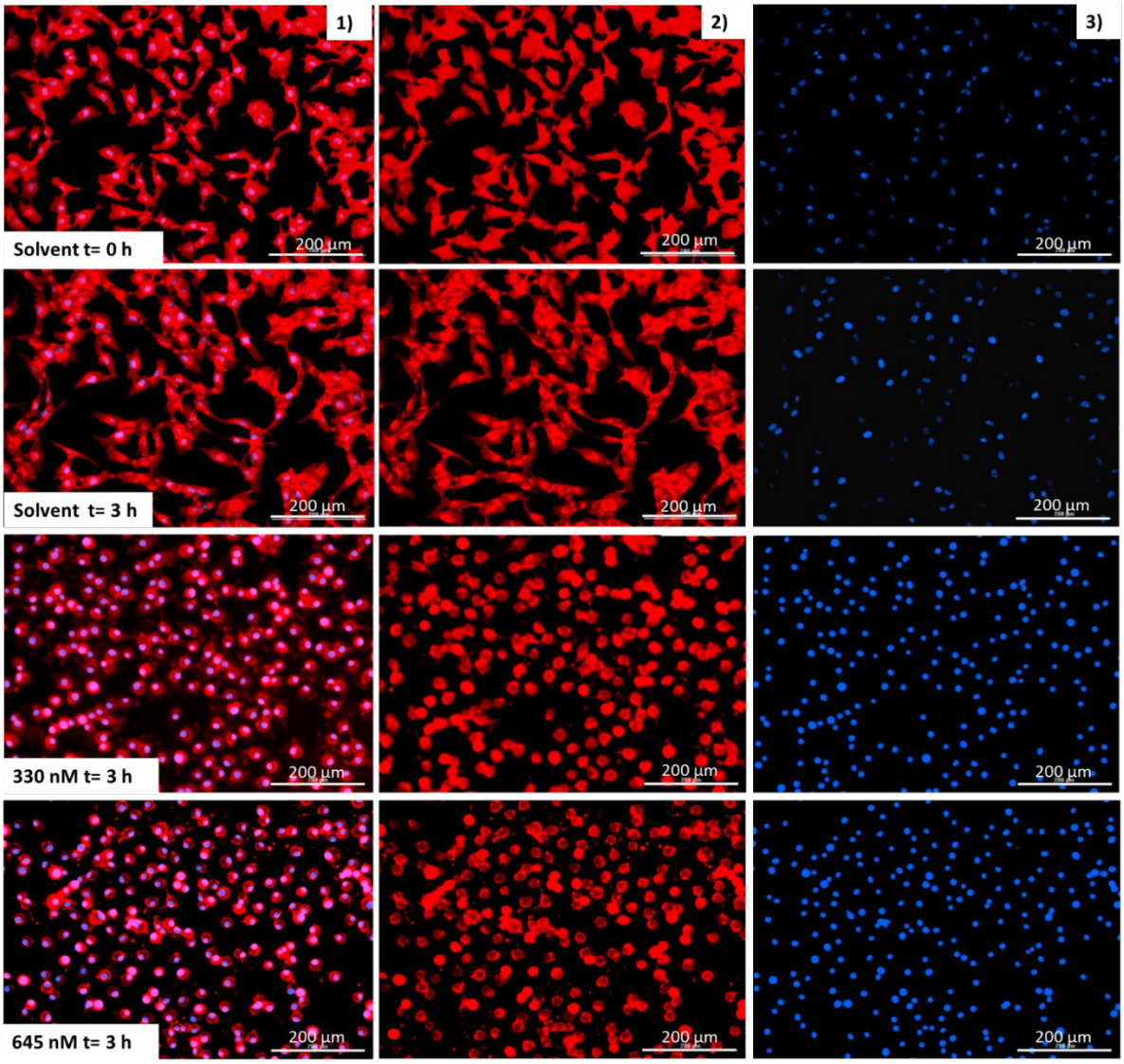

SI Fig. 10 Live cell images of HCEC-1CT cells treated with a K-0081 extract (extract B2) in normal external solution. The figure illustrates the cell morphology at the very start of the incubation period and after a 3-hour treatment with the solvent control (0.5% ethanol) or the toxic extract, respectively. In column 1), the overlay of cell mask and cell nuclei are shown. The cell membrane staining is provided in column 2) and the cell nuclei in column 3).

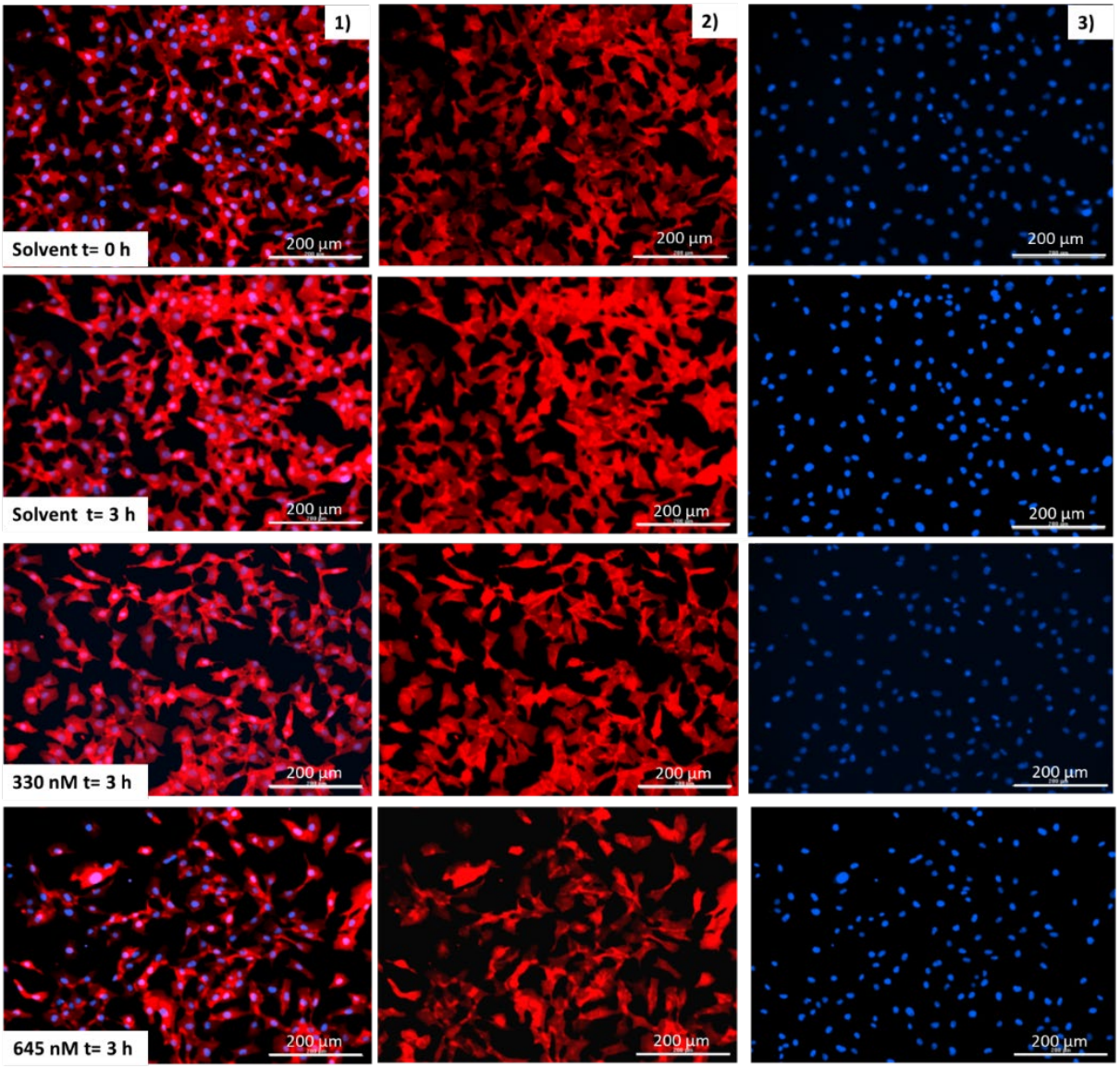

SI Fig. 11 Live cell images of HCEC-1CT cells treated with a K-0081 extract (extract B2) in Cl^--free medium. The figure illustrates the cell morphology at the very start of the incubation period and after a 3-hour treatment with the solvent control (0.5% ethanol) or the toxic extract, respectively. In column 1), the overlay of cell mask and cell nuclei are shown. The cell membrane staining is provided in column 2) and the cell nuclei in column 3).

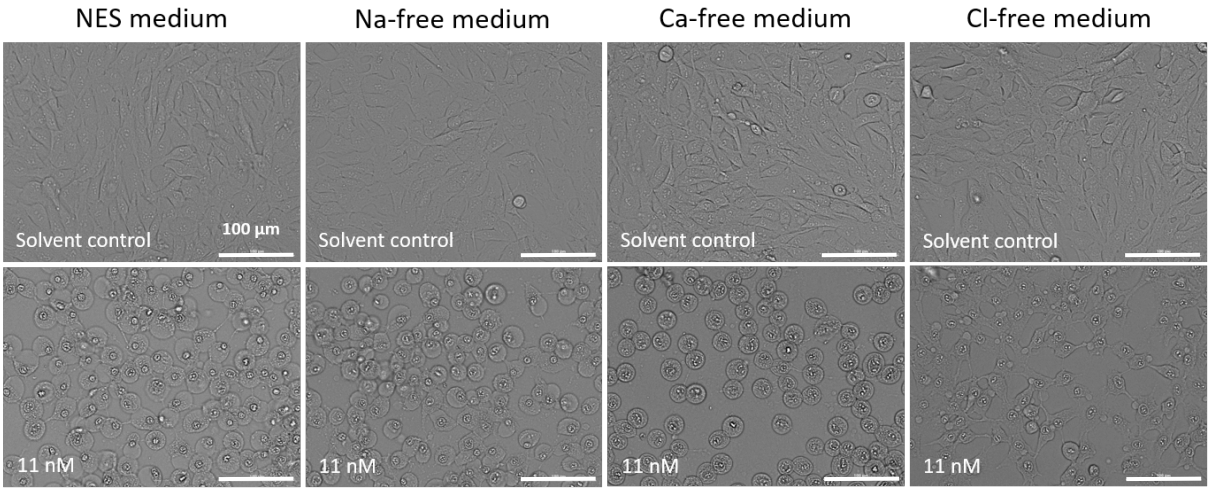

SI Fig. 12 Bright field images of HCEC-1CT cells after 3-hour exposure to A-type prymnesin solution sA1. Bars represent 100 µm.

7.2 Manuscript 2 – “How relevant are sterols in the mode of action of prymnesins?”

This article was published in Aquatic Toxicology, Volume 276, in November 2024. https://doi.org/10.1016/j.aquatox.2024.107080

Author contributions: conceptualization **H.C.P**., G.D.F., A.P., E.V.; data curation, formal analysis, investigation and visualization **H.C.P**., D.B.; funding acquisition; **H.C.P**., D.M., E.V.; methodology; G.D.F., A.P., E.V.; project administration; E.V.; resources C.A.D.S, T.O.L., P.J.H., D.M., G.D.F., A.P., E.V.; supervision D.M, G.D.F., A.P., E.V.; writing - original draft; **H.C.P**.; writing - review & editing; all co-authors

The master student Deniz Berk conducted sterol-addition experiments in RTgill-W1 cells and HCEC-1CT cells (provided in supplementary data) under the co-supervision of the author of this thesis. Prymnesin profile analysis was mostly performed for the previous paper “Cytotoxicity of *Prymnesium parvum* extracts and prymnesin analogs on epithelial fish gill cells RTgill-W1 and the human colon cell line HCEC-1CT” by Elisabeth Varga. All other experiments (cytotoxicity, hemolysis, hemolysis with addition of free sterols, cholesterol modulation and subsequent cytotoxicity tests, SPR), data evaluation and visualization, manuscript drafting and writing were performed by the author of this thesis. Catharina Alves-de-Souza, Per Juel Hansen, and Thomas Ostenfeld Larsen provided biomass for toxicological investigations. Giorgia Del Favero supervised fluorescence imaging and Allen Place mentored the hemolysis and SPR measurements as well as sterol interactions. Doris Marko served as supervisor and provided funding and resources, and Elisabeth Varga was the principal investigator of this work and co-supervisor.

Aquatic Toxicology 276 (2024) 107080

Contents lists available at ScienceDirect

Aquatic Toxicology

journal homepage: www.elsevier.com/locate/aqtox

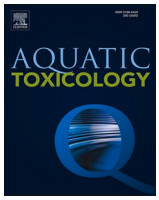

How relevant are sterols in the mode of action of prymnesins?

Hélène-Christine Prause [a,b], Deniz Berk [a], Catharina Alves-de-Souza [c,d], Per J. Hansen [e], Thomas O. Larsen [f], Doris Marko [a], Giorgia Del Favero [a,g], Allen Place [h], Elisabeth Varga [a,i,*]

[a] Department of Food Chemistry and Toxicology, Faculty of Chemistry, University of Vienna, Währinger Str. 38-40, 1090 Vienna, Austria
[b] Vienna Doctoral School in Chemistry, Faculty of Chemistry, University of Vienna, Währinger Str. 42, 1090 Vienna Austria
[c] Departamento de Oceanografía, Facultad de Ciencias Naturales y Oceanográficas, Universidad de Concepción, Concepción 4030000, Chile
[d] Centro de Investigación Oceanográfica COPAS Coastal, Universidad de Concepción, Concepción, Chile
[e] Marine Biological Section, Department of Biology, University of Copenhagen, Strandpromenaden 5, 3000 Elsinore, Denmark
[f] Department of Biotechnology and Biomedicine, Technical University of Denmark, Søltofts Plads 221, 2800 Kgs. Lyngby, Denmark
[g] Core Facility Multimodal Imaging, Faculty of Chemistry, University of Vienna, Währinger Str. 38-42, 1090 Vienna, Austria
[h] Institute of Marine and Environmental Technology, University of Maryland Center for Environmental Science, 701 E. Pratt Street, Baltimore, MD 21202, USA
[i] Unit Food Hygiene and Technology, Centre for Food Science and Veterinary Public Health, Clinical Department for Farm Animals and Food System Science, University of Veterinary Medicine, Vienna, Veterinärplatz 1, 1210 Vienna, Austria

ARTICLE INFO

Keywords:
Prymnesium parvum
Cholesterol
RTgill-W1
Toxin mixture
Hemolysis
Cytotoxicity

ABSTRACT

Prymnesins, produced by the haptophyte *Prymnesium parvum*, are considered responsible for fish kills when this species blooms. Although their toxic mechanism is not fully understood, membrane disruptive properties have been ascribed to A-type prymnesins. Currently it is suggested that pore-formation is the underlying cause of cell disruption. Here the hypothesis that A-, B-, and C-type prymnesins interact with sterols in order to create pores was tested. Prymnesin mixtures containing various analogs of the same type were applied in hemolysis and cytotoxicity assays using Atlantic salmon *Salmo salar* erythrocytes or rainbow trout RTgill-W1 cells. The hemolytic potency of the prymnesin types reflected their cytotoxic potential, with approximate concentrations reaching 50 % hemolysis (HC_{50}) of 4 nM (A-type), 54 nM (C-type), and 600 nM (B-type). Variabilities in prymnesin profiles were shown to influence potency. Prymnesin-A (3 Cl) + 2 pentose + hexose was likely responsible for the strong toxicity of A-type samples. Co-incubation with cholesterol and epi-cholesterol prehemolysis reduced the potential by about 50 % irrespective of sterol concentration, suggesting interactions with sterols. However, this effect was not observed in RTgill-W1 toxicity. Treatment of RTgill-W1 cells with 10 μM lovastatin or 10 μM methyl-β-cyclodextrin-cholesterol modified cholesterol levels by 20-30 %. Regardless, prymnesin cytotoxicity remained unaltered in the modified cells. SPR data showed that B-type prymnesins likely bound with a single exponential decay while A-types seemed to have a more complex binding. Overall, interaction with cholesterol appeared to play only a partial role in the cytotoxic mechanism of pore-formation. It is suggested that prymnesins initially interact with cholesterol and stabilize pores through a subsequent, still unknown mechanism possibly including other membrane lipids or proteins.

1. Introduction

The haptophyte *Prymnesium parvum* is considered one of the most persistent harmful algal bloom-forming microalgae in brackish water (Hallegraeff, 1993; Kaartvedt *et al.*, 1991). It was recently (2022) the cause of a massive bloom followed by a major fish-killing event in the Oder/Odra River in Europe (Free *et al.*, 2023). *P. parvum* produces a group of toxins called prymnesins which have ichthyotoxic and hemolytic effects and are believed to be the cause of fish kills ensuing from such blooms (Binzer *et al.*, 2019; Igarashi *et al.*, 1999, Igarashi *et al.*, 1996; Rasmussen *et al.*, 2016; Yariv and Hestrin, 1961). Currently, prymnesins are characterized as either A-, B-, and C-types, depending on the length of their carbon-backbone (Binzer *et al.*, 2019; Rasmussen *et al.*, 2016). To date, only four structures have been fully elucidated (Igarashi *et al.*, 1996; Igarashi *et al.*,1999; Rasmussen *et al.*, 2016). Many different analogs have been found since, for which no elucidation has been performed, with varying degrees of chlorination and glycosylation. The structure of C-type prymnesins remains to be elucidated. It was

* Corresponding author.
E-mail address: Elisabeth.Varga@vetmeduni.ac.at (E. Varga).

https://doi.org/10.1016/j.aquatox.2024.107080
Received 8 June 2024; Received in revised form 2 September 2024; Accepted 2 September 2024
Available online 3 September 2024
0166-445X/

suggested that prymnesin toxicity is pH-dependent, which has been tentatively examined previously (Caron *et al.*, 2023; Igarashi *et al.*, 1998; Moran & Ilani, 1974; Shilo and Aschner, 1953; Ulitzur and Shilo, 1964). A common feature all identified prymnesins share is a primary amine in their lipophilic moiety (Igarashi *et al.*, 1999, Igarashi *et al.*, 1996; Rasmussen *et al.*, 2016). The protonation of this amine group is believed to play an important role in the "charge distribution" of the molecule and thus its toxicity (Igarashi *et al.*, 1998; Moran & Ilani, 1974; Valenti *et al.*, 2010). While changes in pH may modify toxin activity, the hypothesis of reduced toxicity at pH 6.5 due to larger relative amounts of ionized prymnesins as suggested by Valenti *et al.*, (2010) is debated and further research is needed to elucidate the relationship between prymnesin toxicity and pH (Cichewicz and Hambright 2010). Differences in the potential of the three groups have been shown for ichthyotoxic as well as cytotoxic potential (Blossom *et al.*, 2014; Rasmussen *et al.*, 2016; Varga and Prause *et al.*, 2024). Interestingly, one strain of *P. parvum* can only produce one type of toxin, namely A, B, or C, but various analogs thereof (Binzer *et al.*, 2019; Rasmussen *et al.*, 2016).

Upon contact with the fish gills, prymnesins can increase cell membrane permeability, wreaking havoc on the osmotic balance, ultimately causing the fish to succumb to suffocation (Bergsson *et al.*, 2019; Ulitzur and Shilo, 1966; Yariv and Hestrin, 1961). At the molecular level, this effect is supposedly achieved through pore formation in the gill cells (Ulitzur and Shilo, 1966; Yariv and Hestrin, 1961). Despite numerous studies and the current knowledge on prymnesins at the time of writing, it remains unclear how prymnesins can accomplish such damage to the fish gill cells. Given their structural similarities to karlotoxin, with a terminally chlorinated aliphatic chain, or to amphidinol, an aliphatic chain without chlorination (Fig. 1), and the currently available toxicity data, it is postulated that prymnesins can interact directly with the cell membrane (Igarashi *et al.*, 1998; Imai and Inoue, 1974; Shilo, 1981; Waters *et al.*, 2015).

This study aimed at providing more detail regarding the mode of action of prymnesins by trying to understand the relevance of sterols in their toxicity. It was hypothesized that prymnesins can interact with cell membrane lipids, such as cholesterol, to exert their toxic effects upon the cells. As the difference in cytotoxicity between the groups has been established already, it was intriguing whether this would be the case for their hemolytic potency as well. To answer the question of whether prymnesins are able to interact with sterols, hemolysis as well as cytotoxicity were tested for toxins that had previously been combined with sterols. In addition, RTgill-W1 cell membranes were modified to either contain more or less cholesterol and subsequently exposed to prymnesins. This would help better understand the relevance of membrane cholesterol for the cytotoxic mechanism of prymnesins, and whether the exertion of toxic activity is dependent on the levels of cholesterol in the membrane. Moreover, it was of interest to examine if variances in analog profiles would influence the toxicity. Two A-type and two B-type strains were used for this comparison. Finally, the interactions between A- and B-type prymnesins with selected sterols were also recorded via surface plasmon resonance (SPR) measurements.

2. Materials and methods

2.1. Samples

Prymnesin samples were obtained from biomass of *P. parvum* cultures. One A-type prymnesin sample, originally a hemolysis solution from Sigma Aldrich (No. P-1389, St. Louis, MO, USA), was kindly gifted by T. Shier (Department of Medicinal Chemistry, College of Pharmacy, University of Minnesota, MN, USA). Another A-type and one B-type strain were cultivated and harvested by the Algal Resources Collection (ARC) in the Center of Marine Sciences at the Marine Biotechnology in North Carolina, University of North Carolina at Wilmington (strains UNCW-ARC140 and UNCW-ARC66, respectively). One B-type strain (K-0081), was obtained from the Scandinavian Culture Collection of Algae and Protozoa (SCCAP, now incorporated in the Norwegian Culture Collection of Algae, NORCCA). Lastly, the C-type strain RCC-1436 was purchased from the Roscoff Culture Collection (RCC, France).

Culture conditions for *P. parvum* strains were previously described in Varga and Prause *et al.* (2024) and briefly described as follows. For strains UNCW-ARC140 and UNCW-ARC66, F/2 medium was prepared from filtered and autoclaved natural seawater collected 40 miles off the Wilmington coast and adjusted to 4 ppt. The microalgae were cultivated with an initial density of ~1,000 cells mL^{-1} in a 10-L photobioreactor (IKA Algaemaster 10 control, IKA® Works Inc., Wilmington, NC, USA) at 20 °C, 70 µmol m^{-2} s^{-1} and a 12:12 dark:light photoperiod (LED Light). Air bubbling and CO_2 injection were used to maintain a pH ~8. Cells counts were determined every 3 days using a Sedwick-Rafter chamber and cells were harvested after 2 weeks (190,000 cells mL^{-1}) by

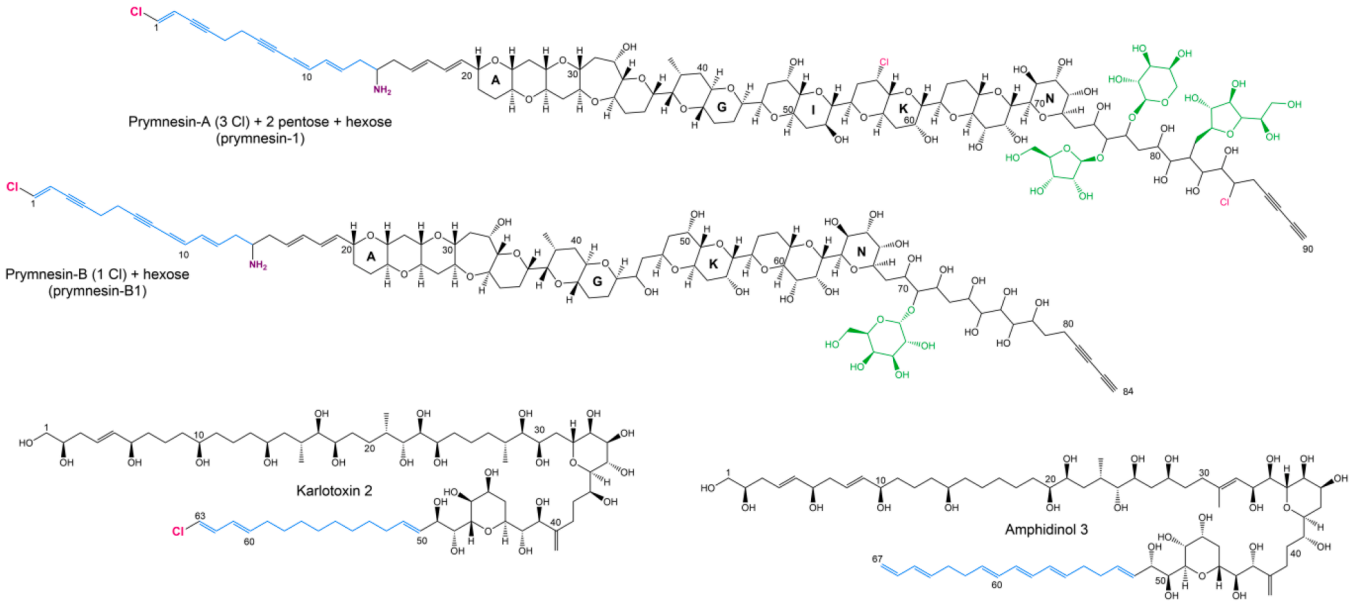

Fig. 1. Structures of one A- type and one B-type prymnesin, respectively, from the haptophyte Prymnesium parvum as examples for comparison to dinoflagellate toxins karlotoxin 2 from Karlodinium veneficum and amphidinol 3 from Amphidinium klebsii.

centrifugation in a Sorvall superspeed RC2-B centrifuge at 4 °C and 12, 000 × g. For strains K-0081 and RCC-1436. For strains K-0668 and RCC-1436 F/2 medium was prepared from filtered and pasteurized natural seawater off the coast of Elsinore at 30 ppt (Guillard, 1975). The microalgae were maintained in 10-L glass bottles, at 15 °C with a 14:10 h light-dark cycle and 450-500 μmol photons m^{-2} s^{-1} irradiance. Cell concentrations were monitored every two to three days by manual cell counting under the microscope to ensure these strains remained in the exponential growth phase. The algal biomass of all strains was harvested in the late exponential phase by centrifugation at 4,000 relative centrifugal force (rcf) for 15 min at 4 °C, and the biomass pellet separated from the supernatant.

For all the strains, the pellets were then stored at -80 °C until extraction using the protocol provided by Binzer *et al.* (2019). First, the algal cell pellet was thawed, then centrifuged at 4,000 rcf for 5 min to remove any remaining supernatant. Second, the pellets were extracted several times with ice-cold acetone to remove chlorophyll, until a light green supernatant was obtained. Third, prymnesins were subsequently extracted with methanol (MeOH). The MeOH was then evaporated with a rotavapor (R-114, Büchi Labortechnik AG, Flawil, Switzerland) or a CentriVap Benchtop Vacuum Concentrator coupled to a CentriVap Coldtrap (both Labconco Corp., Kansas City, MO, USA), and the samples were reconstituted in absolute ethanol (EtOH). Finally, the samples were placed in an ultrasonic bath for several minutes, centrifuged, and the particle-free supernatant was transferred to HPLC vials and stored at -20 °C. The two A-type samples will henceforward be referred to as the A-type solution (Sigma Aldrich) and the A-type extract, from Sigma Aldrich of unknown strain origin and strain UNCW-ARC140 respectively.

2.1.1. Prymnesin profiles

The prymnesin profile was analyzed using ultra-high performance liquid chromatography coupled with high-resolution mass spectrometry (UHPLC-HRMS) exactly as described in Varga and Prause *et al.* (2024). Toxin concentrations for prymnesin samples were estimated through high-performance liquid chromatography and fluorescence detection (HPLC-FLD), as previously described (Svenssen *et al.*, 2019; Varga and Prause *et al.*, 2024). In short, prymnesins were labeled with a fluorescent tag (AccQ-Tag Fluor Reagent Kit, Waters Corp., Milford, MA, USA) through derivatization of their primary amines. A 1200 HPLC system (Agilent Technologies, Waldbronn, DE), using an Agilent Poroshell C18 column (2.1 × 50 mm 2.7 μm) with water as eluent A and acetonitrile as eluent B, both containing 0.1 % formic acid, were used for chromatographic separation. Prymnesins were detected via fluorescence at excitation/emission wavelengths of 250/395 nm. The data were analyzed with ChemStation for LC Rev. B.04.01 SP1 from Agilent Technologies.

2.2. Cell culture

Both the rainbow trout (*Oncorynchus mykiss*) gill cell line RTgill-W1, obtained from K. Schirmer (Department of Environmental Toxicology, EAWAG, Dübendorf, CH), and the human epithelial colon cell line HCEC-1CT, provided by J. W. Shay, UT Southwestern Medical Center, Dallas, TX, USA, were chosen for cytotoxicity tests and cultivated as described in Varga and Prause *et al.*, (2024).

RTgill-W1 cells were kept at 19 °C in Leibovitz's 15 medium (L-15) supplemented with 1 % (*v/v*) penicillin/streptomycin (Thermo Fisher Scientific, Waltham, MA, USA) and 10 % (*v/v*) fetal calf serum (EuroBio, Le Ulis, France) (Bols *et al.*, 1994). HCEC-1CT cells were cultured at 37 °C with 5 % CO_2 in Dulbecco's Modified Eagle's Medium (DMEM (Thermo Fisher Scientific, Waltham, MA, USA)). For the complete cultivation medium 500 mL DMEM were supplemented with 10 mL Medium 199 (10x), 10 mL HEPES buffer solution 1 M, 5.2 mL Insulin-Transferrin-Selenium-G Supplement (Thermo Fisher Scientific, Waltham, MA, USA), 10 mL HyClone™ Cosmic Calf™ Serum (GE Healthcare Life Sciences HyClone Laboratories, Danaher Corp., Washington DC, USA), 0.6 mL gentamycin solution (Sigma Aldrich GmbH, St. Louis, MO, USA), 100 μL Recombinant Human Epidermal Growth Factor (100 μg/mL, Szabo-Scandic HandelsgmbH & Co KG, Vienna, Austria), and 100 μL hydrocortisone (5 mg/mL, Merck KGaA, Darmstadt, Germany). Both cell lines were kept in cell+ surface (Sarstedt AG & Co KG, Nürnbrecht, Germany) flasks or plates.

2.3. Toxicity tests

2.3.1. Cell viability assays

Cell viability of RTgill-W1 and HCEC-1CT cells upon exposure to ichthyotoxin samples was mainly determined with the CellTiter-Blue® (CTB (Promega, Madison, WI, USA)) assay according to the manufacturer's instructions. The protocol used for exposing RTgill-W1 cells to ichthyotoxins was adapted from the one described previously (Dayeh *et al.*, 2005; Rasmussen *et al.* 2016) Cells were seeded onto an F-bottom 96-well polystyrene plate at a density of 2×10^4 cells per well (RTgill-W1) or 5×10^3 cells per well (HCEC-1CT) and grown for 48 h. Cells were then exposed to 100 μL prymnesin sample diluted in culture medium with a final EtOH concentration of 0.5 % (*v/v*). Medium containing 0.5 % (*v/v*) EtOH was used as solvent control, and medium containing 0.05 % and 0.1 % (*v/v*) Triton™ X-100 (Sigma Aldrich, St. Louis, MO, USA) as positive control. Following a 3-h incubation at 21 °C (RTgill-W1) or 37 °C (HCEC-1CT) in the dark, 100 μL of 1:10 diluted CTB reagent in culture medium was added to the previously aspirated cells and incubated for 1 h at room temperature in the dark.

The WST-1 Assay (Abcam, Cambridge, United Kingdom) was performed according to the manufacturer's protocol to detect cytotoxicity in RTgill-W1 cells after treatment with cholesterol altering substances (section 2.4.2). After the wells had been aspirated and rinsed with Dulbecco's phosphate buffered saline (DPBS, Thermo Scientific Waltham, MA, USA), 80 μL of WST-1 reagent were added to the wells and incubated for 1.5 h in the dark, after which the absorbance was taken at 450 and 650 nm. The cells were then fixed and stained with a fluorescent dye, visualizing cellular cholesterol (2.4.3).

The lactate dehydrogenase (LDH) assay (Pierce CyQuant™, Thermo Scientific, Waltham, MA, USA) was used to evaluate lytic effects on the cells. The manufacturer's protocol was followed for LDH testing, where 50 μL of supernatant were combined with 50 μL reaction mix. The reaction was stopped after 30 min by adding 50 μL stop solution, and finally the absorbance was measured at 490 and 680 nm.

2.3.2. Hemolytic assay

Red blood cells (RBCs) from the Atlantic salmon (*Salmo salar*) were utilized to assess the hemolytic potential of the prymnesin samples with the exception of the extract of strain UNCW-ARC66. The assay protocol was adapted from the one described by Deeds *et al.* (2002). Blood was drawn from the caudal vein using heparin-treated needles and collected in a falcon tube for centrifuging at 1,250 rcf and 4 °C for 25 min to remove serum. The remaining RBCs were subsequently washed three times (1,250 rcf, 4 °C, 5 min) with cold Tris-buffer I, which consisted of 150 mM NaCl, 3.2 mM KCl, 1.25 mM $MgSO_4$, 12.2 mM Tris base in MilliQ water. RBCs were then diluted in Tris-buffer II (Tris-buffer I + 3.75 mM $CaCl_2$) to 1.25 % (*v/v*) of their original concentration and stored at 4 °C for up to 10 days. Both buffers were adjusted to pH 7.4 at 10 °C before filter sterilization (0.22 μm). A calibration curve was obtained by preparing a dilution series of the hemolytic reference compound saponin (Quillaja bark, CAS No.: 8047-15-2; Sigma Chemical Co., St. Louis, MO, USA) (Lorent *et al.*, 2014). Hemolytic assays were performed in 96-well plates (V-bottom, polystyrene, non-treated, Corning Inc., Corning, NY, USA) by preparing desired dilutions of the ichthyotoxin samples in Tris-buffer II, with a final EtOH concentration of 0.5 % (*v/v*) and adding 100 μL sample per well. Hemolysis was started once 100 μL of 1.25 %-RBC solution were added to the samples. The plate was placed on an orbital shaker (80-100 rotations per minute) and incubated at room temperature for 1 h. The solvent control was 0.5 % EtOH (*v/v*) in

Tris-buffer II, and 8 μg/mL saponin in Tris-buffer II served as positive control. After incubation, the plate was centrifuged at 600 rcf for 5 min, after which 100 μL of the supernatant were transferred into a clear F-bottom 96-well polystyrene plate (Corning Inc., Corning, NY, USA). The absorbance of hemoglobin released from the RBCs was then read at 540 nm. The RBC solution was monitored for its stability by checking the optical density of the solution supernatant without addition of any hemolysins. Ideally the absorbance of the supernatant would remain around 0.2, and the maximal acceptable value was set at 0.4. When an absorbance of $\geq$0.4 was reached the solution was discarded and a new batch of 1.25 %-RBC solution was prepared. Sensitivities of the individual batches were tested by obtaining a saponin curve.

The B-type prymnesin extract of strain UNCW-ARC66 was the only sample not tested for hemolysis since it was not able to cause cell viability of RTgill-W1 cells to fall below 50 %, and therefore considered not potent enough.

All experiments involving fish were carried out in accordance with the guidelines at the Institutional Animal Care and Use Committee (IACUC) of the University of Maryland Medical School: protocol No. 0014 and No. 0522012. Fish used for tissue sampling were anesthetized with tricaine methanesulfonate (MS-222, 10 mg/L) for blood sampling and then euthanized with MS-222 (150 mg/L).

2.4. Impact of sterols on toxicity

2.4.1. Combination assays

Possible interactions between prymnesins and cholesterol (5(6)-cholesten-3-ol, Sigma, St. Louis, MO, USA) and epicholesterol (5-cholesten-3a-ol, Steraloids Inc., Newport, RI, USA) were tested in hemolytic assays. Again, the protocol described by Deeds *et al.* (2002) was followed. Briefly, samples (extracts of UNCW-ARC140, K-0081, and RCC-1436, and the Sigma Aldrich prymnesin solution) were diluted to their EC_{50} values and then combined with the equivalent volume of sterol in solution at 0.1 – 10,000 nM before starting hemolysis assays.

This assay was adapted for cytotoxicity in RTgill-W1 and HCEC-1CT cells. Sterol concentrations were adjusted to range from 1 nM to 50,000 nM for RTgill-W1 and HCEC-1CT cells, in the respective cultivation media. Cells were seeded as per usual, and the A-type prymnesin solution was diluted to twice the concentration of the EC_{50} obtained for either cell line. The sample was then combined with the equivalent volume of sterol at various concentrations, and a total volume of 100 μL was added to the cells, which were then incubated for 3 h. Cell viability was measured in CTB and LDH assays.

Sterols were dissolved in EtOH.

2.4.2. Cholesterol modulation in RTgill-W1 cells

Whether the cytotoxicity of prymnesins is dependent on the cholesterol content of the target cell membrane was assessed via fluorescence microscopy combined with cell viability testing as previously described (Rebhahn *et al.*, 2022). Conditions to achieve a desirable change in membrane cholesterol content while maintaining acceptable cell viability of RTgill-W1 cells were determined as follows: cells were seeded into 96-well plates at a density of 1.5×10^4 cells per well for 48 h followed by a 24 h incubation with the cholesterol content-altering agents. To increase the cholesterol content cells were treated with water-soluble cholesterol in the form of cholesterol-loaded methyl--beta-cyclodextrin (MbCD-Chol, Sigma Aldrich GmbH, St. Louis, MO, USA) at 10 and 50 μM (Del Favero *et al.*, 2020). Lovastatin (lovastatin sodium salt, Enzo, Farmingdale, NY, USA) at 0.1, 1, and 10 μM was used to test for depletion of membrane cholesterol. These treatments were controlled for cytotoxicity in a WST-1 assay while establishing this protocol. Cholesterol was relatively quantified using a fluorescent stain as described in 2.4.3. Based on the results of these testing conditions, MbCD-Chol and lovastatin at 10 μM were chosen for further testing with prymnesins. After the 24-h cholesterol-altering treatment, 100 μL of the A-type prymnesin solution at approximately EC_{90} (12 nM) and the UNCW-ARC66 extract (B-type) at approximately EC_{60} (113 nM) were added to the cells and incubated for 3 h. The resulting cell viability was measured via the CTB assay using the usual controls. As lovastatin was dissolved in dimethylsulfoxide (DMSO), the solvent control for this compound consisted of 0.25 % (*v/v*) DMSO in culture medium.

2.4.3. Fluorescence microscopy

After manipulating the cholesterol content of the cells and cell viability testing through WST-1, the cells were fixed with 1 % (*v/v*) paraformaldehyde (PFA) in DPBS for 30 min, followed by quenching the PFA with 100 mM glycine in DPBS for 1-2 min. Next, the cholesterol in the cells was stained with filipin III ready-made solution (25 μg/mL in DPBS (Sigma Aldrich GmbH, St. Louis, MO, USA) for 1 h. In between all steps and after staining, the cells were rinsed three times with DPBS, and finally ROTI®Mount FluoroCare mounting medium (Carl Roth GmbH + Co. KG, Karlsruhe, Germany) was added to each well. Fluorescence spectra were recorded between excitation at 340-380 nm and emission at 385-470 nm with the Lionheart FX automated microscope (BioTek Instruments Inc., Winooski, VT, USA) using the DAPI channel. For quantification the ImageJ 1.54f Fiji Software was used, where gray-scale images were converted to RBG images, and keeping only the blue-channel image, 7 single cells per image were selected and measured for their area and integrated intensity of filipin fluorescence. The background intensity was measured and subtracted from the intensities obtained for the cells.

2.5. Surface plasmon resonance (SPR)

After performing co-incubation assays of these ichthyotoxins with selected sterols, surface plasmon resonance (SPR) measurements were performed for assessing interactions between the A-type prymnesin solution and the K-0081 extract (B-type) with cholesterol, epicholesterol, and ergosterol (Fluka Chemie GmbH, Buchs, Switzerland). The experiments were run on a T200 Biacore system using the Series S Sensor Chip HPA (Cytiva, Danaher Corp., Washington DC, USA). The three sterols were diluted in HBS buffer (10 mM HEPES, 150 mM NaCl, pH 7.4) to reach a concentration of 10 μM. The sensor chip was prepared by first pre-conditioning all four flow cells (Fc) with 40 mM octyl-D-glucoside for 5 min at a flow rate of 10 μL/min. The sterol were subsequently immobilized at about 1,000 responsive units (RU) with a flowrate of 2 μL/min for 30 min. Fc1 with only octyl-D-glucoside served as control. The baseline was stabilized by rinsing all Fcs with 10 mM NaOH for 30 s, followed by a 5 min blocking with bovine serum albumin (0.1 mg/mL in dH_2O). HBS buffer was run over all Fcs three times, followed by 1 μM of A-type prymnesins (Sigma Aldrich) and 1 μM B-type prymnesin extract (strain K-0081) for 2 min at 10 μL/min. In-between samples the Fcs were washed with HBS buffer. Responses were fitted on a 1:1 model, and kinetic values were calculated with the program Biacore T200 software 3.2.1 (Cytiva, Danaher Corp., Washington DC, USA). As these samples were mixtures of different analogs, SPR served only as a way of confirming whether sterol-interactions take place. Specific reaction kinetics were not calculated, but the overall ability of prymnesins to bind with sterols was tested and compared between the two prymnesin types.

2.6. Statistics

All assays were carried out in technical triplicates, with the exception of SPR assays, which were performed in duplicates. Statistical significance was calculated with One Way ANOVA followed by the posthoc Fisher's least significant difference test, as well as t-test (one-sample or two-sample) using OriginPro 2020 Version 9.7.0.185 (Academic, OriginLab Corporation, Northampton, MA, USA).

3. Results

3.1. Prymnesin profile

The different prymnesin analogs of all the samples were analyzed and are listed in Table 1. Three of the samples had already been reported by Varga and Prause *et al.* (2024) and are indicated as such. The profiles found for the two A-type samples exhibited various differences. The main components of these samples were analog prymnesin-A (3 Cl) + 2 pentose + hexose (prymnesin-1), making up 60 % of the total prymnesins in the A-type solution (Sigma Aldrich), and analog prymnesin-A (3 Cl) + pentose (prymnesin-2), with 43 % in the extract UNCW-ARC140. Only about 20 % of analog prymnesin-A (3 Cl) + 2 pentose + hexose (prymnesin-1) was found in the A-type extract (UNCW-ARC140). Two analogs containing two Cl-moieties (prymnesin-A (2 Cl) + pentose and prymnesin-A (2 Cl) + 2 pentose + hexose) were detected in the A-type sample from Sigma Aldrich. The only analog containing two Cl-moieties in the UNCW-ARC140 extract was prymnesin-A (2 Cl + DB) + pentose, which was not found in the solution from Sigma Aldrich. The two B-type samples were more similar to one another, with analog prymnesin-B (1 Cl) accounting for 35 % in the UNCW-ARC66 and 24 % in the K-0881 extract. The dominant analog of the K-0881 extract was prymnesin-B (1 Cl) + hexose (known as prymnesin-B1) with 41 %. The main difference between these two was that no analogs containing 2 Cl were present in the UNCW-ARC66 extract. The most abundant analog in the RCC-1436 extract was prymnesin-C (4 Cl+ DB) + pentose. An estimate of the total concentration (μM) was calculated for each sample based on the analogs present, accounting for all prymnesin analogs. From this point onwards, all concentrations provided will reflect the concentration of the analog mixture of the prymnesin samples.

Table 1
Prymnesin profiles of samples used in this project reported as percentages of the total peak areas. The total concentration of the prymnesin sample based on the total analog content is also given (μM).

A-type prymnesins	ARC140	Sigma Aldrich[1) *]
PRM-A (2 Cl + DB) + pentose	12	-
PRM-A (2 Cl) + pentose	-	2
PRM-A (2 Cl) + 2 pentose + hexose	-	4
PRM-A (3 Cl)	6	-
PRM-A (3 Cl) + pentose	43	18
PRM-A (3 Cl) + 2 pentose	4	3
PRM-A (3 Cl) + pentose + hexose	13	9
PRM-A (3 Cl) + pentose + 2 hexose	-	2
PRM-A (3 Cl) + 2 pentose + hexose	21	61
Concentration (μM)	9.1 ± 2.4	2.2 ± 0.2

B-type prymnesins	ARC66	K-0081 [1)]
PRM-B (1 Cl)	35	24
PRM-B (1 Cl) + pentose	32	18
PRM-B (1 Cl) + hexose	25	41
PRM-B (1 Cl) + pentose + hexose	4	2
PRM-B (1 Cl) + 2 hexose	5	10
PRM-B (2 Cl) sum of all varieties	-	5
Concentration (μM)	22 ± 6	204 ± 18

C-type prymnesins	RCC-1436 [1)]
PRM-C (2 Cl + DB) + pentose	4
PRM-C (3 Cl + DB)	8
PRM-C (3 Cl + DB) + pentose	17
PRM-C (3 Cl + DB) + pentose + hexose	1
PRM-C (3 Cl) + pentose	8
PRM-C (4 Cl + DB)	28
PRM-C (4 Cl + DB) + pentose	36
Concentration (μM)	15 ± 1

"-" not detected; DB double bond
1) As previously reported in Varga and Prause *et al.* (2024).
* Duplicate of the sample reported previously.

3.2. Toxicity of prymnesins

3.2.1. Cytotoxicity

The cytotoxic potential for most samples had already been described in the previous study by Varga and Prause *et al.* (2024). The A-type prymnesin solution (Sigma Aldrich), the most potent sample, showed a cytotoxic EC_{50} of about 4 nM in RTgill-W1 cells and 6-7 nM in HCEC-1CT cells. The RCC-1436 C-type prymnesin extract was the second most potent, with EC_{50} values of 14 nM for RTgill-W1 cells and approximately 34 nM for the HCEC-1CT cell line. The extract from the B-type producing strain K-0081 exhibited 50 % cytotoxicity at concentrations of 127 nM and 170 nM, respectively. For the purpose of this study, the two UNCW-ARC strain extracts were evaluated for their cytotoxicity as well. The samples were tested for their toxic effects towards RTgill-W1 cells and measured via CTB. A 50 % cytotoxic effect was observed at approximately 5 nM of the UNCW-ARC140 extract (A-type). The highest concentration of the UNCW-ARC66 extract (B-type),113 nM not exceeding the maximum EtOH concentration of 0.5 % (*v/v*), could decrease metabolic activity to about 60 % only (Supplementary information (SI) Fig. 1).

3.2.2. Hemolytic potential

The difference in potency between the three prymnesin groups (A, B, and C) was tested for hemolysis of RBCs obtained from salmon blood. All tested prymnesin samples were potent hemolysins (Fig. 2). Once again, the A-type solution (Sigma Aldrich) was the most potent, with an approximated HC_{50} value of 6 nM. A 50 % hemolysis (HC_{50}) of the RBCs could be achieved at 9 nM of the UNCW-ARC140 A-type extract, and the highest possible concentration of 18.2 nM (maintaining EtOH levels at 0.5 % (*v/v*)) lysed about 70 % of all RBCs. The C-type prymnesin sample had an estimated HC_{50} of about 54 nM, and lastly 600 nM of the B-type extract from strain K-0081 were needed to achieve 50 % lysis of RBCs. The C-type prymnesin sample could only reach a maximal hemolysis of about 60 % at the highest possible concentration while maintaining a 0.5 % (*v/v*) EtOH concentration. The UNCW-ARC66 B-type prymnesin extract was not tested for hemolysis, considering its low cytotoxic potential.

3.3. Impact of sterols on toxicity

3.3.1. Combination assays

In order to assess the influence of sterols on the toxicity, combination assays of toxins with sterols were performed. The samples were diluted to their HC_{50} or EC_{50} values and combined with cholesterol or epicholesterol prior to starting the hemolysis or cytotoxicity assays. The total EtOH concentration was kept at 0.5 % (*v/v*), and therefore this percentage was also used for the solvent control (either in Tris buffer or culture medium). In general, standard deviations for the hemolysis experiments were at times larger than expected. This can be explained by the fact that new batches of 1.25 %-RBC solution had to be prepared often, as their shelf-life is unpredictably short (max. 7-10 days). Thus, the replicates for the assays with the K-0081 B-type prymnesin extract as well as the UNCW-ARC140 A-type extract for instance were conducted using different batches of RBC solution, as it would have been wasteful to restart the experiment and discard previously obtained results. The variance between the RBC batches remained at $\leq$ 10 % for all tested saponin concentrations, with the exception of saponin at 1,600 ng/mL (SI Fig. 2). This concentration was right around the HC_{50} of the saponin control where higher variabilities are always observed. Importantly, the number of RBCs was not counted during the preparation of this solution, which may have had an additional effect on data reproducibility. The C-type prymnesin sample could not be tested for combination with epicholesterol as insufficient sample volume was available.

Neither cholesterol nor epicholesterol showed any hemolytic activity of their own (SI Fig. 3). For all tested prymnesins, a clear decrease of the hemolytic effect could be observed once the sample had been combined

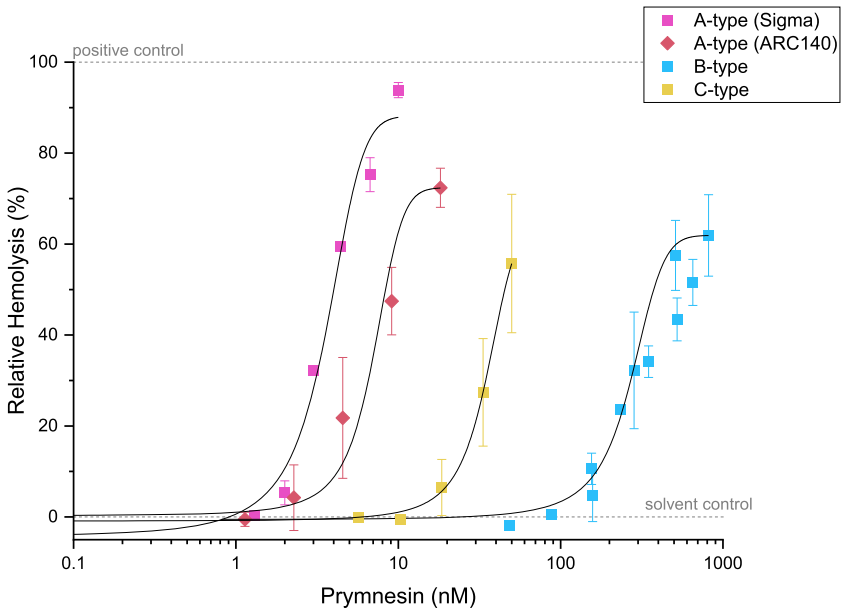

Fig. 2. Hemolytic activity of the A-type solution (Sigma Aldrich), the A-type extract (strain UNCW-ARC140), the B- (strain K-0081), and C-type (strain RCC-1436) prymnesins in red blood cells from Atlantic salmon (*Salmo salar*). Saponin (8 μg/mL) was used as positive control and set as 100 % hemolysis, Tris-buffer II containing 0.5 % (*v/v*) EtOH served as solvent control. The prymnesin concentrations (nM) reflect the total concentration of all analogs present in each sample respectively. Data is provided as mean ± SD of n ≥ 2.

with sterols (Fig. 3). The reduction of hemolysis was seemingly independent of the sterol concentration, with the addition of sterols at 0.1 nM and 1,000 nM resulting in a similar effect for most samples. Only for the A-type prymnesin solution combination with cholesterol or epicholesterol at 10,000 nM led to an even stronger reduction in hemolysis. This reduction was significantly different from the effect obtained with other concentrations of cholesterol. Remarkably, the combination of A-type prymnesin solution with 10,000 nM cholesterol resulted in practically 0 % hemolysis, while with epicholesterol no smaller value than 10 % hemolysis could be reached. It seems important to note that these effects could not be observed in the combination assays with the A-type prymnesin extract (UNCW-ARC140). In this sample, the observed reduction in hemolysis was stable at all concentrations of added sterols, which was similar to the hemolytic activity observed for the K-0081 B-type prymnesin sample.

Given the outcome of the hemolytic potential after combination with sterols, the question was addressed whether pre-incubation of prymnesins with sterols also affects the cytotoxic potential towards fish gill cells (RTgill-W1) or human epithelial cells (HCEC-1CT) (SI Fig. 4 and SI Fig. 5). Interestingly, no discernible change in cytotoxic potential could be measured when the toxin was pre-incubated with sterol, with the exception of a combination with cholesterol at the lowest concentration of 0.1 nM, where a significant decrease in the cytotoxicity of A-type prymnesins at 4 nM could be calculated for the CTB assay (SI Fig. 4A). In the human cell line HCEC-1CT, the A-type solution (Sigma Aldrich) at 7 nM (EC_{50} adjusted for the cell line) combined with cholesterol at 100 nM, 10,000 nM, and 50,000 nM reduced the cytotoxic potential by about 15 %. Nevertheless, this reduction in cytotoxicity did not show a significant difference and thus remains a trend (SI Fig. 4 A).

3.3.2. Modulation of membrane cholesterol content

The cytotoxic potential of prymnesins was tested on RTgill-W1 cells that had been altered in their cholesterol content. More cholesterol was loaded into the cells by treating them with MbCD-Chol and, for comparison, lovastatin was used to deplete the cells of cholesterol. The resulting change in cholesterol content was determined by staining with filipin and measuring the integrated fluorescent intensity (Fig. 4). A concentration of 10 μM MbCD-Chol was effective in significantly increasing the cellular cholesterol content by approximately 30 %. Treatment with lovastatin for 24 h also caused a concentration-dependent change in the cholesterol level. Lovastatin lowered the content by about 25 % and 10 % at 10 μM and 1 μM, respectively. None of these treatments impacted the cell viability, as measured in the WST-1 assay (SI Fig. 6).

Once the cholesterol content could be modulated, cholesterol load (MbCD-Chol) and reduction (Lova) were used to explore the dependency of the toxicity of the prymnesins. To evaluate possible changes in cytotoxic potency, the A-type solution (Sigma Aldrich) and the UNCW-ARC66 B-type prymnesin extract at approximately EC_{90} and EC_{60}, respectively, as well as the A-type extract from strain UNCW-ARC140 at EC_{20} and EC_{70} were added to the cells directly after the 24-h cholesterol modulation. Exposure lasted 3 h and the consequent cell damage was measured via the CTB assay (Fig. 5). Despite altering the cholesterol content of the cells no clear change in the cytotoxicity could be measured for either one of the samples. Although a tendency for a lower cytotoxic potential could be observed when the cells had been treated with lovastatin and then exposed to the B-type sample, this effect was not significantly different to the impact on untreated cells. Exposure to the A-type sample (Sigma Aldrich) resulted in a similar outcome. The metabolic activity was decreased to about 5 % in regular as well as in cholesterol-altered RTgill-W1 cells. Also for the UNCW-ARC140 sample, no difference between the untreated cells and cholesterol-modulated cells could be observed for neither of the toxin concentrations applied (EC_{20}, EC_{70}). No difference between cholesterol depleted and enriched cells could be measured for any of the prymnesin samples.

3.4. Surface plasmon resonance (SPR)

To better understand the interaction between prymnesins and sterols, SPR was used to measure binding of A- and B-type prymnesins to cholesterol, epicholesterol, and ergosterol. Because interactions could not be measured for single prymnesin analogs, SPR data are viewed as indications for sterol affinity and not reaction kinetics. The reaction was fitted to a simple 1:1 kinetics model and tested for the accuracy thereof (Chi^2). When a mixture of analytes is tested for 1:1 binding, it is assumed that they compete for the immobilized ligand, with binding depending

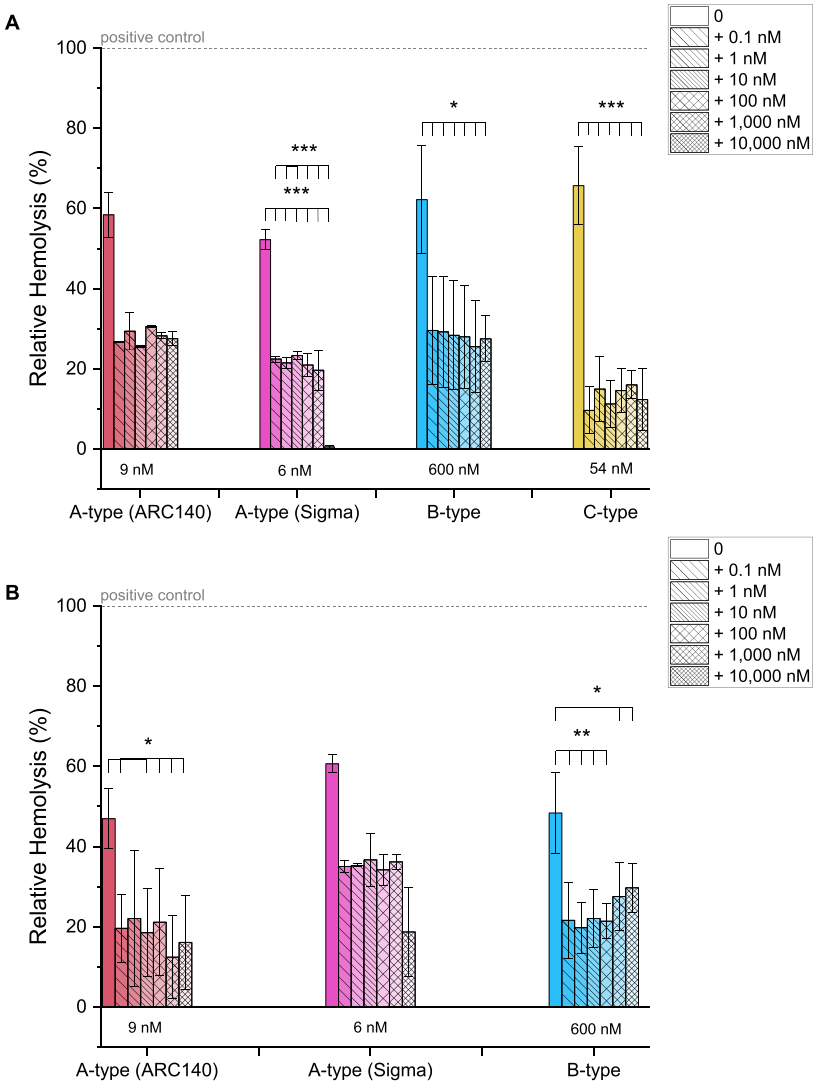

Fig. 3. Potential of both A-type prymnesin samples, the solution from Sigma Aldrich from unknown strain origin and the extract from strain UNCW-ARC140, the extracts from the B-type strain K-0081 and the C-type strain RCC-1436 diluted to their previously established HC_{50} values, compared to hemolytic effects resulting from combination of these samples at their HC_{50} with different concentrations of cholesterol (A) and epicholesterol (B) before incubation with red blood cells. The prymnesin concentrations (nM) reflect the total concentration of all analogs present in each sample respectively. Saponin (8 μg/mL) was used as positive control and set as 100 % hemolysis, and Tris-buffer II containing 0.5 % (*v/v*) EtOH served as solvent control. The sterol control consisted of the highest concentration (10,000 nM) for each sterol in Tris-buffer II and caused 0 % hemolysis. Data is provided as mean ± SD of $n \geq 2$. Where the number of replicates equals $n = 3$ significance was calculated with One Way ANOVA (* = $p < 0.05$; ** = $p < 0.01$; *** = $p < 0.001$). Significance was not calculated for samples with fewer replicates (UNCW-ARC140 sample combined with cholesterol and the Sigma Aldrich solution in combination with epicholesterol).

on analyte concentration and affinity (Gaudreault *et al.*, 2021). Therefore, only the dissociation of the complexes was considered, as dissociation rates are independent of analyte concentrations and can be used to interpret complex stability. The dissociation constants, $k_d(1/2)$, were calculated by the T200 Biacore software and can be found in Table 2. The sensograms are shown in Fig. 6. Both samples, the A-type solution (Sigma Aldrich) and the B-type extract (K-0081) bound to all ligands (sterols), and also non-specifically to the control, octyl-D-glucoside. This unspecific binding can be attributed to the amphipathic properties ascribed to compounds like prymnesins (Andersen *et al.*, 2017; Bachvaroff *et al.*, 2008; Svenssen *et al.*, 2019).

Dissociation rate constants were all within the same range, from 2.59×10^{-3} to 6.72×10^{-3} (1/s), indicating similar complex stability for both toxin mixtures with all three sterols. Notably, no $k_d(1/s)$ was calculated for the A-type sample complexing with cholesterol, as the dissociation range reached RUs below 0. The A-type prymnesin solution seemed to build a more stable complex with epicholesterol, resulting in a $k_d(1/s)$ of 2.59×10^{-3}, compared to ergosterol ($k_d(1/s)$ of 6.64×10^{-3}). Similarly, the B-type mixture formed the most stable complex with epicholesterol, for which a $k_d(1/s)$ of 3.09×10^{-3} was calculated, followed by the stability of the B-type prymnesins-ergosterol complex. Again, considering that these results stem from a toxin mixture, it should be kept in mind that variances in binding stability may be due to changes in affinities depending on the analogs dominating the interaction. Interestingly though, the fit of the 1:1 model differed between the samples. B-type prymnesins generally fit the 1:1 dissociation much better, with lower Chi^2 values of 1.97×10^{-1} for ergosterol, 5.45×10^{-1} for cholesterol, and 1.14 for epicholesterol. The A-type sample, in comparison, did not seem to follow a single exponential decay. This suggests that this sample may have a more complex binding interaction with the ligands. Importantly, the RU values for the A-type sample were higher than for the B-type, likely due to the higher EtOH content. This was unavoidable, as the desired concentration of 1 μM required different dilutions of the prymnesin samples.

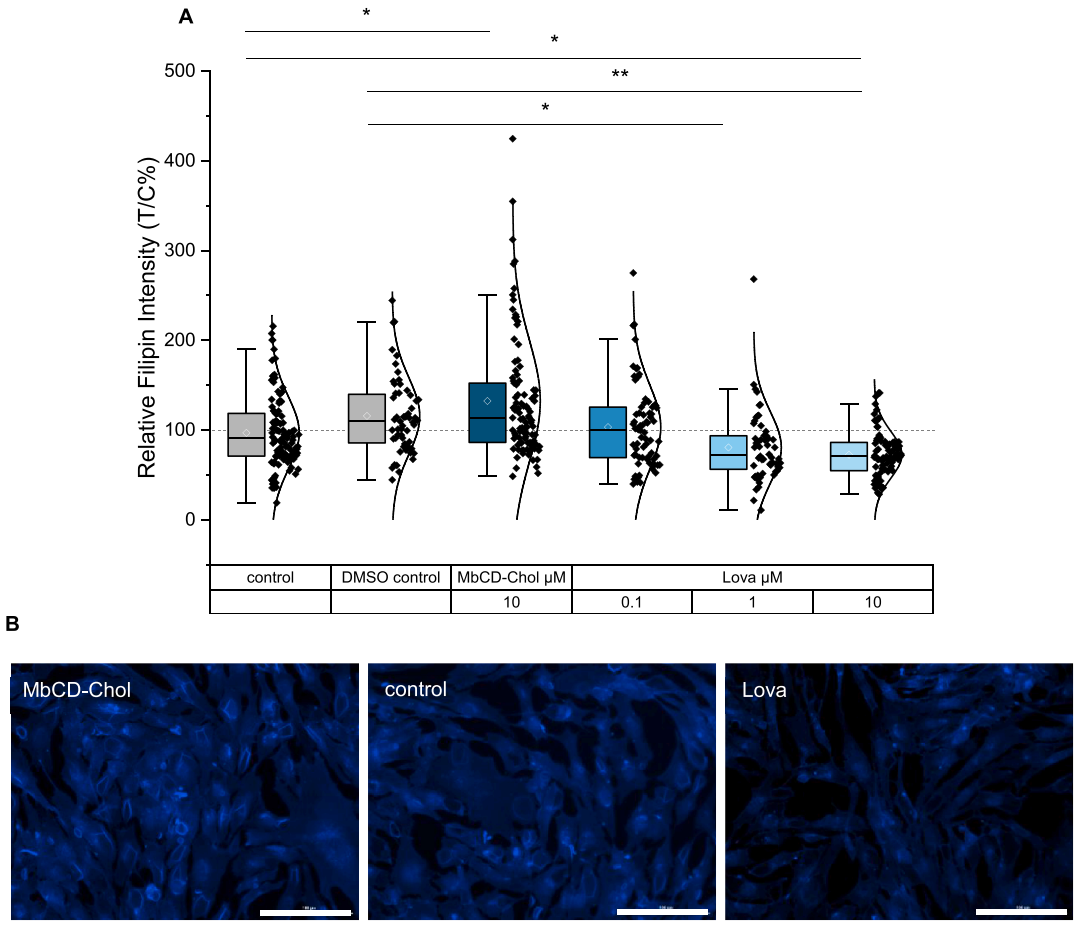

Fig. 4. (A) Relative cholesterol content based on measured filipin intensity of RTgill-W1 cells treated with methyl-β-cyclodextrin loaded with cholesterol (MbCD-Chol) to increase the membrane cholesterol content, and lovastatin (Lova) to deplete the cells of cholesterol. Dimethylsulfoxide (DMSO) at 0.25 % (*v/v*) in culture medium was added as control for treatment with Lova. Unaltered RTgill-W1 cells exposed to culture medium served as control. Data represent mean ± SD of n=105 cells (7 cells per image, 1 image per well, 3 wells per condition (technical triplicates), 5 biological replicates for each condition (* = $p < 0.05$; ** = $p < 0.01$)). (B) RTgill-W1 cells after cholesterol content-modulating treatment stained with filipin. Scale bars represent 100 µm. Lower and upper box boundaries 25th and 75th percentiles, respectively, line inside box median, diamond-shape inside box mean. The black filled diamond shapes represent single data points.

4. Discussion

The observed difference in potency between the two A-type samples used in this study most likely lies in the variability of their analog-profiles. Varga and Prause *et al.* (2024) have already suggested specific prymnesin analogs to be more cytotoxic than others. It seems the analog prymnesin-A (3 Cl) + 2 pentose + hexose (prymnesin-1) played a key role in A-type sample potency. At the respective EC_{50}, approximately 3.7 nM and 1.9 nM of this analog were present in the A-type solution (Sigma Aldrich) and the UNCW-ARC140 extract, respectively. This would explain the stronger effects observed for the A-type solution (Sigma Aldrich). Prymnesin-A (3 Cl) + pentose (known as prymnesin-2) on the other hand may not be as involved in the toxic mechanism, despite being the most abundant analog in the UNCW-ARC140 extract. Analogs prymnesin-B (1 Cl) + hexose (prymnesin-B1) and prymnesin-B (1 Cl) + pentose (prymnesin-B2) were likely the drivers behind the toxic activity of the B-type samples, as their content in both samples was comparable, and the observed potency was similar as well.

It was shown that the order of cytotoxic potency of A > B > C was also reflected in the hemolytic potential (with approximately 6 nM and 9 nM HC_{50} for the A-type samples, about 54 nM for the C-type and 600 nM for the B-type sample) (Binzer *et al.*, 2019; Svenssen *et al.*, 2019; Varga and Prause *et al.*, 2024). Intriguingly, the HC_{50} of 6 nM obtained for the A-type solution (Sigma Aldrich) was very close to the cytotoxic EC_{50} of 4 nM (1.5-fold increase). The C-type extract was about 10-fold less potent while the B-type prymnesin extract (strain K-0081) needed a 3.5- to 5-fold EC_{50} value for hemolysis compared to cytotoxicity. The A-type prymnesin extract (UNCW-ARC140) only needed to be 2-fold more concentrated to reach 50 % hemolysis, which was comparable to the A-type solution (Sigma Aldrich). The procedural variance between the hemolysis and cytotoxicity assays could have impacted the way in which prymnesins target the cells. Although it would be expected that RBCs in suspension are more susceptible than an adherent cell line. Combining prymnesins with sterols before starting hemolysis assays resulted in a significant reduction of hemolytic potential for all tested samples, albeit irrespective of the sterol concentration. This indicates that prymnesins must have interacted with sterols. Previous studies have shown that cholesterol undergoes self-association, forming micelles at a critical concentration of 25 nM to 40 nM at 25 °C. This reversible micelle formation may explain why an increase in cholesterol concentration did not result in an additional decrease in hemolysis (Haberland and Reynolds, 1973). When the micelles are formed it is likely that two phases are created: the aqueous phase containing RBCs, the other the micellar phase into which prymnesins partition due to their lipophilic moiety. Since previous studies on the relevance of cholesterol were conducted using only A-type prymnesins, it was uncertain how B-type prymnesins would perform in such an assay (Igarashi *et al.*, 1998; Imai and Inoue, 1974; Ulitzur and Shilo, 1966). As no strengthened impact on the hemolytic potential was recorded for the other three prymnesin samples, it remains to be examined whether the additional decrease in hemolysis of

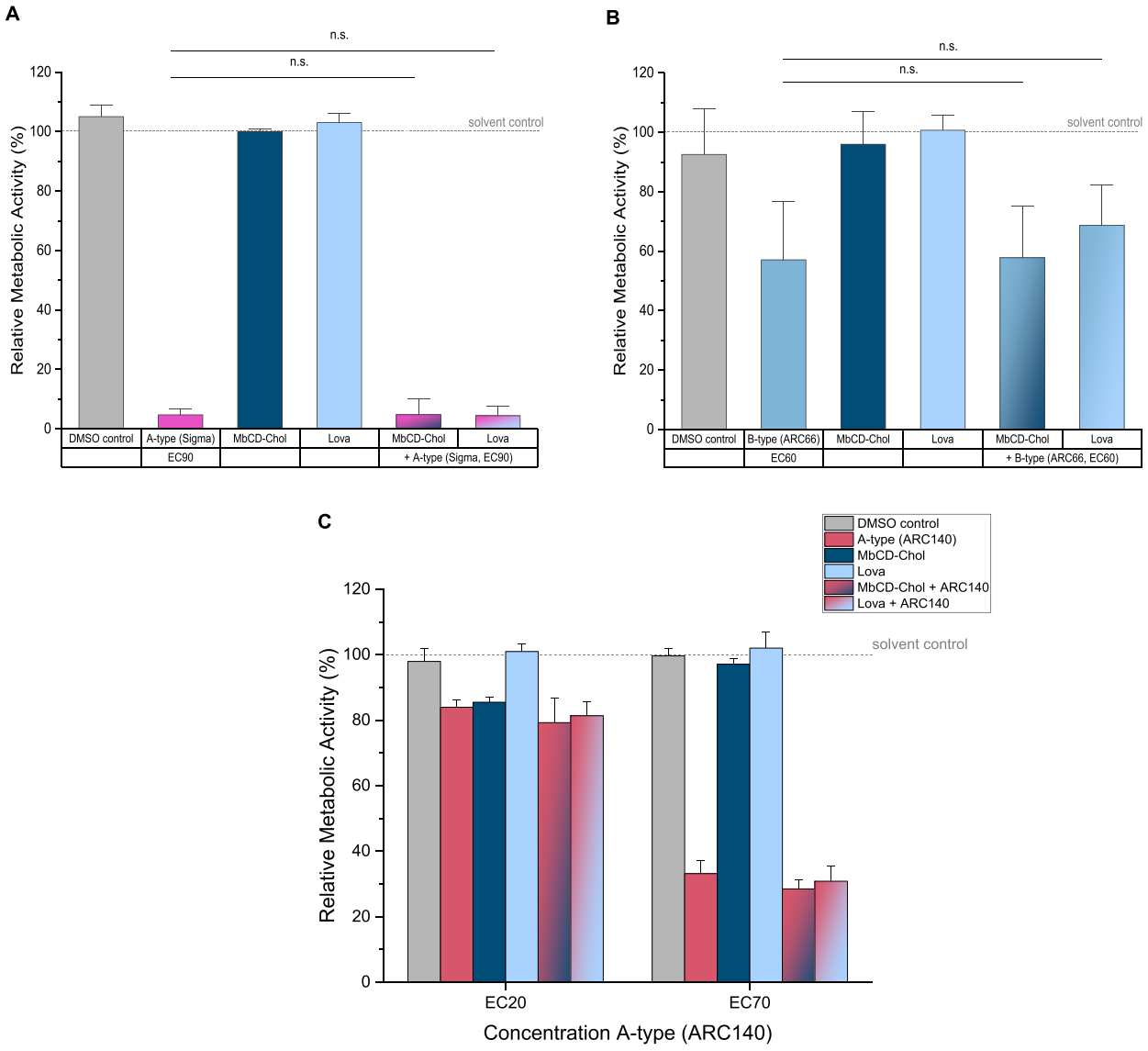

Fig. 5. Metabolic activity of RTgill-W1 cells exposed to the A-type prymnesin solution (Sigma Aldrich) at approximately EC_{90} (12 nM) (**A**), the UNCW-ARC66 extract (B-type prymnesins) at approximately EC_{60} (113 nM) (**B**), and the UNCW-ARC140 extract (A-type) (**C**) at approximately EC_{20} (4 nM) and EC_{70} (14 nM) for 3 h after a 24 h treatment with the cholesterol-altering compounds methyl-β-cyclodextrin loaded with cholesterol (MbCD-Chol, 10 μM) and lovastatin (Lova, 10 μM). The prymnesin concentrations (nM) reflect the total concentration of all analogs present in each sample respectively. Dimethylsulfoxide (DMSO) at 0.25 % (*v/v*) in culture medium was added as control for treatment with Lova, and culture medium containing 0.5 % (*v/v*) EtOH was used as solvent control. Data represent mean ± SD of n ≥ 3. (* = $p < 0.05$; ** = $p < 0.01$; *** = $p < 0.001$; n.s. = no significance), except for the ARC140 sample, where sample size was n = 2 (therefore no statistics were performed for this sample).

Table 2
Dissociation constants k_d (1/s) of the prymnesin samples A-type solution (Sigma Aldrich) and B-type extract (strain K-0081) for the different ligands: cholesterol, epicholesterol, and ergosterol. Chi^2 values indicate the quality of the 1:1 fitting performed for this calculation.

Immobilized ligand	Sample prymnesin	1:1 dissociation k_d (1/s)	Quality Kinetics Chi^2 (RU^2)
Cholesterol	A-type	n.d.	n.d.
	B-type	6.72×10^{-3}	5.45×10^{-1}
Epicholesterol	A-type	2.59×10^{-3}	2.43×10^{2}
	B-type	3.09×10^{-3}	1.14
Ergosterol	A-type	6.64×10^{-3}	5.25×10^{2}
	B-type	5.35×10^{-3}	1.97×10^{-1}

n.d. – no data

the A-type solution (Sigma Aldrich) was caused by something else. Or conversely, whether the presence of unknown compounds in the other samples hindered this effect. As stated in another study, unidentified molecules present in extracts potentially affect the cytotoxic potency of prymnesins (Varga and Prause *et al.*, 2024). The more pronounced differential in potency between the three prymnesin types in the RBCs raises an interesting and potentially important question. The manner in which prymnesins target cell membranes may vary depending on the type of prymnesin and possibly also the specific analog. This variation may become more evident through testing in various cell models. Generally, RBCs from Atlantic salmon were less sensitive toward prymnesins than RTgill-W1 cells, particularly when exposed to B-type and C-type prymnesins. It has already been described in one of the earlier studies on prymnesins that the species origin of RBCs matters greatly when it comes to the hemolytic potential of the analog prymnesin-A (3 Cl) + pentose (Igarashi *et al.*, 1998). This may be caused

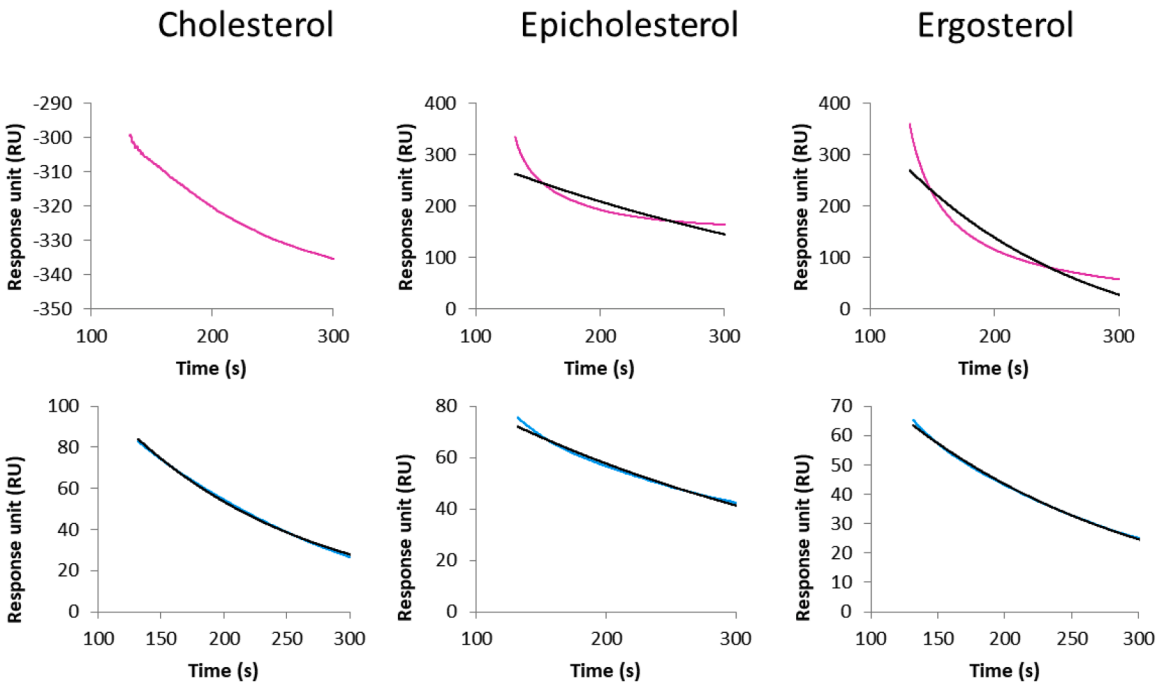

Fig. 6. Sensograms for dissociation kinetics of 1 μM A-type prymnesins (red (Sigma Aldrich solution from unknown strain origin)) and B-type prymnesins (blue (extract from K-0081)) from immobilized ligands; 10 mM ergosterol, 10 mM epicholesterol, and 10 mM cholesterol. Fitted 1:1 dissociation curves are shown in black and measured curves in color. Measurements were performed in duplicates. The dissociation constants (k_d(1/s)) and quality of fit (Chi^2) for the respective ligands are provided in Table 2. The prymnesin concentrations (nM) reflect the total concentration of all analogs present in each sample respectively.

by significant variances in lipid profiles in terms of their content of unsaturated and long chain lipids or the cholesterol-phospholipid molar ratio (Cornwell *et al.*, 1968; O'Brien, 1967).

Generally, a change in cholesterol content of about 10-30 % in RTgill-W1 cells could be achieved, yet unexpectedly it did not affect the overall cytotoxicity of the tested samples. Several studies have shown that altering cholesterol content of cells can disrupt the lipid/cholesterol rafts within the plasma membrane (Gyoten *et al.*, 2023; von Tresckow *et al.*, 2004; Zidovetzki and Levitan, 2007). On the one hand, it may be that changes in membrane cholesterol levels did not occur evenly throughout the membrane. One possibility would be that they took place in the cholesterol-rich rafts, leaving cholesterol located outside those rafts available for prymnesin interaction. This theory would at least in part explain why the samples exhibited the same toxicity and seems plausible assuming prymnesins to prefer or be just as capable of interacting with cholesterol outside those lipid rafts. On the other hand, the cholesterol alteration was likely not specifically located in the plasma membrane, but within the entire cell. Previous findings have shown that modifications of plasma cholesterol can have a substantial effect on the intracellular cholesterol content (Lange *et al.*, 2004; Zidovetzki and Levitan, 2007). By this measure, the 10-30 % cholesterol change in the RTgill-W1 cells does not necessarily refer to the plasma membrane only, but to a global cellular cholesterol content. It should be highlighted that while a significant change in cholesterol content could be achieved, continuous lysis induced by prymnesins, possibly to a lower extent, may still be possible even with a lower membrane sterol content.

It was recently suggested that stabilization of pores caused by amphidinol 3 is achieved by insertion of the lipophilic arm through the membrane (Matsumori *et al.*, 2024). Considering that prymnesins and amphidinols share this lipophilic property, it can be inferred that this hydrocarbon chain is of similar importance for prymnesins. They may be able to insert themselves into the bilayer in a way similar to the first binding step of amphidinol 3 or the interaction of saponin with the plasma membrane (Lorent *et al.*, 2014; Matsumori *et al.*, 2024). Seeing how prymnesins are considerably large molecules, self-aggregation of several toxin-entities, as proposed for saponins, seems doubtful (Lorent *et al.*, 2014). Instead, a prymnesin monomer or dimer may be sufficient to create a channel in the bilayer, enabling ion transport through the membrane as, proposed by the group of Chen *et al.* (2005) for amphiphilic compounds with a more rigid or more flexible core, respectively. At this point it remains to be debated how flexible prymnesin molecules are, and how much the lack of the double-ring structure in B-types influences this compared to the A-type prymnesins. Considering the SPR data of obtained in this study, it could be suggested that B-type and A-type prymnesins have distinct mechanisms of interacting with the bilayer. A-type prymnesins may exhibit a binding similar to that of amphidinol 3, which follows a two-step binding (Matsumori *et al.*, 2024). The significantly lower potency observed for B- and C-type prymnesins in RBCs may hint at an interaction distinct from that of A-types with the plasma membrane.

Based on the results of this study, it seems as though cellular cholesterol of the target cell is not the defining factor for the mode of action of prymnesins, and that the role of cholesterol must be more intricate. *P. parvum* cells contain a very low overall level of sterols, which could be considered a self-protection mechanism (Ghosh *et al.* 1998). This theory would be in line with the fact that prymnesins are able to build stable complexes with cholesterol, as was shown in the SPR experiments. However, modulating the cholesterol content of RTgill-W1 cells had no effect on prymnesin cytotoxicity, which contradicts the previous theory. Considering all the findings discussed thus far an alternative hypothesis could be inferred: prymnesins may require cholesterol as an anchor to the cell membrane, yet the actual pore-formation is in part caused or stabilized by a different mechanism. One suggestion is pore-formation through increased activation of selected ion-channels or ATPases (Haberman, 1989; Cox *et al.* 2019). This hypothesis seems more likely given that prymnesin toxicity is known to be influenced by the presence or absence of certain ions and can affect membrane conductance (Igarashi *et al.* 1998; Moran and Ilani., 1974; Ulitzur and Shilo, 1964; Varga and Prause *et al.*, 2024). It should be kept in mind, that the exact mechanism might look different between each prymnesin type (A,- B-, or C-type)

In conclusion, the lytic mechanism of prymnesins seems to be more

complex than previously believed. The interplay of membrane components with each other and the influence prymnesins may have on this remain to be fully assessed. Thus far, it is evident that prymnesins exhibit strong affinities towards lipids and can induce osmotic imbalance in cells. It is likely that A-type and B-type prymnesins target lipid-bilayers differently, possibly due to variations in their backbone structures. Additionally, the extent of their toxic effects varies depending on the cell type, which was particularly evident for B- and C-type prymnesins. However, the potency ranking observed for the samples in this study remained the same across the test-systems, indicating that the relative toxicity of individual analogs was stable. Further studies on the mode of action of prymnesins should prioritize understanding the differences between plasma membranes of various cell types and species. These investigations should not only include lipids, but also proteins such as ion-channels. Lastly, understanding which aspects of the different prymnesin classes are responsible for variations in their toxic potential could help deepen knowledge of the mode of action greatly.

Author declaration

Submission of an article implies that the work described has not been published previously (except in the form of an abstract or as part of a published lecture or academic thesis), that it is not under consideration for publication elsewhere, that its publication is approved by all authors and tacitly or explicitly by the responsible authorities where the work was carried out, and that, if accepted, it will not be published elsewhere in the same form, in English or in any other language, without the written consent of the copyright-holder.

By attaching this Declaration to the submission, the corresponding author certifies that:

- The manuscript represents original and valid work and that neither this manuscript nor one with substantially similar content under the same authorship has been published or is being considered for publication elsewhere.
- Every author has agreed to allow the corresponding author to serve as the primary correspondent with the editorial office, and to review the edited typescript and proof.
- Each author has given final approval of the submitted manuscript and order of authors. Any subsequent change to authorship will be approved by all authors.
- Each author has participated sufficiently in the work to take public responsibility for all the content.

CRediT authorship contribution statement

Hélène-Christine Prause: Writing – review & editing, Writing – original draft, Visualization, Methodology, Investigation, Funding acquisition, Formal analysis, Data curation, Conceptualization. **Deniz Berk:** Writing – review & editing, Visualization, Investigation, Formal analysis, Data curation. **Catharina Alves-de-Souza:** Writing – review & editing, Resources. **Per J. Hansen:** Writing – review & editing, Resources. **Thomas O. Larsen:** Writing – review & editing, Resources. **Doris Marko:** Writing – review & editing, Supervision, Resources, Funding acquisition. **Giorgia Del Favero:** Writing – review & editing, Supervision, Resources, Methodology, Conceptualization. **Allen Place:** Writing – review & editing, Supervision, Resources, Methodology, Conceptualization. **Elisabeth Varga:** Writing – review & editing, Supervision, Resources, Project administration, Methodology, Funding acquisition, Conceptualization.

Declaration of competing interest

The authors declare that they have no known competing financial interests or personal relationships that could have appeared to influence the work reported in this paper.

Data availability

Data will be made available on request.

Funding

This project was partially funded by the travel grant of the Doctoral School in Chemistry (DoSChem) of the University of Vienna. Furthermore, the research was supported by the University of Vienna, Faculty of Chemistry, Department of Food Chemistry and Toxicology. This research was funded in part by the Austrian Science Fund (FWF) [grant DOI:10.55776/I5707]. C.A.d.S. was funded by COPAS Coastal ANID FB210021. For open access purposes, the author has applied a CC BY public copyright license to any author accepted manuscript version arising from this submission. Open access funding was provided by the University of Veterinary Medicine Vienna.

Acknowledgements

We are grateful for the generous input with the imaging workflows of the Core Facility Multimodal Imaging, member of the VLSI (Vienna Life Science Instruments), Faculty of Chemistry, University of Vienna. Much appreciation is felt for John Stubbelfield, Zohar Laboratory, University of Maryland Baltimore County, for procuring the salmon blood samples. Michael Murphy, Biacore, Cytiva (Danaher Corp., Washington DC, USA), kindly supported the data evaluation for SPR experiments. Tom Shier from the Department of Medicinal Chemistry, College of Pharmacy, University of Minnesota gratefully provided the A-type prymnesin solution previously available from Sigma Aldrich. The pellets of strains UNCW-ARC140 and UNCW-ARC66 were kindly provided by the Algal Resources Collection at the University of North Carolina Wilmington. The RTgill-W1 cell line was provided by Kristin Schirmer, Department of Environmental Toxicology, EAWAG, and the HCEC-1CT cell line by Jerry W. Shay from the UT Southwestern Medical Center. This work is supported by the USDA National Institute of Food and Agriculture through the Food Research Initiative SAS program (award #2021-68012-35922). Peter Frühauf and the Department of Analytical Chemistry at the University of Vienna is acknowledged for the provision of the fluorescence detector and Franz Berthiller of the BOKU University for the opportunity to perform LC-HRMS measurements on the 6550 iFunnel Q-TOF LC-MS system. The authors are grateful to the Mass Spectrometry Centre (MSC), member of the VLSI, Faculty of Chemistry, University of Vienna for technical assistance.

Supplementary materials

Supplementary material associated with this article can be found, in the online version, at doi:10.1016/j.aquatox.2024.107080.

References

Andersen, A., de Medeiros, L., Binzer, S., Rasmussen, S., Hansen, P., Nielsen, K., Jørgensen, K., Larsen, T., 2017. HPLC-HRMS quantification of the ichthyotoxin karmitoxin from *Karlodinium armiger*. Mar. Drugs 15, 278. https://doi.org/10.3390/md15090278.

Bachvaroff, T.R., Adolf, J.E., Squier, A.H., Harvey, H.R., Place, A.R., 2008. Characterization and quantification of karlotoxins by liquid chromatography–mass spectrometry. Harmful. Algae. 7, 473–484. https://doi.org/10.1016/j.hal.2007.10.003.

Bergsson, H., Reducha Andersen, N., Søndergaard Svendsen, M.B., Juel Hansen, P., Fleng Steffensen, J., 2019. Respiratory physiology of European plaice (*Pleuronectes platessa*) exposed to *Prymnesium parvum*. Fishes 4 (2), 32. https://doi.org/10.3390/fishes4020032.

Binzer, S.B., Svenssen, D.K., Daugbjerg, N., Alves-de-Souza, C., Pinto, E., Hansen, P.J., Larsen, T.O., Varga, E., 2019. A-, B- and C-type prymnesins are clade specific compounds and chemotaxonomic markers in *Prymnesium parvum*. Harmful. Algae. 81, 10–17. https://doi.org/10.1016/j.hal.2018.11.010.

Blossom, H.E., Rasmussen, S.A., Andersen, N.G., Larsen, T.O., Nielsen, K.F., Hansen, P.J., 2014. *Prymnesium parvum* revisited: relationship between allelopathy,

ichthyotoxicity, and chemical profiles in 5 strains. Aquat. Toxicol. 157, 159–166. https://doi.org/10.1016/J.AQUATOX.2014.10.006.
Bols, N.C., Barlian, A., Chirino-Trejo, M., Caldwell, S.J., Goegan, P., Lee, L.E.J., 1994. Development of a cell line from primary cultures of rainbow trout, Oncorhynchus mykiss (Walbaum), gills. J. Fish Dis. 17 (6), 601–611. https://doi.org/10.1111/j.1365-2761.1994.tb00258.x.
Chen, W.H., Shao, X.B., Regen, S.L., 2005. Poly (choloyl)-based amphiphiles as pore-forming agents: transport-active monomers by design. J Am Chem S 127 (36), 12727–12735. https://doi.org/10.1021/ja053527q.
Cichewicz, R.H., Hambright, K.D., 2010. A revised amino group pKa for prymnesins does not provide decisive evidence for a pH-dependent mechanism of *Prymnesium parvum*'s toxicity. Toxicon 55 (5), 1035–1037. https://doi.org/10.1016/j.toxicon.2010.02.002.
Cornwell, D.G., Heikkila, R.E., Bar, R.S., Biagi, G.L., 1968. Red blood cell lipids and the plasma membrane. J. Am. Oil. Chem. S 45 (5), 297–304. https://doi.org/10.1007/BF02667099.
Caron, D.A., Lie, A.A., Buckowski, T., Turner, J., Frabotta, K., 2023. The effect of pH and salinity on the toxicity and growth of the golden alga, *Prymnesium parvum*. Protist 174 (1), 125927. https://doi.org/10.1016/j.protis.2022.125927.
Cox, C.D., Gottlieb, P.A., 2019. Amphipathic molecules modulate PIEZO1 activity. Biochem. Soc. Transact. 47 (6), 1833–1842. https://doi.org/10.1042/BST20190372.
Dayeh, V.R., Schirmer, K., Lee, L.E., Bols, N.C., 2005. Rainbow trout gill cell line microplate cytotoxicity test. Small-scale Freshwater Toxicity Investigations: Toxicity Test Methods, pp. 473–503. https://doi.org/10.1007/1-4020-3120-3_16.
Deeds, J.R., Terlizzi, D.E., Adolf, J.E., Stoecker, D.K., Place, A.R., 2002. Toxic activity from cultures of *Karlodinium micrum* (= *Gyrodinium galatheanum*)(Dinophyceae)—a dinoflagellate associated with fish mortalities in an estuarine aquaculture facility. Harmful Algae 1 (2), 169–189. https://doi.org/10.1016/S1568-9883(02)00027-6.
Del Favero, G., Hohenbichler, J., Mayer, R.M., Rychlik, M., Marko, D., 2020. Mycotoxin altertoxin II induces lipid peroxidation connecting mitochondrial stress response to NF-κB inhibition in THP-1 macrophages. Chem. Res. Toxicol. 33 (2), 492–504. https://doi.org/10.1021/acs.chemrestox.9b00378.
Free, G., Van de Bund, W., Gawlik, B., Van Wijk, L., Wood, M., Guagnini, E., Koutelos, K., Annunziato, A., Grizzetti, B., Vigiak, O., Gnecchi, M., Poikane, S., Christiansen, T., Whalley, C., Antognazza, F., Zerger, B., Hoeve, R.J., Stielstra, H., European Commission. Joint Research Centre, 2023. An EU analysis of the ecological disaster in the Oder River of 2022: lessons learned and research-based recommendations to avoid future ecological damage in EU rivers, a joint analysis from DG ENV, JRC and the EEA. Publications Office of the European Union: Luxembourg. https://doi.org/10.2760/067386.
Gaudreault, J., Liberelle, B., Durocher, Y., Henry, O., De Crescenzo, G., 2021. Determination of the composition of heterogeneous binder solutions by surface plasmon resonance biosensing. Sci. Rep. 11 (1), 3685.
Ghosh, P., Patterson, G.W., Wikfors, G.H., 1998. Sterols of some marine Prymnesiophyceae. J. Phycol. 34 (3), 511–514. https://doi.org/10.1046/j.1529-8817.1998.340511.x.
Guillard, R.R.L., 1975. Culture of Phytoplankton for Feeding Marine Invertebrates. Culture of Marine Invertebrate Animals. Springer US, Boston, MA, pp. 29–60. https://doi.org/10.1007/978-1-4615-8714-9_3.
Gyoten, M., Luo, Y., Fujiwara-Tani, R., Mori, S., Ogata, R., Kishi, S., Kuniyasu, H., 2023. Lovastatin treatment inducing apoptosis in human pancreatic cancer cells by inhibiting cholesterol rafts in plasma membrane and mitochondria. Int. J. Mol. Sci. 24, 16814. https://doi.org/10.3390/ijms242316814.
Haberland, M.E., Reynolds, J.A., 1973. Self-association of cholesterol in aqueous solution. Proc. Natl. Acad. Sci. 70 (8), 2313–2316. https://doi.org/10.1073/pnas.70.8.2313.
Habermann, E., 1989. Palytoxin acts through Na^+, K^+-ATPase. Toxicon 27 (11), 1171–1187. https://doi.org/10.1016/0041-0101(89)90026-3.
Hallegraeff, G.M., 1993. A review of harmful algal blooms and their apparent global increase. Phycologia 32, 79–99. https://doi.org/10.2216/I0031-8884-32-2-79.1.
Igarashi, T., Aritake, S., Yasumoto, T., 1998. Biological activities of prymnesin-2 isolated from a red tide alga *Prymnesium parvum*. Nat. Toxins 6, 35–41. https://doi.org/10.1002/(SICI)1522-7189(199802)6:1<35::AID-NT7>3.0.CO;2-7.
Igarashi, T., Satake, M., Yasumoto, T., 1999. Structures and partial stereochemical assignments for prymnesin-1 and prymnesin-2: Potent hemolytic and ichthyotoxic glycosides isolated from the red tide alga *Prymnesium parvum*. J. Am. Chem. Soc. 121, 8499–8511. https://doi.org/10.1021/ja991740e.
Igarashi, T., Satake, M., Yasumoto, T., 1996. Prymnesin-2: a potent ichthyotoxic and hemolytic glycoside isolated from the red tide alga *Prymnesium parvum*. J. Am. Chem. Soc. 118, 479–480. https://doi.org/10.1021/ja9534112.
Imai, M., Inoue, K., 1974. The mechanism of action of *prymnesium* toxin on membranes. Biochim. Biophys. Acta 352, 344–348. https://doi.org/10.1016/0005-2736(74)90226-0.
Kaartvedt, S., Johnsen, T.M., Aksnes, D.L., Lie, U., Svendsen, H., 1991. Occurrence of the toxic phytoflagellate *Prymnesium parvum* and associated fish mortality in a norwegian fjord system. Can J Fish Aquat Sci 48, 2316–2323. https://doi.org/10.1139/f91-272.
Lange, Y., Ye, J., Steck, T.L., 2004. How cholesterol homeostasis is regulated by plasma membrane cholesterol in excess of phospholipids. Proc. Natl Acad. Sci. 101, 11664–11667. https://doi.org/10.1073/pnas.0404766101.
Lorent, J.H., Quetin-Leclercq, J., Mingeot-Leclercq, M.P., 2014. The amphiphilic nature of saponins and their effects on artificial and biological membranes and potential consequences for red blood and cancer cells. Org & Biomol Chem 12 (44), 8803–8822. https://doi.org/10.1039/C4OB01652A.
Matsumori, N., Hieda, M., Morito, M., Wakamiya, Y., Oishi, T., 2024. Truncated derivatives of amphidinol 3 reveal the functional role of polyol chain in sterol-recognition and pore formation. BMCL 98, 129594. https://doi.org/10.1016/j.bmcl.2023.129594.
Moran, A., Ilani, A., 1974. The effect of prymnesin on the electric conductivity of thin lipid membranes. J. Membr Biol 16, 237–256. https://doi.org/10.1007/BF01872417.
O'Brien, J.S., 1967. Cell membranes—composition: structure: function. J. Theoretical. Biol. 15 (3), 307–324. https://doi.org/10.1016/0022-5193(67)90140-3.
Rasmussen, S.A., Meier, S., Andersen, N.G., Blossom, H.E., Duus, J.Ø., Nielsen, K.F., Hansen, P.J., Larsen, T.O., 2016. Chemodiversity of ladder-frame prymnesin polyethers in *Prymnesium parvum*. J. Nat. Prod. 79 (9), 2250–2256. https://doi.org/10.1021/acs.jnatprod.6b00345.
Rebhahn, V.I.C., Kiss, E., Marko, D., Del Favero, G, 2022. Foodborne compounds that alter plasma membrane architecture can modify the response of intestinal cells to shear stress *in vitro*. Toxicol. Appl. Pharmacol. 446, 116034 https://doi.org/10.1016/j.taap.2022.116034.
Shilo, M., 1981. The Toxic Principles of *Prymnesium Parvum*. The Water Environment. Springer US, Boston, MA, pp. 37–47. https://doi.org/10.1007/978-1-4613-3267-1_4.
Shilo, M., Aschner, M., 1953. Factors governing the toxicity of cultures containing the phytoflagellate *Prymnesium parvum* Carter. Microbiology 8 (3), 333–343. https://doi.org/10.1099/00221287-8-3-333.
Svenssen, D.K., Binzer, S.B., Medić, N., Hansen, P.J., Larsen, T.O., Varga, E., 2019. Development of an indirect quantitation method to assess ichthyotoxic B-type prymnesins from *Prymnesium parvum*. Toxins 11, 251. https://doi.org/10.3390/toxins11050251.
Ulitzur, S., Shilo, M., 1966. Mode of action of *Prymnesium parvum* ichthyotoxin. J. Protozool. 13, 332–336. https://doi.org/10.1111/J.1550-7408.1966.TB01915.X.
Ulitzur, S., Shilo, M., 1964. A sensitive assay system for determination of the ichthyotoxicity of *Prymnesium parvum*. J. Gen. Microbial. 36, 161–169. https://doi.org/10.1099/00221287-36-2-161.
Valenti Jr, T.W., James, S.V., Lahousse, M.J., Schug, K.A., Roelke, D.L., Grover, J.P., Brooks, B.W, 2010. A mechanistic explanation for pH-dependent ambient aquatic toxicity of *Prymnesium parvum* Carter. Toxicon 55 (5), 990–998. https://doi.org/10.1016/j.toxicon.2009.09.014.
Varga, E., Prause, H.-C., Riepl, M., Hochmayr, N., Berk, D., Attakpah, E., Kiss, E., Medić, N., Del Favero, G., Larsen, T.O., Hansen, P.J., Marko, D., 2024. Cytotoxicity of *Prymnesium parvum* extracts and prymnesin analogs on epithelial fish gill cells RTgill-W1 and the human colon cell line HCEC-1CT. Arch. Toxicol. 98 (2024), 999–1014. https://doi.org/10.1007/s00204-023-03663-5.
von Tresckow, B., Kallen, K.-J., von Strandmann, E.P., Borchmann, P., Lange, H., Engert, A., Hansen, H.P., 2004. Depletion of cellular cholesterol and lipid rafts increases shedding of CD30. J. Immunol. 172, 4324–4331. https://doi.org/10.4049/jimmunol.172.7.4324.
Waters, A.L., Oh, J., Place, A.R., Hamann, M.T., 2015. Stereochemical studies of the karlotoxin class using NMR Spectroscopy and DP4 chemical-shift analysis: insights into their mechanism of action. Angew. Chem. 127, 15931–15936. https://doi.org/10.1002/ange.201507418.
Yariv, J., Hestrin, S., 1961. Toxicity of the extracellular phase of *Prymnesium parvum* cultures. J. Gen. Microbiol. 24, 165–175. https://doi.org/10.1099/00221287-24-2-165.
Zidovetzki, R., Levitan, I., 2007. Use of cyclodextrins to manipulate plasma membrane cholesterol content: Evidence, misconceptions and control strategies. *Biochim et Biophys Act - Biomembranes* 1768, 1311–1324. https://doi.org/10.1016/j.bbamem.2007.03.026.

Supplementary information of

the mode of action of prymnesins How relevant are sterols for the mode of action of prymnesins?

Hélène-Christine Prause[1,2], Deniz Berk[1], Catharina Alves-de-Souza[3,4], Per J. Hansen[5], Thomas O. Larsen[6], Doris Marko[1], Giorgia Del Favero[1,7], Allen Place[8], Elisabeth Varga[1,9,*]

[1] Department of Food Chemistry and Toxicology, Faculty of Chemistry, University of Vienna, Währinger Str. 38-40, 1090 Vienna, Austria.

[2] Vienna Doctoral School in Chemistry, Faculty of Chemistry, University of Vienna, Währinger Str. 42, 1090 Vienna Austria.

[3] Departamento de Oceanografía, Facultad de Ciencias Naturales y Oceanográficas, Universidad de Concepción, Concepción 4030000, Chile

[4] Centro de Investigación Oceanográfica COPAS Coastal, Universidad de Concepción, Concepción, Chile

[5] Marine Biological Section, Department of Biology, University of Copenhagen, Strandpromenaden 5, 3000 Elsinore, Denmark.

[6] Department of Biotechnology and Biomedicine, Technical University of Denmark, Søltofts Plads 221, 2800 Kgs. Lyngby, Denmark.

[7] Core Facility Multimodal Imaging, Faculty of Chemistry, University of Vienna, Währinger Str. 38-42, 1090 Vienna, Austria.

[8] Institute of Marine and Environmental Technology, University of Maryland Center for Environmental Science, 701 E. Pratt Street, Baltimore, MD 21202, USA.

[9] Unit Food Hygiene and Technology, Centre for Food Science and Veterinary Public Health, Clinical Department for Farm Animals and Food System Science, University of Veterinary Medicine, Vienna, Veterinärplatz 1, 1210 Vienna, Austria

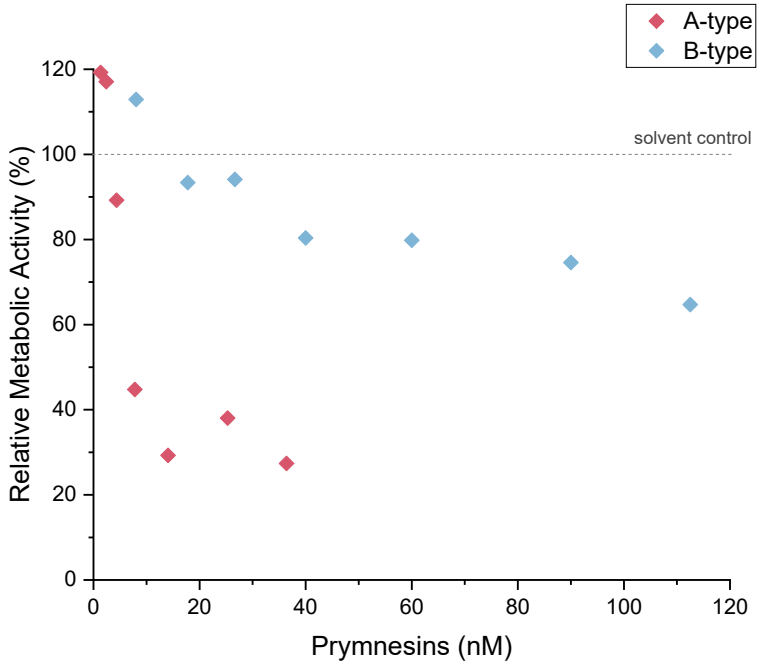

SI Figure 6 – Cytotoxic activity of UNCW-ARC prymnesin extracts for strains ARC140 (A-type) and ARC66 (B-type) in RTgill-W1 cells. Each data point represents the mean of a technical triplicate.

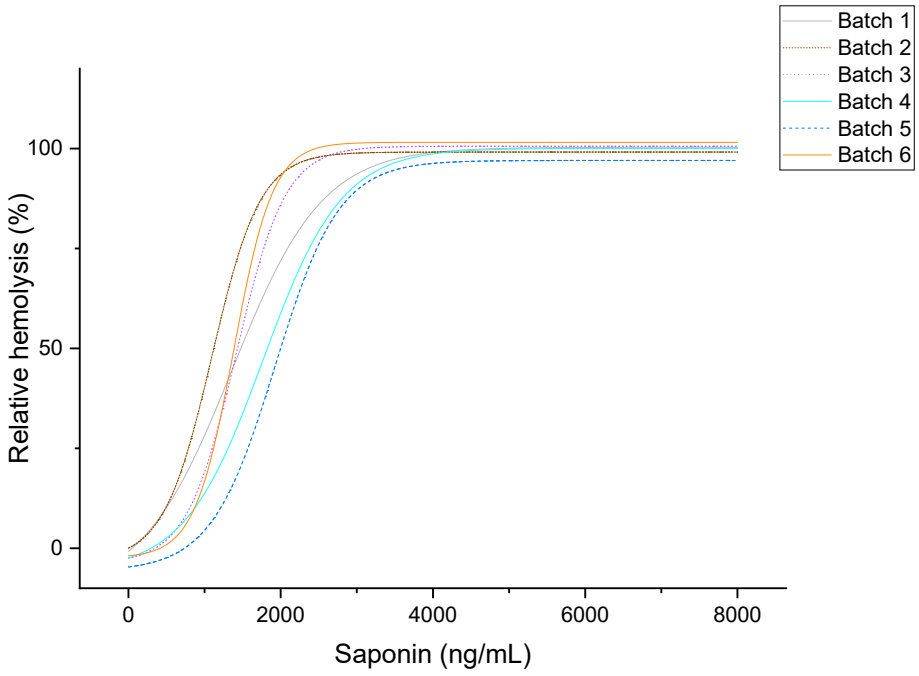

SI Figure 7 - Fitted dose-response curves obtained for hemolysis caused by saponin for each batch of 1.25 % (*v*/*v*)-red blood cell solution prepared from Atlantic salmon blood. Data lines represent fitted curves of mean ± SD of n ≥ 3

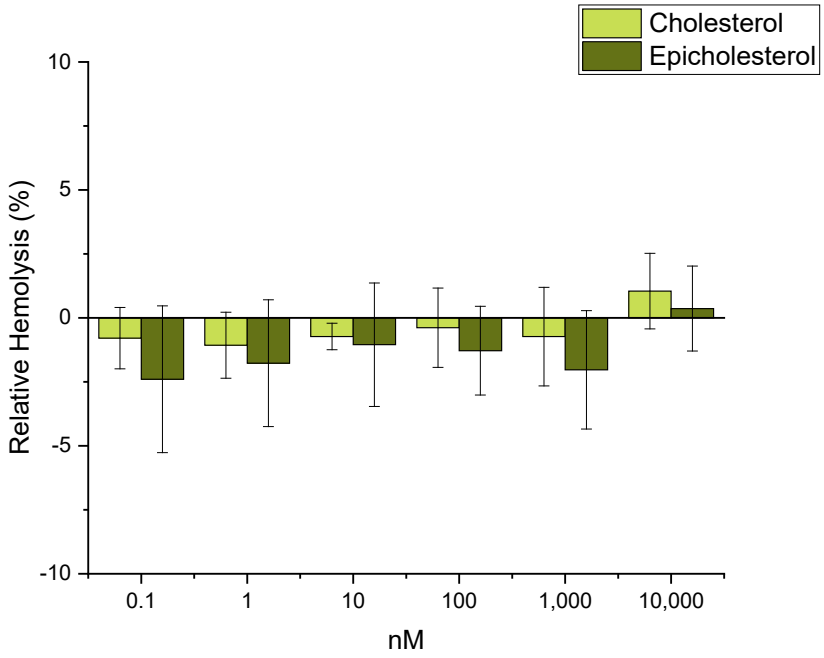

SI Figure 8 – Sterol control from hemolysis assays where prymnesin samples were combined with either cholesterol or epicholesterol. Data represent mean ± SD of n ≥ 5

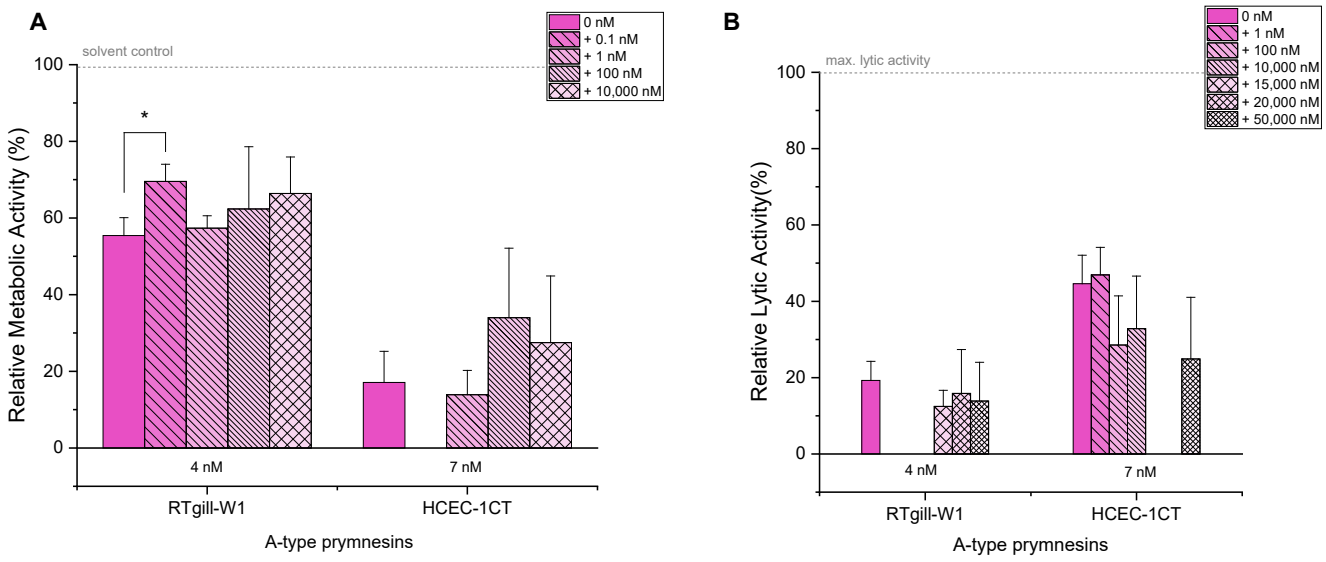

SI Figure 9 – Combination of the A-type prymnesin solution (Sigma Aldrich from the unknown strain origin) with different concentrations of cholesterol in RTgill-W1 cells and HCEC-1CT cells. Cytotoxic measurements were taken in the CTB assay (**A**), and lytic activity was recorded with the LDH assay (**B**). Data represent mean ± SD of n ≥ 2.[#]

[#]Missing bars indicate that the combination with the respective concentration of cholesterol was not performed.

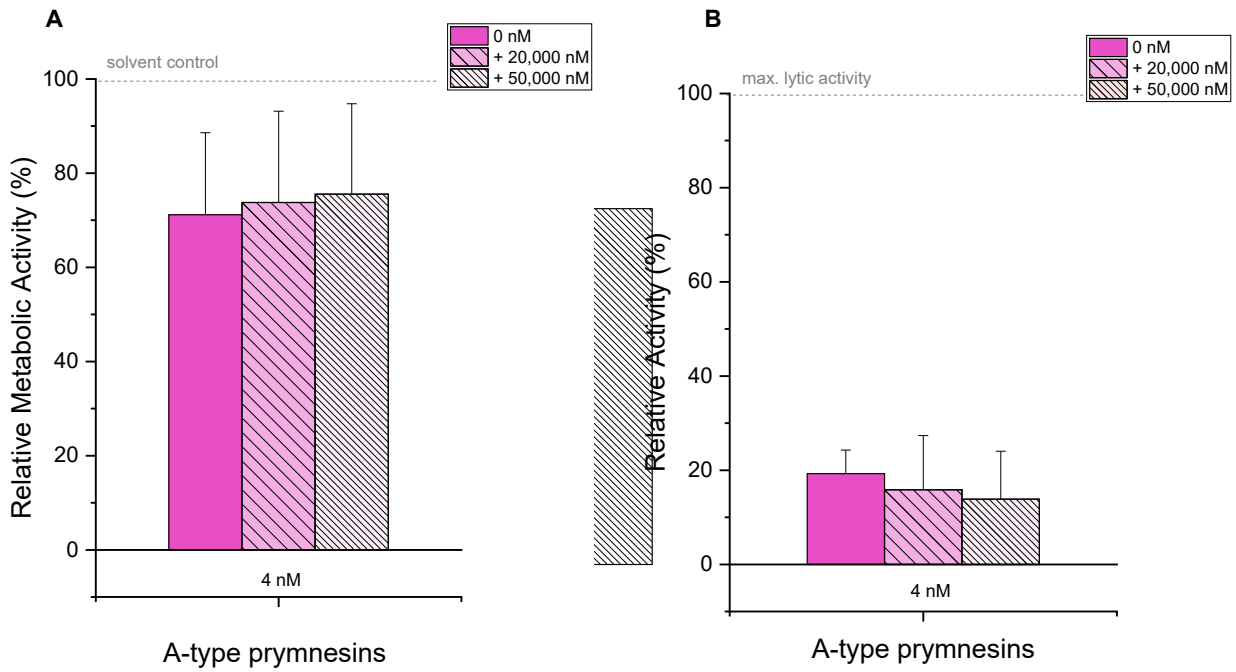

SI Figure 10 – Combination of the A-type prymnesin solution (Sigma Aldrich from the unknown strain origin) with different concentrations of epicholesterol in RTgill-W1 cells. Cytotoxic measurements were taken in the CTB assay (**A**), and lytic activity was recorded with the LDH assay (**B**). Data represent mean ± SD of n ≥ 2.

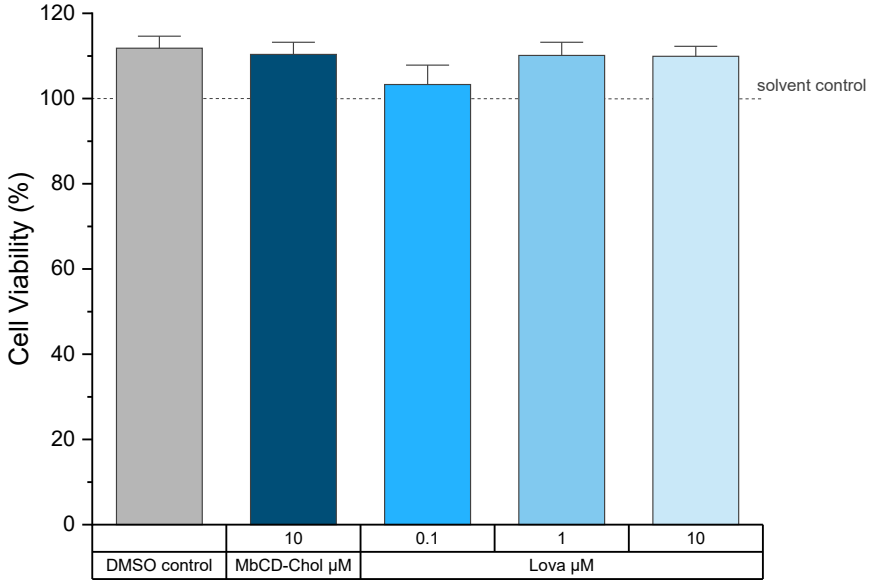

SI Figure 11 – Cell viability resulting from RTgill-W1 cells treated with methyl-β-cyclodextrin loaded with cholesterol (MbCD-Chol), and lovastatin (Lova) for 24 h measured via the WST-1 assay. The solvent control consisted of only culture medium, and culture medium containing 0.25 % (*v/v*) dimethylsulfoxide (DMSO) was added as control for treatment with Lova. Data represent mean ± SD of n=3.

7.3 Manuscript 3 – “The cytotoxic and hemolytic potential of karmitoxin from *Karlodinium armiger* and how it interacts with sterols”

This paper was published in Harmful Algae, Volume 143, in February 2025. https://doi.org/10.1016/j.hal.2025.102817

Author contributions: conceptualization **H.C.P**., G.D.F., A.P., E.V.; data curation, formal analysis, investigation, and visualization **H.C.P**., N.H., Y.Y.; funding acquisition **H.C.P**., D.M., E.V.; methodology **H.C.P.,** T.O.L., P.J.H., G.D.F., A.P., E.V.; project administration E.V.; resources T.O.L., P.J.H., G.D.F., D.M., A.P., E.V.; supervision G.D.F., D.M., A.P., E.V.; writing - original draft **H.C.P.**; writing - review & editing all co-authors.

The master student Nadine Hochmayr performed initial cytotoxicity tests in HCEC-1CT and RTgill-W1 cells, including comparison of 3 vs. 24 h exposure. Yanan Yu was responsible for *K. armiger* cultivation and toxin purification and worked under the supervision of Thomas Ostenfeld Larsen and Per Juel Hansen. The remaining assays (hemolysis, hemolysis with addition of free sterols, SPR, cholesterol modulation and cytotoxicity in modulated RTgill-W1 cells) were performed by the author of this thesis, as well as data evaluation/visualization and paper drafting/writing. Giorgia Del Favero mentored the fluorescence microscope part and Allen Place supervised the hemolysis and SPR measurements as well as sterol interactions. In her role as supervisor, Doris Marko provided resources and funding. Elisabeth Varga was the principal investigator of this work and co-supervisor of the students.

Harmful Algae 143 (2025) 102817

Contents lists available at ScienceDirect

Harmful Algae

journal homepage: www.elsevier.com/locate/hal

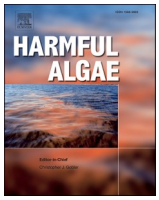

The cytotoxic and hemolytic potential of karmitoxin from *Karlodinium armiger* and how it interacts with sterols

Hélène-Christine Prause [a,b], Nadine Hochmayr [a], Yanan Yu [c,d], Thomas Ostenfeld Larsen [c], Per Juel Hansen [e], Giorgia Del Favero [a,f], Doris Marko [a], Allen Place [g], Elisabeth Varga [a,h,*]

[a] Department of Food Chemistry and Toxicology, Faculty of Chemistry, University of Vienna, Währinger Str. 38-40, 1090 Vienna, Austria
[b] Vienna Doctoral School in Chemistry, Faculty of Chemistry, University of Vienna, Währinger Str. 42, 1090 Vienna Austria
[c] Department of Biotechnology and Biomedicine, Technical University of Denmark, Søltofts Plads 221, 2800 Kgs. Lyngby, Denmark
[d] Key Laboratory of Oceanic and Polar Fisheries, Ministry of Agriculture and Rural Affairs, East China Sea Fisheries Research Institute, Chinese Academy of Fishery Sciences, Jungong Road 300, Shanghai, 200090, China
[e] Marine Biological Section, Department of Biology, University of Copenhagen, Strandpromenaden 5, 3000 Elsinore, Denmark
[f] Core Facility Multimodal Imaging, Faculty of Chemistry, University of Vienna, Währinger Str. 38-42, 1090 Vienna, Austria
[g] Institute of Marine and Environmental Technology, University of Maryland Center for Environmental Science, 701 E. Pratt Street, Baltimore, MD 21202, USA
[h] Unit Food Hygiene and Technology, Centre for Food Science and Veterinary Public Health, Clinical Department for Farm Animals and Food System Science, University of Veterinary Medicine, Vienna, Veterinärplatz 1, 1210 Vienna, Austria

ARTICLE INFO

Keywords:
Ichthyotoxin
Mode of action
Lysis
Cholesterol
RTgill-W1
HCEC-1CT

ABSTRACT

Karmitoxin, produced by *Karlodinium armiger*, is structurally related to karlotoxin and amphidinols, two potent ichthyotoxic hemolysins with high affinity for sterols. Given these structural similarities, karmitoxin is believed to exhibit comparable toxic effects. Cytotoxicity was assessed in the fish gill cell line RTgill-W1 and the human epithelial colon cell line HCEC-1CT. The hemolytic potential with and without added sterols was tested on fish erythrocytes to investigate possible impacts of toxin-sterol interactions. Sterol interactions were further evaluated using surface plasmon resonance. A 3-h incubation returned an EC_{50} of 111 and 175 nM in RTgill-W1 and in HCEC-1CT cells, respectively. Lactate dehydrogenase (LDH) release increased with toxin concentration, reaching 11 % in the fish and 40 % in the human cell line. Extended exposure (24 h) increased the toxicity in RTgill-W1 cells (EC_{50} 74 nM, 40 % LDH release). In parallel, hemolytic potential of karmitoxin was confirmed, as well as its interaction with free sterols. Interaction kinetics revealed complex stabilities with $k_d(s^{-1})$ constants of 1.13×10^{-2} (cholesterol), 5.48×10^{-3} (epicholesterol), and 4.72×10^{-3} (ergosterol). Interaction with cholesterol followed the single-exponential model well, while data indicated more complex binding with epicholesterol and ergosterol. Altering the RTgill-W1 cholesterol content did not impact cytotoxicity at the tested concentration. Overall, karmitoxin showed potent cytotoxic and hemolytic properties in human and fish models. Complex formation with sterols may play a role in membrane targeting, yet cellular cholesterol quantity might not affect cytotoxicity.

1. Introduction

The dinoflagellate species *Karlodinium armiger* was identified and isolated from the Mediterranean Sea two decades ago (Bergholtz et al., 2006; Garcés et al., 2006). This species has been associated with several fish kills and has since its discovery been found to produce an ichthyotoxin called karmitoxin which is structurally similar to karlotoxins and amphidinols (Fig. 1) (Rasmussen et al., 2017). The key feature distinguishing karmitoxin from karlotoxin and amphidinols is the primary amine group at the end of the lipophilic arm. The mode of action (MOA) of karlotoxin and amphidinols is an ongoing area of research and is tentatively understood. It has been shown that these toxins can create pores in the plasma membrane, a process which is supported by their high affinity for membrane sterols, cholesterol or ergosterol (Deeds and Place, 2006; Deeds et al., 2002; Place et al., 2009; Swasono et al., 2010; Waters et al., 2015; Place et al. 2024). Their ability to create pores has

* Corresponding author.
E-mail address: elisabeth.varga@vetmeduni.ac.at (E. Varga).

https://doi.org/10.1016/j.hal.2025.102817
Received 15 November 2024; Received in revised form 4 February 2025; Accepted 7 February 2025
Available online 10 February 2025

also been described to be largely aided by their hairpin structure, which all of these compounds have in common (Houdai et al., 2005; Waters et al., 2015). The information available on the MOA of karlotoxins and amphidinols may suggest that karmitoxin could likewise possess affinity towards cholesterol, and that its lytic potency is influenced by or dependent on the presence of cholesterol.

Therefore, the purpose of this project was to shed light on the interaction with sterols, particularly cholesterol, as well as on the importance of sterols in the MOA of karmitoxin. Interactions with different types of sterols were tested in hemolysis assays using blood from Atlantic salmon (*Salmo salar*) and were also assessed using surface plasmon resonance (SPR) to gain insight into the binding kinetics. *In-vitro* cytotoxicity tests were performed in the rainbow trout gill cell line RTgill-W1 and the epithelial human colon cell line HCEC-1CT. This human cell line was selected to demonstrate that karmitoxin toxicity is not limited to fish gill cells. It may also provide insights into potential adverse effects in the event of human exposure to this ichthyotoxin. The effect of altering the cholesterol content of RTgill-W1 cells on the potential of karmitoxin was also assessed in cytotoxicity experiments.

2. Materials and methods

2.1. Algal culture and toxin purification

K. armiger strain K-0668 was acquired from the Scandinavian Culture Collection of Algae and Protozoa (SCCAP now part of Norwegian Culture Collection of Algae (NORCCA)). The algae were grown in modified f/2 medium with 50 μM NH_4^+, replacing NO_3^-, in autoclaved natural sea water at a salinity of 30. This was done according to the findings of Binzer et al. (2020), who showed that the mixotrophic algae *K. armiger* can grow well with the addition of NH_4^+ as a food source. $NaHCO_3$ at a final concentration of 0.5 mM was added to media after autoclaving the sea water. Cultures were grown at a constant temperature of 15 °C with aeration, a light-dark cycle of 14:10 h, and an irradiance of 150 μmol photons $m^{-2}{\cdot}s^{-1}$. Once the algae had reached stationary phase they were centrifuged, the supernatant was then loaded onto a C18 Sepra material (Phenomenex) in a SNAP column (60 g) and eluted with 80 % methanol containing 10 mM formic acid using an Isolera autoflash system (both Biotage, Uppsala, Sweden). Karmitoxin was then isolated by semipreparative HPLC on a Luna C18(2) column using an acetonitrile−H_2O gradient from 30 % to 50 % acetonitrile containing 50 ppm trifluoroacetic acid over 40 min at a flow rate of 4 mL/min. The purified karmitoxin was then reconstituted in ethanol (EtOH) and the protocol using high performance liquid chromatography and fluorescent detection (HPLC-FLD) for toxin semi-quantitation described for prymnesins by Svenssen et al. (2019) was applied to estimate the karmitoxin concentration. In short, the primary amine of karmitoxin was derivatized through labeling with a fluorescent tag (AccQ-Tag Fluor Reagent Kit, Waters Corporation, Milford, MA, USA). The chromatographic separation was performed on a 1200 HPLC system (Agilent Technologies, Waldbronn, Germany), using an Agilent Poroshell C18 column (2.1 × 50 mm, 2.7 μm) using water (0.1 % formic acid) as eluent A and acetonitrile (0.1 % formic acid) as eluent B. The toxin was detected at a fluorescence excitation wavelength of 250 nm and an emission wavelength of 395 nm. Data were evaluated using ChemStation for LC Rev. B.04.01 SP1 from Agilent Technologies.

2.2. Cell culture

Cell viability tests were mainly performed on the rainbow trout (*Oncorynchus mykiss*) gill cell line RTgill-W1. This cell line was provided by K. Schirmer, Department of Environmental Toxicology, EAWAG, Dübendorf, Switzerland. Cultivation was performed as previously described, at 19 °C in Leibovitz's 15 medium (L-15) supplemented with 1 % (*v/v*) penicillin/streptomycin (Thermo Fisher Scientific, Waltham, MA, USA) and 10 % (*v/v*) fetal calf serum (EuroBio, Le Ulis, France) (Bols et al., 1994).

Cytotoxicity tests were also conducted on the human epithelial colon cell line HCEC-1CT, which was kindly provided by J.W. Shay, UT Southwestern Medical Center, Dallas, TX, USA, and cultured at 37 °C and 5 % CO_2. Cultivation medium was prepared with 500 mL Dulbecco's Modified Eagle's Medium (DMEM (Thermo Fisher Scientific, Waltham, MA, USA)) supplemented with 10 mL HEPES buffer solution 1 M, 10 mL Medium 199 (10x), 10 mL HyClone™ Cosmic Calf™ Serum (GE Healthcare Life Sciences HyClone Laboratories, Danaher Corporation, Washington DC, USA), 5.2 mL Insulin-Transferrin-Selenium-G Supplement (Thermo Fisher Scientific, Waltham, MA, USA), 0.6 mL gentamycin solution (Sigma Aldrich GmbH, St. Louis, MO, USA), 100 μL Recombinant Human Epidermal Growth Factor (100 μg/mL, Szabo-Scandic HandelsgmbH & Co KG, Vienna, Austria), and 100 μL hydrocortisone (5 mg/mL, Merck KGaA, Darmstadt, Germany).

2.3. Toxicity assays

2.3.1. Hemolytic assay

The hemolytic potential of karmitoxin was evaluated using red blood cells (RBCs) obtained from Atlantic salmon (*Salmo salar*). The protocol for preparation of the buffers and the RBC-solution was adapted from Deeds et al. (2002) and followed as described in Prause et al. (2024). Briefly, heparin-treated needles were used to draw blood, which was subsequently centrifuged at 1250 rcf and 4 °C for 25 min and washed with Tris-buffer I, consisting of 150 mM NaCl, 3.2 mM KCl, 1.25 mM $MgSO_4$, 12.2 mM Tris base in MilliQ water. A 1.25 % (*v/v*) RBCs solution in Tris-buffer II (Tris-buffer I+ 3.75 mM $CaCl_2$) was prepared and stored

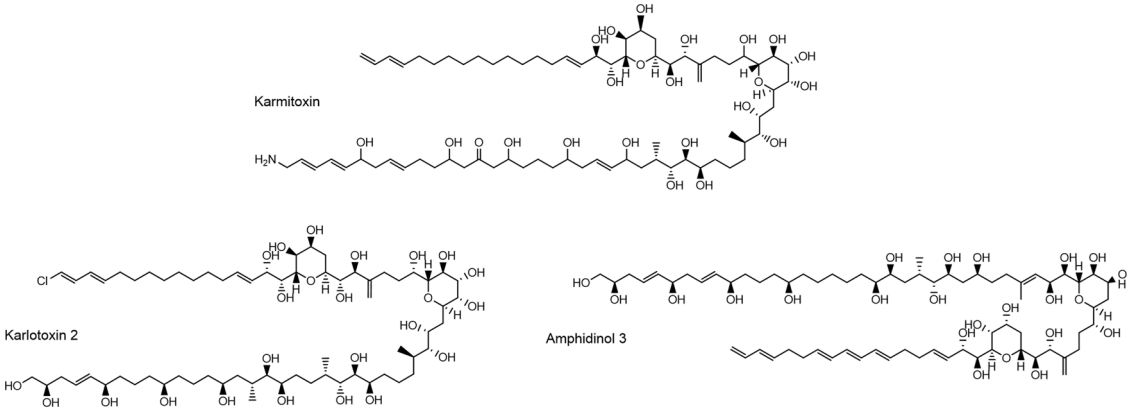

Fig. 1. Structures of karmitoxin produced by the dinoflagellate *Karlodinium armiger* in comparison to karlotoxin 2 from *Karlodinium veneficum* and amphidinol 3 from *Amphidinium klebsii*.

at 4 °C for up to 10 days. The pH of both buffers was adjusted before sterile filtration (0.22 μm) to pH 7.4 at 10 °C, and a hemolytic calibration curve using saponin (Quillaja bark, CAS No.: 8047–15–2; Sigma Chemical Co., St. Louis, MO, USA) was created for each new batch of 1.25 %-RBC solution. The stability of the RBC solution was monitored by observing the absorbance value obtained for incubation with only Tris-buffer II. Saponin (8 μg/mL) was also used as positive control, and the solvent control consisted of Tris buffer II containing 0.5 % (*v/v*) EtOH. The assays were carried out in 96-well plates (V-bottom, polystyrene, non-treated, Corning Inc., Corning, NY, USA). All experiments involving fish were carried out in accordance with the guidelines at the Institutional Animal Care and Use Committee (IACUC) of the University of Maryland Medical School: protocol No 0014 and No 0522012. Fish used for tissue sampling were anesthetized with tricaine methanesulfonate (MS-222, 10 mg/L) for blood sampling and then euthanized with MS-222 (150 mg/L).

2.3.2. CellTiter blue® (CTB)

The CellTiter Blue® (CTB, (Promega, Madison, WI, USA)) assay was used to determine the cytotoxicity of karmitoxin on RTgill-W1 and HCEC-1CT cells. Cells were seeded onto 96-well plates at a density of 2×10^4 cells per well (RTgill-W1) or 5×10^3 cells per well (HCEC-1CT). Following a 48-h growing period, they were exposed to karmitoxin diluted in culture medium (final EtOH concentration 0.5 % (*v/v*)). The solvent control consisted of medium containing 0.5 % (*v/v*) EtOH, and the positive control was 0.05 % and 0.1 % Triton™ X-100 (Triton X, (Sigma-Aldrich, St. Louis, MO, USA)) in culture medium. The cells were incubated with karmitoxin for 3 or 24 h in the dark at 19 °C (RTgill-W1) or 37 °C (HCEC-1CT). Subsequently, the solutions were aspirated and 100 μL 1:10 diluted CTB reagent in the respective culture medium was added to the cells. After a 1-h reaction time, 80 μL of the CTB-supernatant were transferred into a black 96-well plate and fluorescence was measured according to the manufacturer's instructions.

2.3.3. Lactate dehydrogenase (LDH) assay

Lytic effects of karmitoxin were assessed with the lactate dehydrogenase (LDH) assay (Pierce CyQuant™, Thermo Scientific, Waltham, MA, USA). The manufacturer's protocol was followed. Briefly, after the 3-h toxin incubation 50 μL supernatant were transferred onto a new F-bottom 96-well plate, and by adding 50 μL LDH reaction mix the reaction was initiated. After 30 min 50 μL stop solution were added and the absorbance was read at 490 and 680 nm.

2.4. Interaction with sterols

2.4.1. Sterol combinations

In order to understand whether karmitoxin can interact with sterols, cholesterol (5(6)-cholesten-3-ol, Sigma St. Louis, MO, USA) and epicholesterol (5-cholesten-3a-ol, Steraloids Inc., Newport, RI, USA) were combined with karmitoxin before starting a hemolytic assay. The selection of these sterols was based on previous work showing that karlotoxin built highly stable complexes with cholesterol, but not with its epimer epicholesterol (Place et al., 2024). The assay protocol of Prause et al. (2024) was followed. Shortly, the karmitoxin sample diluted to the HC_{50}[1] value was combined with the equivalent volume of either one of the sterols ranging from 0.1 nM to 10,000 nM. Sterols had previously been dissolved in EtOH, and dilutions were performed to maintain a total EtOH concentration of 0.5 % (*v/v*). Hemolysis was performed as described previously, by adding 100 μL 1.25 % (*v/v*) RBC solution.

2.4.2. Surface plasmon resonance (SPR)

Binding interactions of karmitoxin with cholesterol, epicholesterol, and ergosterol (Fluka Chemie GmbH, Buchs, Switzerland) were also recorded via surface plasmon resonance (SPR). The protocol, originally described by Place et al. (2024) was followed precisely, using the T200 Biacore system with a Series S Sensor Chip HPA (Cytiva, Danaher Corporation, Washington, DC, USA). The flow cells (Fcs) of the sensor chip were first pre-conditioned with 40 mM octyl-d-glucoside for 5 min at a flow rate of 10 μL/min. The sterols were diluted to 10 μM in HBS buffer (10 mM HEPES, 150 mM NaCl, pH 7.4) and immobilized on the Fcs at about 1000 responsive units (RUs) with a flowrate of 2 μL/min for 30 min. The Fcs were rinsed with 10 mM NaOH for 30 s and then blocked for 5 min using bovine serum albumin (0.1 mg/mL in dH_2O). HBS buffer was run over the sensor chip three times before karmitoxin at 1 μM was run over the Fcs for 2 min at 10 μL/min. The responses were fitted on a 1:1 model, and complex stabilities were evaluated by calculating the dissociation rate constant $k_d(s^{-1})$ with the program Biacore T200 Evaluation Software version 3.2.1 (Cytiva, Danaher Corporation, Washington, DC, USA).

2.4.3. Membrane cholesterol in RTgill-W1 cells

To get a better understanding of the relevance of cholesterol in the cytotoxic potential of karmitoxin the cholesterol content of the cells was modified to contain more or less cholesterol as described in Prause et al. (2024). A 24-h cholesterol-altering treatment was conducted using 10 μM lovastatin (lovastatin sodium salt, Enzo, Farmingdale, NY, USA) for depletion and 10 μM methyl-β-cyclodextrin (MbCD) loaded with cholesterol (MbCD-Chol (Sigma Aldrich GmbH, St. Louis, MO, USA)) to augment cholesterol contents (Del Favero et al., 2020; Rebhahn et al., 2022). The cellular cholesterol content was relatively quantified via fluorescence microscopy as reported in the previous paper, and a total cholesterol increase of about 30 % and a decrease of approximately 25 % could be achieved (Prause et al., 2024). Following the 24-h treatment, karmitoxin at approximately EC_{80} was added to the cholesterol-modified as well as unaltered cells and incubated for 3 h. The resulting cell viability was measured via CTB assay.

2.5. Statistics

All assays were carried out in technical triplicates, with the exception of SPR assays, which were performed in duplicates. The number of biological replicates is provided below the figures. Significance (* = $p < 0.05$; ** = $p < 0.01$; *** = $p < 0.001$) was calculated with One Way ANOVA followed by the posthoc Fisher's least significant difference test, as well as *t*-test (one-sample or two-sample) using OriginPro 2020 Version 9.7.0.185 (Academic) from OriginLab Corporation (Northampton, MA, USA). RStudio version 4.0.2 (RStudio Inc., Boston, MA, US) was used for calculating EC_{50} values.

3. Results

3.1. Toxicity

3.1.1. Hemolytic activity

Karmitoxin was tested for hemolysis of RBCs obtained from salmon blood. Concentrations ranging from 15 – 240 nM were applied to obtain a hemolytic response curve (Fig. 2). Strong hemolytic potential was observed, and an HC_{50} value of 160 nM could be estimated. The highest concentration, 290 nM, caused 90 % hemolysis of RBCs.

3.1.2. Cytotoxicity and lytic activity in RTgill-W1 cells

RTgill-W1 cells were used to assess the cytotoxic potential of the karmitoxin sample for both 3-h and 24-h exposure. Following a 3-h incubation (Fig. 3**A**) a linear decline in the metabolic activity was measured, with a 50 % cell viability (EC_{50}) achieved by approximately 111 nM karmitoxin. The release of intracellular LDH was positively correlated to cytotoxicity, with the largest release (about 11 %) at the highest tested concentration (191 nM). The first significant reduction in metabolic activity was observed at 78 nM karmitoxin, yet the first

[1] Concentration at which 50 % of all RBCs are lysed.

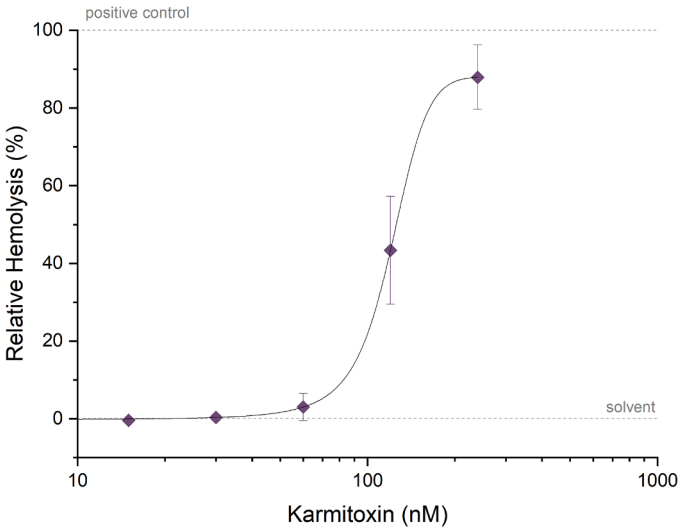

Fig. 2. Hemolytic activity of karmitoxin in erythrocytes of Atlantic salmon (*Salmo salar*). Saponin (8 μg/mL) was used as positive control and set as 100% hemolysis, Tris-buffer II containing 0.5% (*v/v*) EtOH was used as solvent control. Data is given as mean ± SD of n = 3 biological replicates fitted on a non-linear dose-response using the Levenberg Marquardt algorithm.

concentration at which a significant LDH release was observed was 122 nM. A 24-h incubation (Fig. 3**B**) was performed and compared to the standard incubation time of 3 h. The three lowest concentrations (40, 50, and 63 nM) caused an increase in metabolic activity to about 150 %, yet the higher concentrations (78 nM onwards) exhibited significantly stronger cytotoxic effects compared to the 3-h incubation. Exposure to 122 nM karmitoxin for 24 h decreased the metabolic activity by about 95 %, while a 3-h exposure only resulted in a 60 % reduction. The calculated corresponding EC_{50} for the 24-h incubation was thus approximately 74 nM. Interestingly, LDH release did not exceed 40 %, even at the highest concentrations of karmitoxin where the relative metabolic activity was at 0 %. In fact, the extracellular LDH content dropped back to 20 % at the highest concentration.

3.1.3. Cytotoxicity and lytic activity in HCEC-1CT cells

The cytotoxic potential of karmitoxin was also evaluated in a human cell line for the first time (Fig. 4). A slightly higher concentration range, from 80 nM to 382 nM, needed to be applied to the cells for the standard incubation time of 3 h. These concentrations were based on preliminary assays, demonstrating a lower sensitivity of this cell line towards karmitoxin. Both CTB and LDH measurements were performed. Interestingly, the cellular metabolic activity increased when exposed to the two lowest concentrations (80 nM and 100 nM), with no LDH release. A significant decrease in cell viability, to 30 % metabolic activity, was first observed at 196 nM. This concentration had reduced metabolic activity to about 10 % in RTgill-W1 cells. The first significant LDH leakage of 24 % from HCEC-1CT cells also took place after incubation with 196 nM karmitoxin. A concentration of approximately 300 nM was needed to achieve 0 % metabolic activity in HCEC-1CT cells. The highest LDH release of about 40 % occurred at 245 nM. This level of release remained consistent for the two subsequent highest concentrations tested (306 nM and 382 nM). The calculated EC_{50} value for karmitoxin in this cell line was approximately 175 nM.

Morphological changes of the cells after exposure to karmitoxin were observed in bright field images (Fig. 5). Upon coming in contact with karmitoxin the cells would change their shape and become more rounded, and with increasing concentrations the cells started detaching from the well bottom (Fig. 5**A**). Cells for which no metabolic activity was measured were generally presumed to be dead, which was supported by their swollen appearance and the fact that they had fully detached from the well bottom. This can be observed for exposure of HCEC-1CT cells to 382 nM karmitoxin (Fig. 5B).

3.2. Sterol interactions

3.2.1. Combination assays

Whether karmitoxin can interact with sterols was evaluated by combining the toxin at its HC_{50} with different concentrations of cholesterol or epicholesterol. It was hypothesized that an interaction would subsequently affect the hemolytic potential (Place et al. 2024). Once the sterols were combined with the toxin, the expected 50 % hemolysis was reduced to 0 % with cholesterol, and nearly 0 % with epicholesterol (Fig. 6). This outcome was irrespective of the sterol concentration. Neither sterol exhibited hemolytic effects at any of the applied concentrations (supplementary information (SI) Fig. 1).

3.2.2. Surface plasmon resonance (SPR)

Following the hemolytic combination assays, the interaction between karmitoxin and sterols was studied more closely via SPR (Fig. 7). The T200 Biacore Evaluation Software (Cytiva, Danaher Corp., Washington, DC, USA) was used for the calculation of the dissociation rate constant $k_d(s^{-1})$, which can be used to interpret complex stability. Karmitoxin bound to all three sterols, and to octyl-d-glucoside (control) most likely due to an amphipathic character, as described for the structurally very close karlotoxin (Van Wagoner et al., 2008). Differences were observed between the three sterols, with $k_d(s^{-1})$ values of 1.13×10^{-2} for cholesterol, 5.48×10^{-3} for epicholesterol, and 4.72×10^{-3} for ergosterol. From these constant rates it can be inferred that karmitoxin-cholesterol complexes decayed more quickly than the complexes formed with ergosterol or epicholesterol. The dissociation from ergosterol and epicholesterol on the other hand was nearly equal. The difference between the three sterols was further highlighted by the different fit quality (Chi^2) of the single exponential model. Karmitoxin-cholesterol complexes seemingly followed this model well ($Chi^2(RU^2)$ of 5.29), while the fitting of the karmitoxin-epicholesterol or -ergosterol complex decay exhibited larger Chi^2 values, indicating more intricate binding interactions.

3.2.3. Membrane cholesterol in RTgill-W1 cells

Considering that karmitoxin supposedly binds to membrane cholesterol and the high complex stability obtained via SPR, it was of interest to see whether altering the cholesterol content of RTgill-W1 cells would impact its cytotoxicity. Indeed, effective modification of the lipid can be achieved by treating the cells with either MbCD-Chol (10 μM) to augment, or lovastatin (10 μM) to reduce cholesterol content. This treatment and a subsequent relative quantification of the cellular cholesterol was previously reported in Prause et al. (2024), where the cholesterol content could be increased by approximately 30 % and lowered by about 25 %. The cells were then exposed to karmitoxin at approximately EC_{80} (approximately 160 nM) for 3 h. There was seemingly no difference between the cells regarding the impact on the metabolic activity (Fig. 8). A tendency for both treatments to exhibit a protective effect on the cells could be seen, but no significance could be calculated.

4. Discussion

Karmitoxin is considered a very potent hemolysin, and its structural similarity to karlotoxin and amphidinols serves as a key feature in understanding its chemical as well as functional and toxic properties (Rasmussen et al., 2017; Waters et al., 2015; Place et al. 2024). The cytotoxic potential of karmitoxin has already been established in previous studies using the RTgill-W1 cell line (Binzer et al., 2020; Rasmussen et al., 2017). The EC_{50} of 111 nM for a 3-h incubation obtained in this work was similar to the 125 nM found by Rasmussen et al. (2017). In general, exposure of RTgill-W1 cells to karmitoxin for 24 h led to

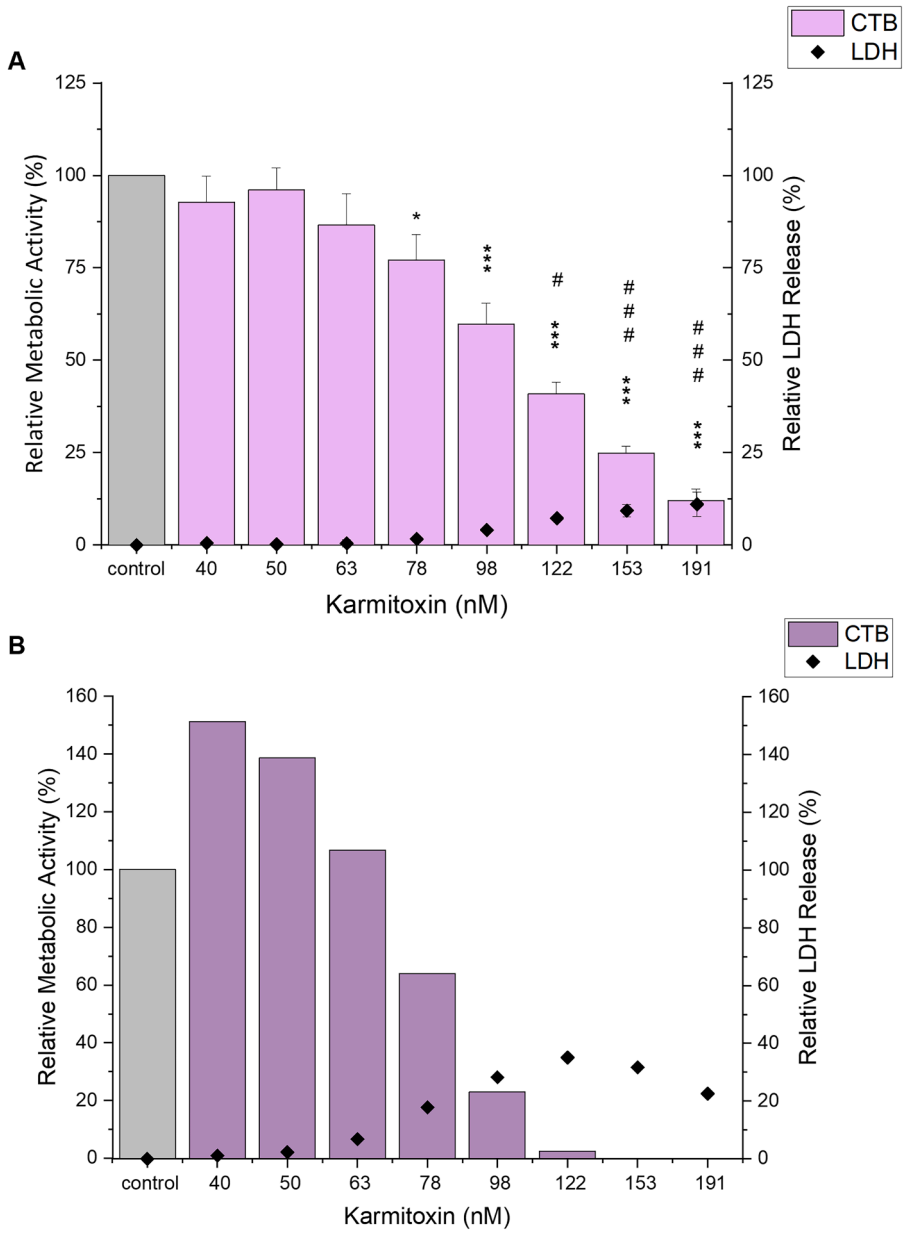

Fig. 3. Cytotoxic potency of karmitoxin in RTgill-W1 cells after 3h (**A**) and 24h (**B**), measured as metabolic activity of the cells via the CellTiter-Blue® (CTB) assay and the lactate dehydrogenase (LDH) assay. Medium containing 0.5% (*v/v*) EtOH was used as solvent control (100% for the CTB assay and 0% for the LDH assay). Data from **A** is presented as mean ± SD of n ≥ 4 biological replicates, significant differences between the measurements are labeled with * (CTB) or # (LDH). Normal distribution of the data was analyzed with the Shapiro-Wilk normality test ($p < 0.05$). Outliers according to Nalimov were eliminated. Data from **B** represent results of technical triplicates, therefore, no statistics were performed.

apparently stronger cytotoxicity, with a lower concentration (74 nM) reaching a 50 % decrease in metabolic activity. Interestingly, the metabolic activity resulting from 24-h exposure to the lower toxin range was drastically higher than the control, with close to no LDH release. This behavior could be attributed to activation of repair mechanisms aimed at maintaining cellular homeostasis as a response to stress induced by karmitoxin (Fulda et al., 2010; Welch, 1993). It can be assumed that lower concentrations of karmitoxin contributed to cellular stress, initiating a pro-survival signaling pathway. However, once a certain threshold is surpassed, either due to the severity or persistence of the stress factor, cells are no longer able to counteract the damage and switch to a cell death signaling pathway (Fulda et al., 2010). This phenomenon explains the higher metabolic activity measured for the lower concentrations of karmitoxin after 24 h compared to the 3-h incubation time. The activation of such repair mechanisms may not be immediate, resulting in an initial disruption on cellular homeostasis (as observed after 3 h), which can later be repaired by the cellular stress response (as observed after 24 h).

The human epithelial cell line seemed to be less sensitive towards karmitoxin, with an EC_{50} value of 175 nM compared to 111 nM in RTgill-W1 cells. It should be noted that cell numbers for seeding were selected based on their ability to reproduce and create a 100 % confluent monolayer within 48 h, in order to maintain testing conditions across both cell lines. As HCEC-1CT cells reproduce more quickly than RTgill-W1 cells, a lower cell number is required to reach confluence. Still, both values are comparable to each other as well as to the hemolytic potential towards Atlantic salmon RBCs, with an HC_{50} of approximately 160 nM karmitoxin. Since membrane damage was also measured in RTgill-W1 and HCEC-1CT cells, it can be assumed that the cytotoxic effects were at least in part caused by lytic activity of karmitoxin. Surprisingly, the

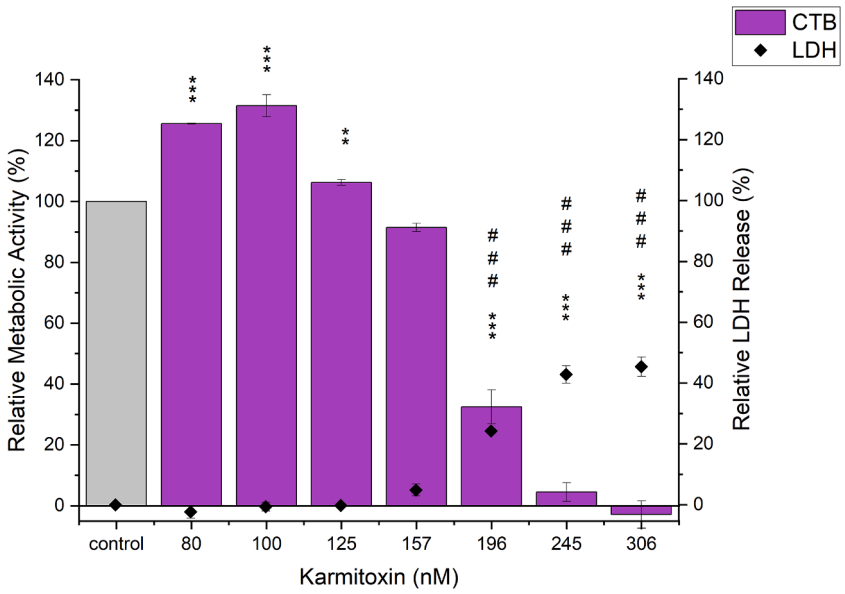

Fig. 4. Cytotoxic potency of karmitoxin in HCEC-1CT cells after 3 h, measured as metabolic activity of the cells via the CellTiter-Blue® (CTB) assay and the lactate dehydrogenase (LDH) assay. Medium containing 0.5 % (*v*/*v*) EtOH was used as solvent control (100 % for the CTB assay and 0 % for the LDH assay). Data is given as mean ± SD of n = 3 biological replicates. Significant differences between the measurements are labeled with * (CTB) or # (LDH). Normal distribution of the data was analyzed with the Shapiro-Wilk normality test ($p < 0.05$). Outliers according to Nalimov were eliminated.

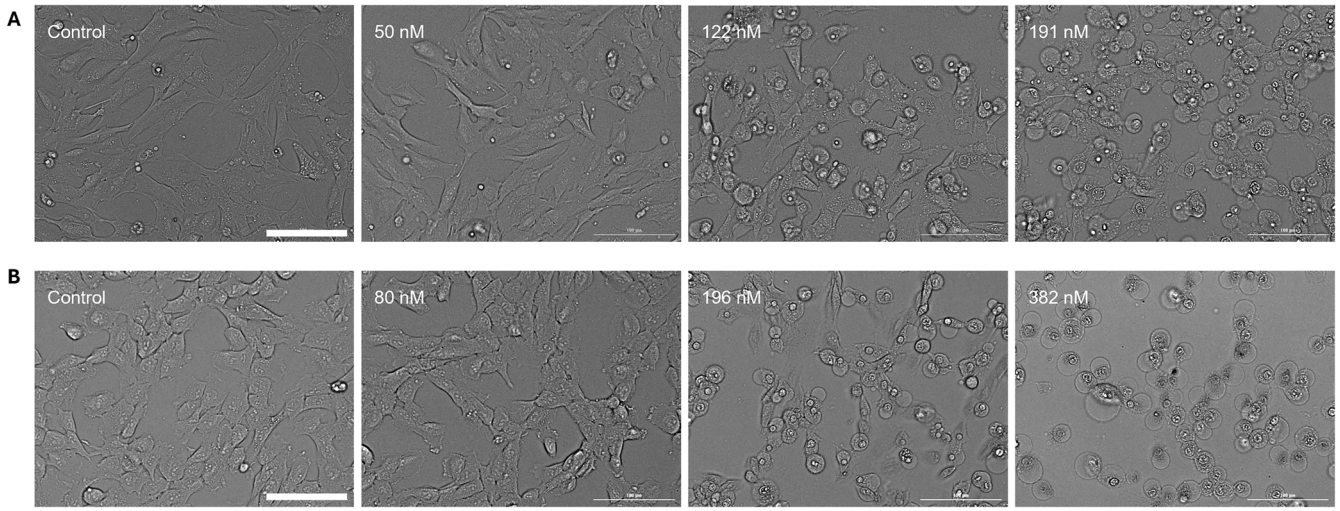

Fig. 5. Bright field images of RTgill-W1 cells (**A**) and HCEC-1CT cells (**B**) after 3-h exposure to various concentrations of karmitoxin in comparison to the control. The control consisted of the respective culture medium containing 0.5 % (*v*/*v*) EtOH. Image contrast and brightness were adjusted for better visibility. Scale bars represent 100 μm.

LDH release in both cell lines was much lower than expected, despite the positive control that represented the amount of LDH released from fully lysed RTgill-W1 or HCEC-1CT cells.

The enzyme LDH plays an essential role in the anaerobic breakdown of glucose, and its cellular levels may be impacted by the activation of pro-survival signaling pathways, which demand increased energy from cells (Brooks et al., 1999). This rationale may in part account for the low LDH values of cells exposed to high toxin concentrations, although it appears to be an oversimplification of this phenomenon. Despite an initial decrease in metabolic activity at the lower toxin concentrations, no LDH release was observed. LDH release increased only at higher concentrations, suggesting that higher toxin concentrations may stabilize or enlarge pore diameter, thereby delaying LDH release relative to metabolic effects. Furthermore, pore-formation may not be the only mechanism causing the cell death. A premise that might be supported by the morphological state of the cells. To test this hypothesis, assays providing more information on cellular processes, such as cell cycle analyses, or monitoring dysregulation of cell signaling pathways including endoplasmic reticulum stress or oxidative stress are necessary (Fulda et al., 2010). Another option would be staining cellular structures such as cytoskeleton, nuclei, or mitochondria, to monitor changes thereof. Deeds et al. (2015) showed that karlotoxin can cause a non-selective pre-lytic increase in cellular cations. It may be that karmitoxin behaves in a similar way.

Generally, these results showed a rapid onset of cytotoxic effects induced by karmitoxin, which can be enhanced by longer incubation time, and possibly also reversed given that the concentration is low enough. This implies that the duration of toxin-exposure could impact the overall toxicity in the target organism. It would be of interest to assess whether RTgill-W1 cells exposed to karmitoxin, at various

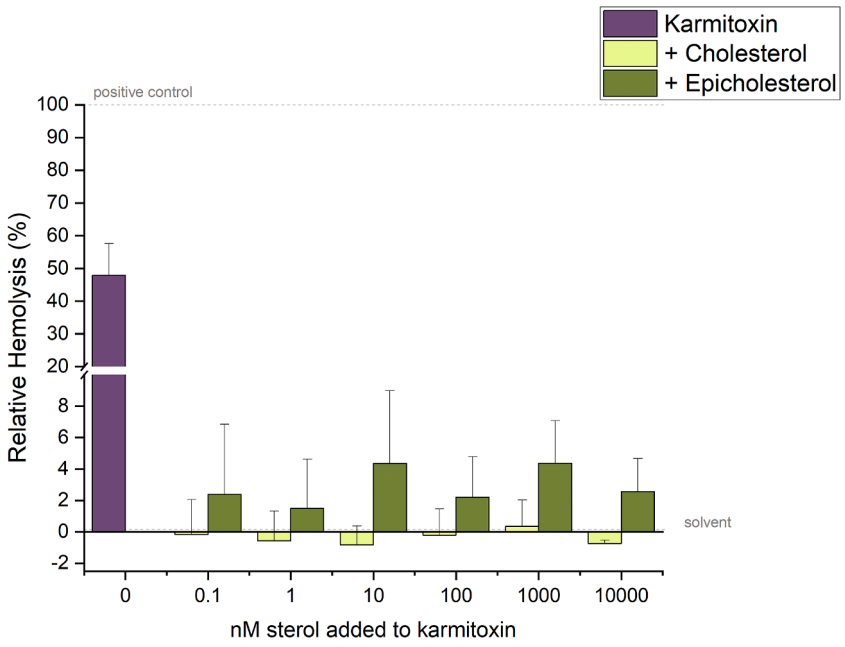

Fig. 6. Hemolytic potential of karmitoxin at HC_{50} (approximately 160 nM) compared to hemolytic effects resulting from combination of karmitoxin at HC_{50} combined with cholesterol or epicholesterol at different concentrations. Saponin (8 μg/mL) was used as positive control and set as 100 % hemolysis, Tris-buffer II containing 0.5 % (*v/v*) EtOH was used as solvent control. Data is given as mean ± SD of n = 2 for cholesterol and n = 3 for epicholesterol.

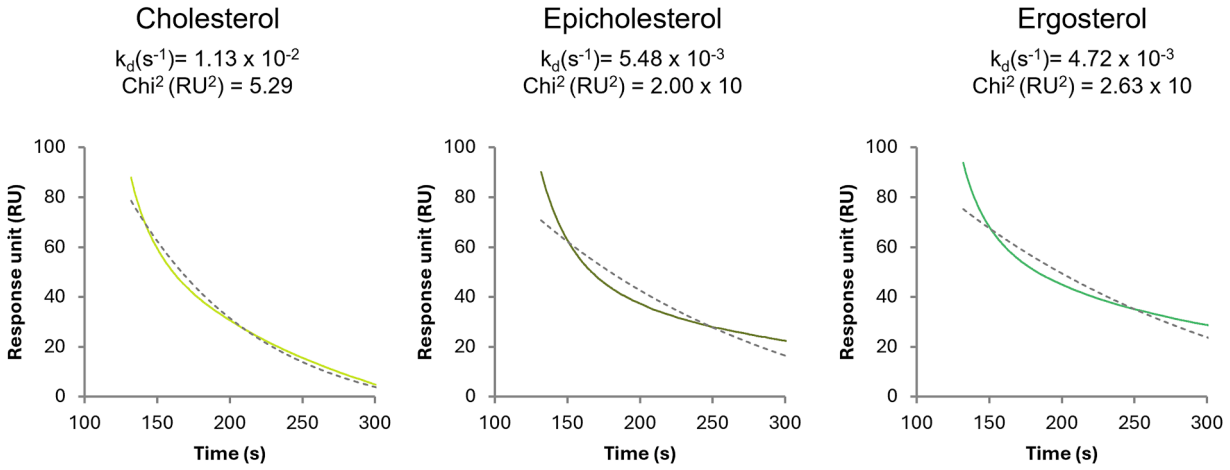

Fig. 7. Sensograms for 1 μM karmitoxin binding to immobilized ligands; 10 mM cholesterol, 10 mM epicholesterol, and 10 mM ergosterol. The measured curves are shown in a solid line in color and the fitted curves in a dark gray dashed line. Measurements were performed in duplicates. The dissociation rate constant $k_d(s^{-1})$ and the quality of the fitted model $Chi^2(RU^2)$ are provided above the graphs.

concentrations and duration times, can recover from the cytotoxic damage during a recuperation period in toxin-free medium. This evaluation would help determine the efficacy of cellular repair mechanisms and identify a concentration threshold for successful repair. With information from such an *in-vitro* experiment it might be easier to estimate how fish would recover from short-term exposure to karmitoxin, similar to fish exposed to prymnesins from the haptophyte *Prymnesium parvum* (Svendsen et al., 2018). Importantly it could elucidate until which concentration such a recovery would be feasible.

The hemolytic potency of karmitoxin was similar to that of karlotoxin, albeit karmitoxin seemed to be more potent (Deeds et al., 2015). To lyse about 90 % of salmon RBCs, 290 nM karmitoxin were sufficient, yet 500 ng/mL (≈370 nM) karlotoxin 2 were necessary to lyse 90 % of trout RBCs (Deeds et al., 2015). We hypothesize that the unique amine group at the lipophilic arm of karmitoxin may be the reason for its stronger potency (Rasmussen et al., 2017). As a result, interaction with phospholipids may be increased in comparison to karlotoxin, which would facilitate the insertion of karmitoxin into the cellular membrane (Place et al., 2009; Rasmussen et al., 2017). Of course, it should be noted that physiological differences between the RBC sources (salmon vs. trout) may exist. The combination of karmitoxin with sterols lowered the expected hemolysis significantly. This effect had already been documented for karlotoxin 2 in trout RBCs (Deeds and Place, 2006). No difference could be observed between the effects of cholesterol or epicholesterol. These results were corroborated by the SPR data, which showed that complex stabilities with cholesterol and epicholesterol were comparable, with dissociation rate constants of $1.13 \times 10^{-2}\ s^{-1}$ and $5.48 \times 10^{-3}\ s^{-1}$, respectively. These $k_d(s^{-1})$ values are similar to the ones previously obtained for karlotoxin 2 and amphidinol 18 interacting with cholesterol ($2.45 \times 10^{-3}\ s^{-1}$ and $1.69 \times 10^{-2}\ s^{-1}$, respectively) (Place et al., 2024). Interestingly, the lowest dissociation rate was found for the complex with ergosterol, the main membrane sterol in fungi (Axelsson

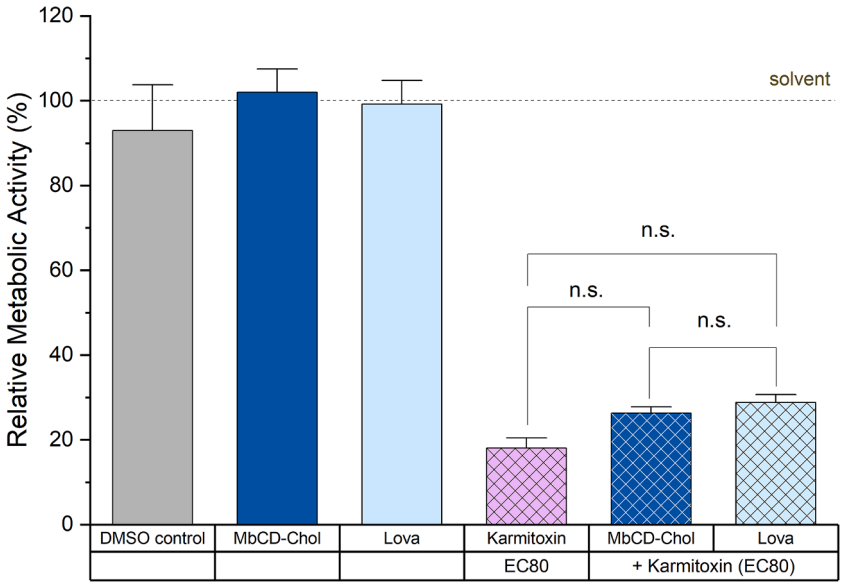

Fig. 8. Metabolic activity of regular and cholesterol-altered RTgill-W1 cells after 3-h exposure to karmitoxin at approximately EC_{80} (approximately 160 nM). Methyl-β-cyclodextrin loaded with cholesterol (MbCD-Chol, 10 μM) was used to increase, and lovastatin (Lova, 10 μM) to lower cellular cholesterol. Culture medium containing 0.5 % (*v/v*) EtOH served as solvent control and medium containing 0.25 % (*v/v*) dimethyl sulfoxide (DMSO) was used as solvent control for the Lova treatment. No significant difference between the karmitoxin treatments could be measured (n.s.). Data represent the mean ± SD of n = 3 biological replicates.

et al., 1995; Dufourc, 2008). Amphidinols and karlotoxins have both been described as potent antifungal agents (Place et al., 2009; Satake et al., 1991; Van Wagoner et al., 2008). For amphidinols the strong affinity towards ergosterol was recently shown to be correlated to their antifungal potency (Matsumori et al., 2024; Swasono et al., 2010). With this information in mind, it can be assumed that karmitoxin also possesses antifungal capacities, and that these are likewise related to their affinity to ergosterol. Matsumori et al. (2024) also showed that amphidinol 3 seems to follow a 2-step reaction model. The authors proposed that the first binding step reflects sterol recognition and binding to the surface, while the second step, which the presence of ergosterol affected significantly more, represents an orientational change and most likely pore-formation (Matsumori et al., 2024). Based on the SPR results obtained here it could be argued that also karmitoxin follows a 2-step binding with ergosterol and epicholesterol.

Possibly the most unexpected result was that alteration of the cholesterol content of RTgill-W1 cells had no impact on the cytotoxic potency of karmitoxin. This indicates that sufficient cholesterol was still present in the membrane, allowing karmitoxin to target the cell membrane regardless of the ~25 % decrease in cholesterol. As discussed in Prause et al. (2024), sterol modulation may take place throughout the entire cell, and not specifically in the cell membrane (Lange et al., 2004). This would mean that the actual change in membrane cholesterol was probably smaller than the measured 25 %. It is also likely that only small amounts of cholesterol are necessary for karmitoxin to target the cell membrane, just as it is likely for karmitoxin to interact with other lipids in the plasma membrane, such as the phospholipids. Regardless, both the increase and decrease of cholesterol resulted in the same tendency for somewhat lower cytotoxicity, which should be further examined. Creating liposomes with different sterol compositions would be valuable in assessing the significance of sterols for the MOA. Calcein leakage experiments previously performed for amphidinols have shown significantly higher leakage from liposomes containing ergosterol (Matsumori et al., 2024). Future studies may focus on conducting a similar experiment with karmitoxin.

Overall, this study demonstrates that the hemolytic potential of karmitoxin parallels its cytotoxic potential. While lytic activities were also observed in the RTgill-W1 and HCEC-1CT cell lines, the LDH leakage was considerably low. This raises the question whether the cytotoxic potential of karmitoxin is reversible when cells are exposed to a low concentration for a limited amount of time. Despite karmitoxin exhibiting a strong affinity towards ergosterol, cholesterol, and epicholesterol, a ± 25 % modulation of (membrane) cholesterol could not affect cytotoxicity of the tested concentration (EC_{80}). For a better understanding of the role of membrane sterols on the MOA of karmitoxin an assessment of lytic activity against liposomes with various lipid profiles is needed. In addition, assessing the impact on cellular mechanisms, such as disruption of cell signaling pathways, oxidative stress, or osmoregulation, is crucial for providing a more comprehensive picture of the MOA of karmitoxin. Another interesting aspect to evaluate is the influence of karmitoxin on the membrane permeability to Ca^{2+}, Na^{+}, and K^{+}.

CRediT authorship contribution statement

Hélène-Christine Prause: Writing – review & editing, Writing – original draft, Visualization, Methodology, Investigation, Funding acquisition, Formal analysis, Data curation, Conceptualization. **Nadine Hochmayr:** Writing – review & editing, Visualization, Investigation, Formal analysis, Data curation. **Yanan Yu:** Writing – review & editing, Visualization, Investigation, Formal analysis, Data curation. **Thomas Ostenfeld Larsen:** Writing – review & editing, Resources, Methodology. **Per Juel Hansen:** Writing – review & editing, Resources, Methodology. **Giorgia Del Favero:** Writing – review & editing, Supervision, Resources, Methodology, Conceptualization. **Doris Marko:** Writing – review & editing, Supervision, Resources, Funding acquisition. **Allen Place:** Writing – review & editing, Supervision, Resources, Methodology, Conceptualization. **Elisabeth Varga:** Writing – review & editing, Supervision, Resources, Project administration, Methodology, Funding acquisition, Conceptualization.

Declaration of competing interest

The authors declare that they have no known competing financial interests or personal relationships that could have appeared to influence the work reported in this paper.

Acknowledgements

Kristin Schirmer, Department of Environmental Toxicology, EAWAG, provided the RTgill-W1 cell line. The HCEC-1CT cell line was obtained from Jerry W. Shay from the UT Southwestern Medical Center. We want to acknowledge Michael Murphy, Biacore, Cytiva (Danaher Corp., Washington DC, USA) who supported the data evaluation for SPR experiments. We are grateful to Peter Frühauf and the Department of Analytical Chemistry at the University of Vienna for the provision of the fluorescence detector. This work is partially supported by the USDA National Institute of Food and Agriculture through the Food Research Initiative SAS program (award #2021–68012–35922).

Funding

This research was supported by the University of Vienna, Faculty of Chemistry, Department of Food Chemistry and Toxicology, and was partly funded by the travel grant of the Doctoral School in Chemistry (DoSChem) of the University of Vienna. Open access funding was provided by the University of Veterinary Medicine Vienna. This research was funded in whole or in part by the Austrian Science Fund (FWF) [grant DOI: 10.55776/I5707]. For open access purposes, the corresponding author has applied for a CC BY public copyright license to any author accepted manuscript version arising from this submission.

Supplementary materials

Supplementary material associated with this article can be found, in the online version, at doi:10.1016/j.hal.2025.102817.

Data availability

Data will be made available on request.

References

Axelsson, B.-O., Saraf, A., Larsson, L., 1995. Determination of ergosterol in organic dust by gas chromatography-mass spectrometry. J. Chromatogr. B 666, 77–84. https://doi.org/10.1016/0378-4347(94)00553-H.

Bergholtz, T., Daugbjerg, N., Moestrup, Ø., Fernández-Tejedor, M., 2006. On the identity of *Karlodinium veneficum* and description of *Karlodinium armiger* sp. nov. (Dinophyceae), based on light and electron microscopy, nuclear-encoded LSU RDNA, and pigment composition. J. Phycol. 42 (1), 170–193. https://doi.org/10.1111/j.1529-8817.2006.00172.x.

Binzer, S.B., Varga, E., Andersen, A.J.C., Svenssen, D.K., de Medeiros, L.S., Rasmussen, S. A., Larsen, T.O., Hansen, P.J., 2020. Karmitoxin production by *Karlodinium armiger* and the effects of *K. armiger* and karmitoxin towards fish. Harmful. Algae 99, 101905. https://doi.org/10.1016/j.hal.2020.101905.

Bols, N.C., Barlian, A., Chirino-Trejo, M., Caldwell, S.J., Goegan, P., Lee, L.E.J., 1994. Development of a cell line from primary cultures of rainbow trout, *Oncorhynchus mykiss* (Walbaum), gills. J. Fish. Dis. 17 (6), 601–611. https://doi.org/10.1111/j.1365-2761.1994.tb00258.x.

Brooks, G.A., Dubouchaud, H., Brown, M., Sicurello, J.P., Butz, C.E., 1999. Role of mitochondrial lactate dehydrogenase and lactate oxidation in the intracellular lactate shuttle. Physiology 96, 1129–1134. https://doi.org/10.1073/pnas.96.3.112.

Deeds, J., Place, A., 2006. Sterol-specific membrane interactions with the toxins from *Karlodinium micrum* (Dinophyceae) — A strategy for self-protection? Afr. J. Mar. Sci. 28 (2), 421–425. https://doi.org/10.2989/18142320609504190.

Deeds, J.R., Hoesch, R.E., Place, A.R., Kao, J.P.Y., 2015. The cytotoxic mechanism of karlotoxin 2 (KmTx 2) from *Karlodinium veneficum* (Dinophyceae). Aquatic Toxicology 159, 148–155. https://doi.org/10.1016/j.aquatox.2014.11.028.

Deeds, J.R., Terlizzi, D.E., Adolf, J.E., Stoecker, D.K., Place, A.R., 2002. Toxic activity from cultures of *Karlodinium micrum* (=*Gyrodinium galatheanum*) (Dinophyceae)—A dinoflagellate associated with fish mortalities in an estuarine aquaculture facility. Harmful. Algae 1 (2), 169–189. https://doi.org/10.1016/S1568-9883(02)00027-6.

Del Favero, G., Mayer, R.M., Dellafiora, L., Janker, L., Niederstaetter, L., Dall'Asta, C., Gerner, C., Marko, D., 2020. Structural similarity with cholesterol reveals crucial insights into mechanisms sustaining the immunomodulatory activity of the mycotoxin alternariol. Cells 9 (4), 847. https://doi.org/10.3390/cells9040847.

Dufourc, E.J., 2008. Sterols and membrane dynamics. J. Chem. Biol. 1 (1–4), 63–77. https://doi.org/10.1007/s12154-008-0010-6.

Fulda, S., Gorman, A.M., Hori, O., Samali, A., 2010. Cellular stress responses: cell survival and cell death. Int. J. Cell Biol. 2010, 214074. https://doi.org/10.1155/2010/214074.

Garcés, E., Fernandez, M., Penna, A., Van Lenning, K., Gutierrez, A., Camp, J., Zapata, M., 2006. Characterization of new Mediterranean *Karlodinium* spp. (Dinophyceae) Strains using morphological, chemical, and physiological methodologies. J. Phycol. 42 (5), 1096–1112. https://doi.org/10.1111/j.1529-8817.2006.00270.x.

Houdai, T., Matsuoka, S., Morsy, N., Matsumori, N., Satake, M., Murata, M., 2005. Hairpin conformation of amphidinols possibly accounting for potent membrane permeabilizing activities. Tetrahedron. 61 (11), 2795–2802. https://doi.org/10.1016/j.tet.2005.01.069.

Lange, Y., Ye, J., Steck, T.L., 2004. How cholesterol homeostasis is regulated by plasma membrane cholesterol in excess of phospholipids. Proc. Natl. Acad. Sci. 101 (32), 11664–11667. https://doi.org/10.1073/pnas.0404766101.

Matsumori, N., Hieda, M., Morito, M., Wakamiya, Y., Oishi, T., 2024. Truncated derivatives of amphidinol 3 reveal the functional role of polyol chain in sterol-recognition and pore formation. Bioorg. Med. Chem. Lett. 98, 129594. https://doi.org/10.1016/j.bmcl.2023.129594.

Place, A.R., Bai, X., Kim, S., Sengco, M.R., Coats, D.W., 2009. Dinoflagellate host-parasite sterol profiles dictate karlotoxin sensitivity. J. Phycol. 45 (2), 375–385. https://doi.org/10.1111/J.1529-8817.2009.00649.X.

Place, A.R., Ramos-Franco, J., Waters, A.L., Peng, J., Hamann, M.T., 2024. Sterolysin from a 1950s culture of *Karlodinium veneficum* (aka *Gymnodinium veneficum* Ballantine) forms lethal sterol dependent membrane pores. Sci. Rep. 14 (1), 17998. https://doi.org/10.1038/s41598-024-68669-0.

Prause, H.C., Berk, D., Alves-de-Souza, C., Hansen, P.J., Larsen, T.O., Marko, D., Favero, G.Del, Place, A., Varga, E, 2024. How relevant are sterols in the mode of action of prymnesins? Aquat. Toxicol. 276, 107080. https://doi.org/10.1016/j.aquatox.2024.107080.

Rasmussen, S.A., Binzer, S.B., Hoeck, C., Meier, S., De Medeiros, L.S., Andersen, N.G., Place, A., Nielsen, K.F., Hansen, P.J., Larsen, T.O., 2017. Karmitoxin: an amine-containing polyhydroxy-polyene toxin from the marine dinoflagellate *Karlodinium armiger*. J. Nat. Prod. 80 (5), 1287–1293. https://doi.org/10.1021/acs.jnatprod.6b00860.

Rebhahn, V.I.C., Kiss, E., Marko, D., Del Favero, G., 2022. Foodborne compounds that alter plasma membrane architecture can modify the response of intestinal cells to shear stress in vitro. Toxicol. Appl. Pharmacol. 446, 116034. https://doi.org/10.1016/j.taap.2022.116034.

Satake, M., Murata, M., Yasumoto, T., Fujita, T., Naoki, H., 1991. Amphidinol, a polyhydroxy-polyene antifungal agent with an unprecedented structure, from a marine dinoflagellate, *Amphidinium klebsii*. J. Am. Chem. Soc. 113 (26), 9859–9861. https://doi.org/10.1021/ja00026a027.

Svendsen, M.B.S., Andersen, N.R., Hansen, P.J., Steffensen, J.F., 2018. Effects of harmful algal blooms on fish: insights from *Prymnesium parvum*. Fishes. 3 (1), 11. https://doi.org/10.3390/FISHES3010011.

Svenssen, D.K., Binzer, S.B., Medić, N., Hansen, P.J., Larsen, T.O., Varga, E., 2019. Development of an indirect quantitation method to assess ichthyotoxic B-type prymnesins from *Prymnesium parvum*. Toxins 11 (5), 251. https://doi.org/10.3390/toxins11050251.

Swasono, R.T., Mouri, R., Morsy, N., Matsumori, N., Oishi, T., Murata, M., 2010. Sterol effect on interaction between amphidinol 3 and liposomal membrane as evidenced by surface plasmon resonance. Bioorg. Med. Chem. Lett. 20 (7), 2215–2218. https://doi.org/10.1016/J.BMCL.2010.02.025.

Van Wagoner, R.M., Deeds, J.R., Satake, M., Ribeiro, A.A., Place, A.R., Wright, J.L.C., 2008. Isolation and characterization of karlotoxin 1, a new amphipathic toxin from *Karlodinium veneficum*. Tetrahedron. Lett. 49 (45), 6457–6461. https://doi.org/10.1016/j.tetlet.2008.08.103.

Waters, A.L., Oh, J., Place, A.R., Hamann, M.T., 2015. Stereochemical studies of the karlotoxin class using NMR spectroscopy and DP4 chemical-shift analysis: insights into their mechanism of action. Angew. Chem. 127 (52), 15931–15936. https://doi.org/10.1002/ange.201507418.

Welch, W.J., 1993. How cells respond to stress. Sci. Am. 268 (5), 56–62. http://www.jstor.org/stable/24941478.

Supplementary Information for:

The cytotoxic and hemolytic potential of karmitoxin from *Karlodinium armiger* and how it interacts with sterols

Hélène-Christine Prause[1,2], Nadine Hochmayr[1], Yanan Yu[3,4], Thomas Ostenfeld Larsen[3], Per Juel Hansen[5], Giorgia Del Favero[1,6], Doris Marko[1], Allen Place[7], Elisabeth Varga[1,8,*]

[1] Department of Food Chemistry and Toxicology, Faculty of Chemistry, University of Vienna, Währinger Str. 38-40, 1090 Vienna, Austria.

[2] Vienna Doctoral School in Chemistry, Faculty of Chemistry, University of Vienna, Währinger Str. 42, 1090 Vienna Austria.

[3] Department of Biotechnology and Biomedicine, Technical University of Denmark, Søltofts Plads 221, 2800 Kgs. Lyngby, Denmark.

[4] Key Laboratory of Oceanic and Polar Fisheries, Ministry of Agriculture and Rural Affairs; East China Sea Fisheries Research Institute, Chinese Academy of Fishery Sciences, Jungong Road 300, Shanghai, 200090, China.

[5] Marine Biological Section, Department of Biology, University of Copenhagen, Strandpromenaden 5, 3000 Elsinore, Denmark.

[6] Core Facility Multimodal Imaging, Faculty of Chemistry, University of Vienna, Währinger Str. 38-42, 1090 Vienna, Austria.

[7] Institute of Marine and Environmental Technology, University of Maryland Center for Environmental Science, 701 E. Pratt Street, Baltimore, MD 21202, USA.

[8] Unit Food Hygiene and Technology, Centre for Food Science and Veterinary Public Health, Clinical Department for Farm Animals and Food System Science, University of Veterinary Medicine, Vienna, Veterinärplatz 1, 1210 Vienna, Austria.

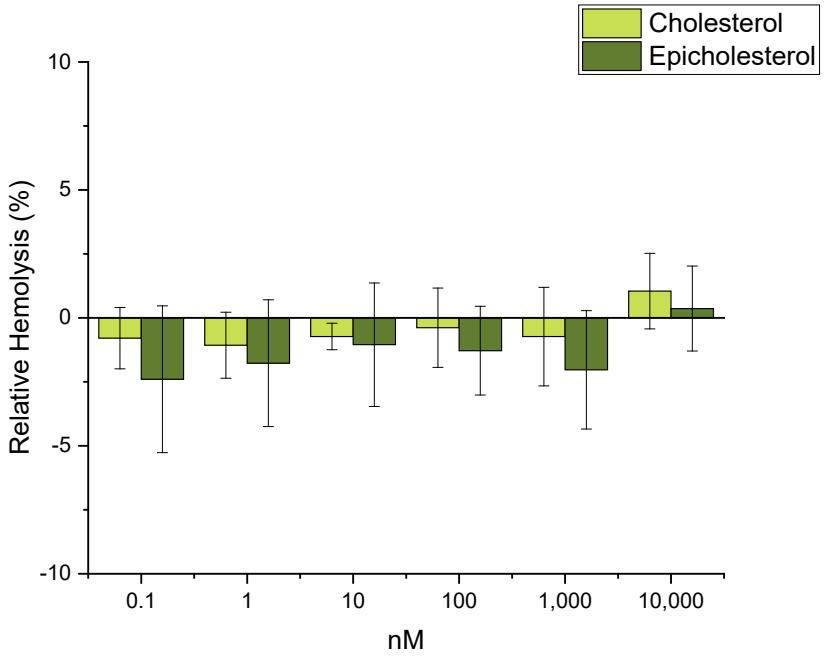

SI Figure 12 – Hemolysis of salmon (*Salmo salar*) red blood cells after exposure to various concentrations of sterols as reported in Prause *et al*., (2024).